Southeastern Geology: Volume 35, No. 2 June 1995

Editor in Chief: S. Duncan Heron, Jr.

Abstract

Academic journal published quarterly by the Department of Geology, Duke University.

SOUTHEASTERN GEOLOGY

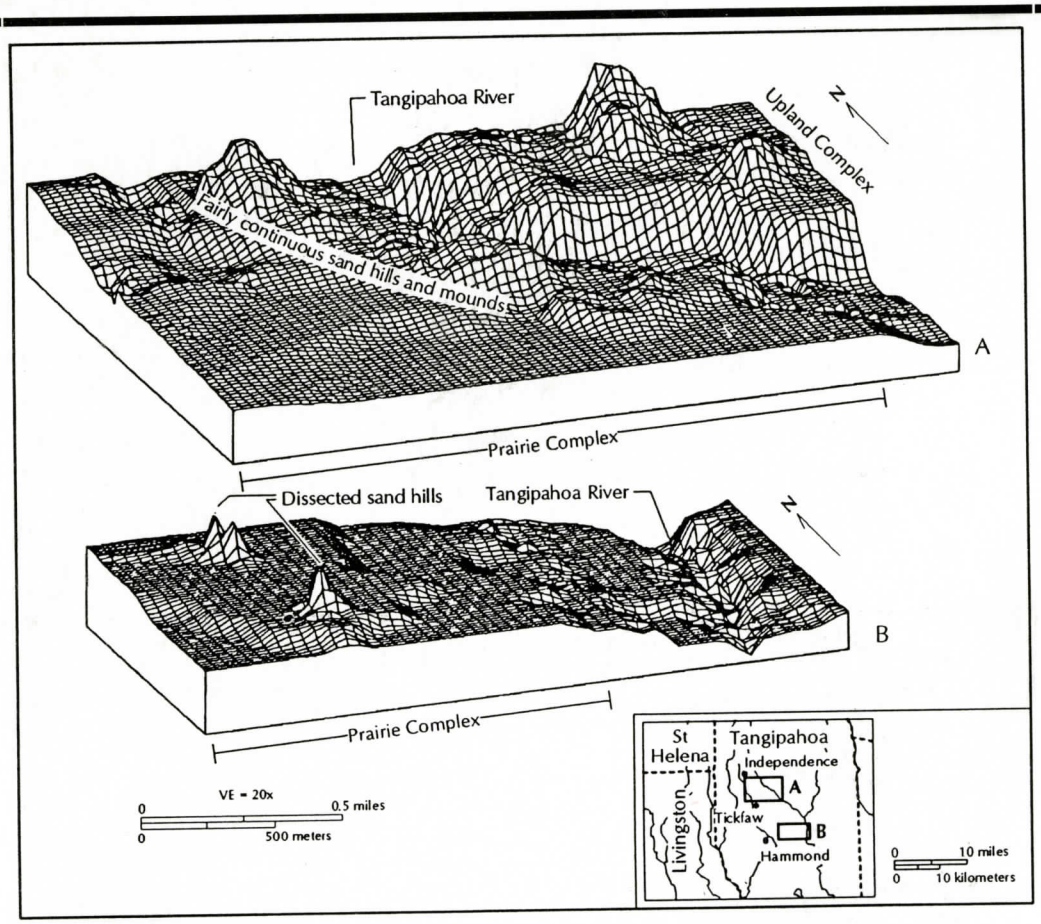

VOL. 35, NO. 2 **JUNE 1995**

SOUTHEASTERN GEOLOGY

PUBLISHED

at

DUKE UNIVERSITY

Editor in Chief:

Duncan Heron

This journal publishes the results of original research on all phases of geology, geophysics, geochemistry and environmental geology as related to the Southeast. Send manuscripts to **DUNCAN HERON, DUKE UNIVERSITY, DEPARTMENT OF GEOLOGY, BOX 90233, DURHAM, NORTH CAROLINA 27708**. Phone 919-684-5321, Fax 919-684-5833, E Mail heron@.geo.Duke.edu. Please observe the following:

1) Type the manuscript with double space lines and submit in duplicate.
2) Cite references and prepare bibliographic lists in accordance with the method found within the pages of this journal.
3) Submit line drawings and complex tables reduced to final publication size (no bigger than 8 x 5 3/8 inches).
4) Make certain that all photographs are sharp, clear, and of good contrast.
5) Stratigraphic terminology should abide by the North American Stratigraphic Code (American Association Petroleum Geologists Bulletin, v. 67, p. 841-875).

Subscriptions to *Southeastern Geology* for volume 35 are: individuals - $16.00 (paid by personal check); corporations and libraries - $21.00; foreign $25. Inquires should be sent to: **SOUTHEASTERN GEOLOGY, DUKE UNIVERSITY, DEPARTMENT OF GEOLOGY, BOX 90233, DURHAM, NORTH CAROLINA 27708**. Make checks payable to: *Southeastern Geology.*

Information about SOUTHEASTERN GEOLOGY is now on the World Wide Web. You may access the web station at this address:

http://www.geo.duke.edu/seglgy.htm

SOUTHEASTERN GEOLOGY is a peer review journal.

ISSN 0038-3678

SOUTHEASTERN GEOLOGY

Table of Contents

Volume 35, No. 2

June 1995

SOUTHEASTERN GEOLOGY
V. 35, No. 2, June 1995, p. 59-77

STYLE AND AGE OF DEFORMATION, CAROLINA SLATE BELT, CENTRAL NORTH CAROLINA

TERRY W. OFFIELD, MICHAEL J. KUNK, AND ROBERT P. KOEPPEN

U.S. Geological Survey
Reston, VA 22092

ABSTRACT

A good illustration of Carolina slate belt deformation style is seen in Late Proterozoic mudstone exposed in a quarry at the east edge of the Albemarle basin. All structures are east vergent. Well-developed axial-planar cleavage dips northwest; gentle to tight folds all are asymmetric to overturned southeastward; and shear-sense indicators all record northwest-over-southeast movement. Structures were rotated around NE-SW-trending, gently-plunging axes as deformation proceeded, with discontinuities (rhyolite dikes and shears) separating zones in which rotations and tightness of folding were different. Structural geometry is interpreted as indicating southeast-directed thrusting. The deformation was accompanied by greenschist-facies metamorphism. $^{40}Ar/^{39}Ar$ dating of biotite that grew during cleavage formation and white mica that grew as porphyroblasts across cleavage gives ages of 456 and 444 Ma, respectively. The slate belt as a whole shows similar structural development, and it is suggested that the quarry provides a small-scale model of belt-wide deformation style, kinematics, and associated metamorphism.

INTRODUCTION

The Carolina slate belt is anomalous within the southeastern Piedmont setting of polydeformed, high-grade schists and gneisses; it consists largely of rocks only weakly to moderately deformed and of low greenschist-facies metamorphism. Furthermore, the structure is anomalous in that folds and faults are dominantly east vergent, especially in the southern two-thirds of the belt in North Carolina, as recorded by cleavage dip, fold asymmetry, shear-sense indicators, and fault displacement (Offield, 1994). The east vergence of structure is a salient feature of the slate belt little discussed in the literature. Northwest-dipping cleavage was noted by Stuckey (1928, p. 24-25) as a general condition in the southern part of the belt, and east-vergent folds were mentioned by Conley and Bain (1965, p. 120). Northwest-dipping cleavage is abundantly recorded on published maps (e.g., Stromquist and Sundelius, 1975; Conley, 1962a, 1962b) and many unpublished thesis maps (e.g., Harris, 1982), but typically without much discussion. In general, detailed descriptions of slate-belt structure are rare, and discussions of deformational style correspondingly sparse, both because structure has not been a focus for studies, and because of a general lack of very good exposures.

A quarry operated by Martin Marietta Aggregates about 6 km north of Asheboro, NC (Figure 1) offers an excellent exposure of slate-belt structure. The quarry, about 550m long, 330m wide, and 55m deep, with 6 vertical working faces 8-10m high, displays folds that range from gentle to tight and cleavage that ranges in dip from gentle northwestward to near vertical. The variations in folds and cleavage are influenced in part by discontinuities such as faults and, especially, dikes that serve as local buttresses. Similar structural features and geometries have been found throughout the Carolina slate belt in six years of reconnaissance study (Offield, 1994), and we believe the Asheboro quarry provides a generally applicable example of structural style seen across much of the slate belt.

The pervasive and characteristic structure in

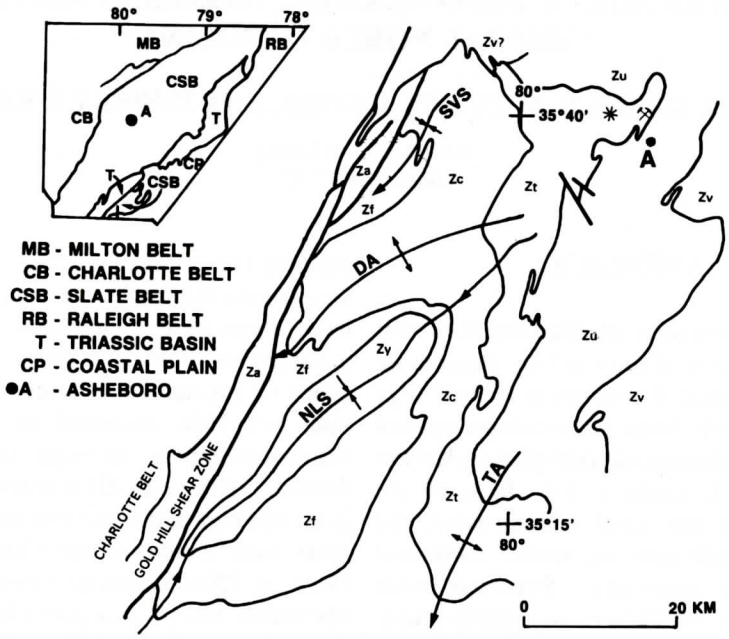

Figure 1. Map of quarry-area geologic setting. A, Asheboro; crossed picks, quarry; *, volcanic center. Geologic units: Zv, Virgilina sequence; Zu, Uwharrie Formation; Zt, Tillery Formation; Zc, Cid Formation; Zf, Floyd Church Formation; Zy, Yadkin Formation; Za, Albemarle Group undivided. Regional folds: TA, Troy anticlinorium; NLS, New London syncline; DA, Denton anticline; SVS, Silver Valley syncline. Modified after Geologic Map of North Carolina (North Carolina Geological Survey, 1985). Inset, index map showing regional lithotectonic assemblages in the North Carolina Piedmont.

the slate belt generally has been inferred to be a product of the Middle to Late Ordovician Taconian orogenic event (Vick and others, 1987; Butler and Secor, 1991), although overprinting by later structures clearly is present in local zones, and earlier folds and faults have been inferred in the northern part of the belt (Glover and Sinha, 1973). The regional low-grade metamorphic imprint on slate-belt rocks generally has been inferred to be associated with the main structural event (Glover and others, 1983; Butler and Secor, 1991). Kish and others (1979) interpreted K-Ar whole-rock ages of 483±15 Ma for rocks of the Albemarle area as dating the time of metamorphism. More recently, $^{40}Ar/^{39}Ar$ whole-rock ages of 455 Ma for samples of the Tillery Formation 45 km south of the Asheboro quarry suggest that the metamorphism was Late Ordovician in age (Noel and others, 1988). $^{40}Ar/^{39}Ar$ spectra of metamorphic biotite that crystallized during formation of cleavage and of metamorphic white mica that overgrew cleavage in the quarry rocks provide new dates which constrain the time of cleavage formation and peak metamorphism.

GEOLOGIC SETTING

Regional

The Albemarle basin occupies a large area in the western part of the Carolina slate belt in North Carolina. It is filled by the Albemarle Group, a sequence of mudstones and siltstones with interbeds of felsic and intermediate to mafic volcanic rocks, deformed in gentle regional folds across the basin (Figure 1; Goldsmith and others, 1988; North Carolina Geological Survey, 1985). The Asheboro quarry is located in the Tillery Formation at the base of

the Albemarle Group (Figure 1; Milton, 1984), at the east edge of the Albemarle basin. The Tillery overlies rhyolite of the Uwharrie Formation along the west flank of a broad regional fold, the Troy anticlinorium (Conley, 1962a; Seiders, 1981). Rocks near the top of the Albemarle sequence contain a Late Proterozoic Ediacaran index fossil (Gibson and others, 1984), and rhyolite of the Uwharrie has a reported U-Pb zircon date of 586±10 Ma (Wright and Seiders, 1980), so the whole regional sequence appears to be of Late Proterozoic age.

Geologic reconnaissance of structure in the Carolina slate belt (Offield, 1994) indicates that the intensity of deformation increases from west to east across the belt, as measured by cleavage development, occurrence of thrusts, and tightness and degree of eastward overturning of folds. In rocks susceptible to cleavage development throughout the slate belt, the morphology of cleavage varies zonally from planar, continuous type to rough or anastomosing, spaced type. On the west side of the belt, in mudstones of the Albemarle basin, cleavage is absent or only weakly developed in association with broad folds (Figure 1). Cleavage is concentrated in zones of east-vergent shears and small-scale folds that separate less disturbed areas. Deformation intensifies in a zone one to two kilometers wide along the Uwharrie-Tillery contact, where the quarry study area is located. In that zone, west-dipping cleavage is well developed, bed dips are steeper and somewhat more erratic, and the contact is locally disturbed by thrusting and shearing. Massive volcanic layers of the adjacent Uwharrie Formation are tilted, and east-vergent structures are seen in rare exposures of thin-bedded epiclastic rocks. East of the Uwharrie (Figure 1), older rocks of the Virgilina sequence (Harris and Glover, 1985, 1988; Offield, 1994) include chloritic andesitic rocks with almost schistose cleavage. In these rocks deformation effects typically are most evident in zones of dominantly west-over-east shear, with tight folds overturned eastward (Conley, 1962b). The pervasive structure throughout the slate belt is similar in character and style (Offield, 1994), and appears to be the product of a single regional tectonic episode (e.g., Butler and Secor, 1991), although more complex relations and evidence of older deformation have been reported from the northwest part of the belt (Glover and Sinha, 1973; Hibbard and others, 1994). For most of the slate belt, the general pattern is one of contrasting strain intensities, involving relatively broad zones of mild to moderate deformation (gentle to open folds and moderate cleavage development) and intervening narrower zones of more intense deformation (tight folds, shear, and strong cleavage development). Cleavage related to the major regional deformation is roughly parallel to the trend of the slate belt and dips northwest, axial-planar to east-vergent folds.

The regional structure is cut by discrete vertical zones of phyllitic or semischistose cleavage at the belt margins and elsewhere across the belt, reflecting strong, localized shear during one or more post-Taconian events (Acadian?, Alleghanian?; e.g., Butler and Fullagar, 1978; Farrar, 1985). Examples of this superposed shear are present in the Asheboro vicinity, but have not been recognized at the quarry.

Quarry

The quarry is located 800m west of the Uwharrie-Tillery contact, in the deformation zone along the east side of the Albemarle basin and the west flank of the Troy anticlinorium (Figure 1). This site is at the northeast corner of the Albemarle basin, where Tillery rocks lie in an apparent synclinal keel.

Laminated mudstone with micrograded sequences, characteristic of the Tillery, is the dominant rock type exposed in the quarry. Lamination typically is on a scale of a few millimeters, and involves alternation of medium gray and darker gray layers that vary slightly in the size and amount of fine silt particles. The laminations do not impart a fissility to the mudstone. Both thick and thin nonlaminated beds also are present, some containing several percent calcite. In a few places, syndepositional volcanic activity is recorded by conformable

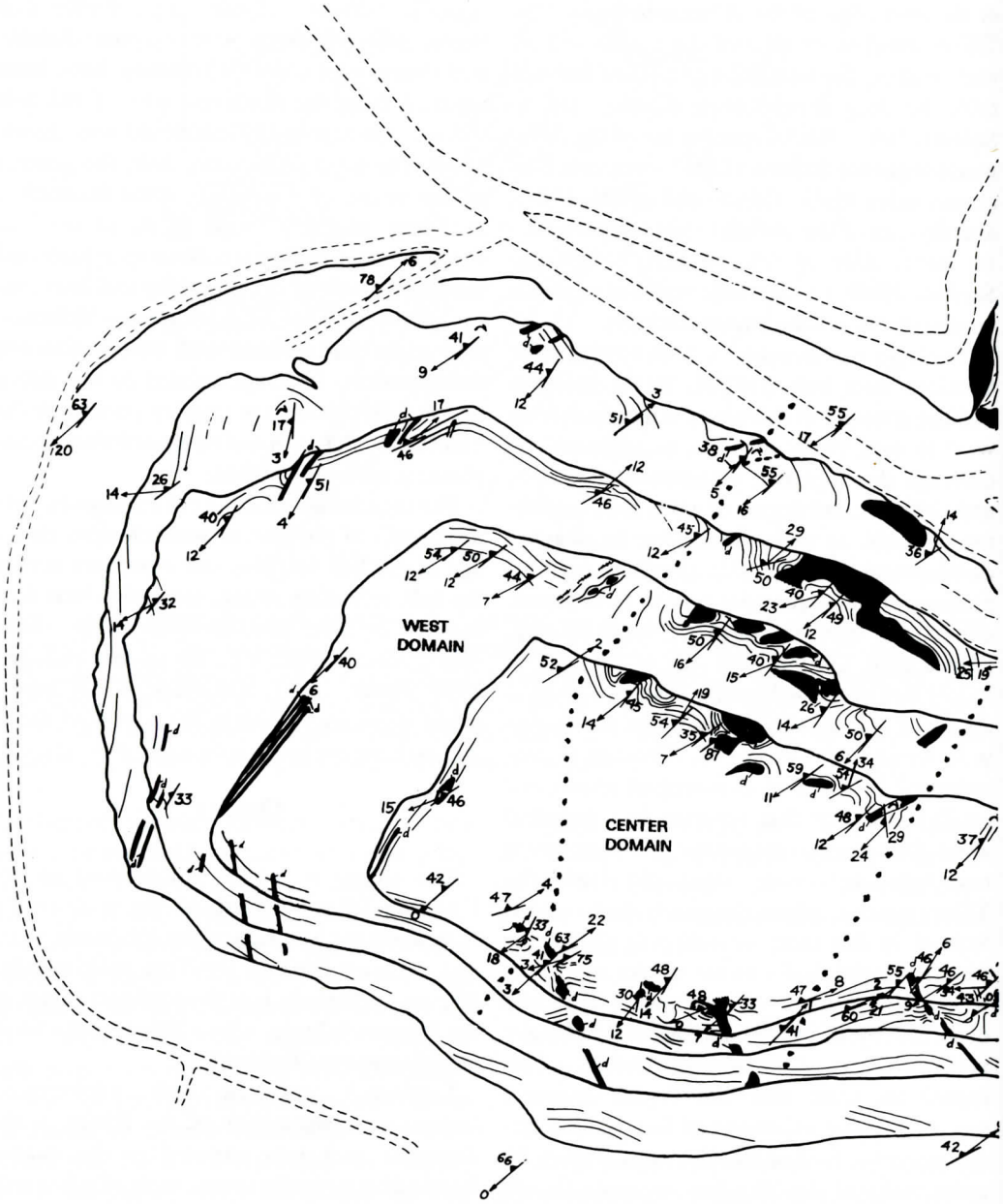
WEST
DOMAIN
CENTER
DOMAIN

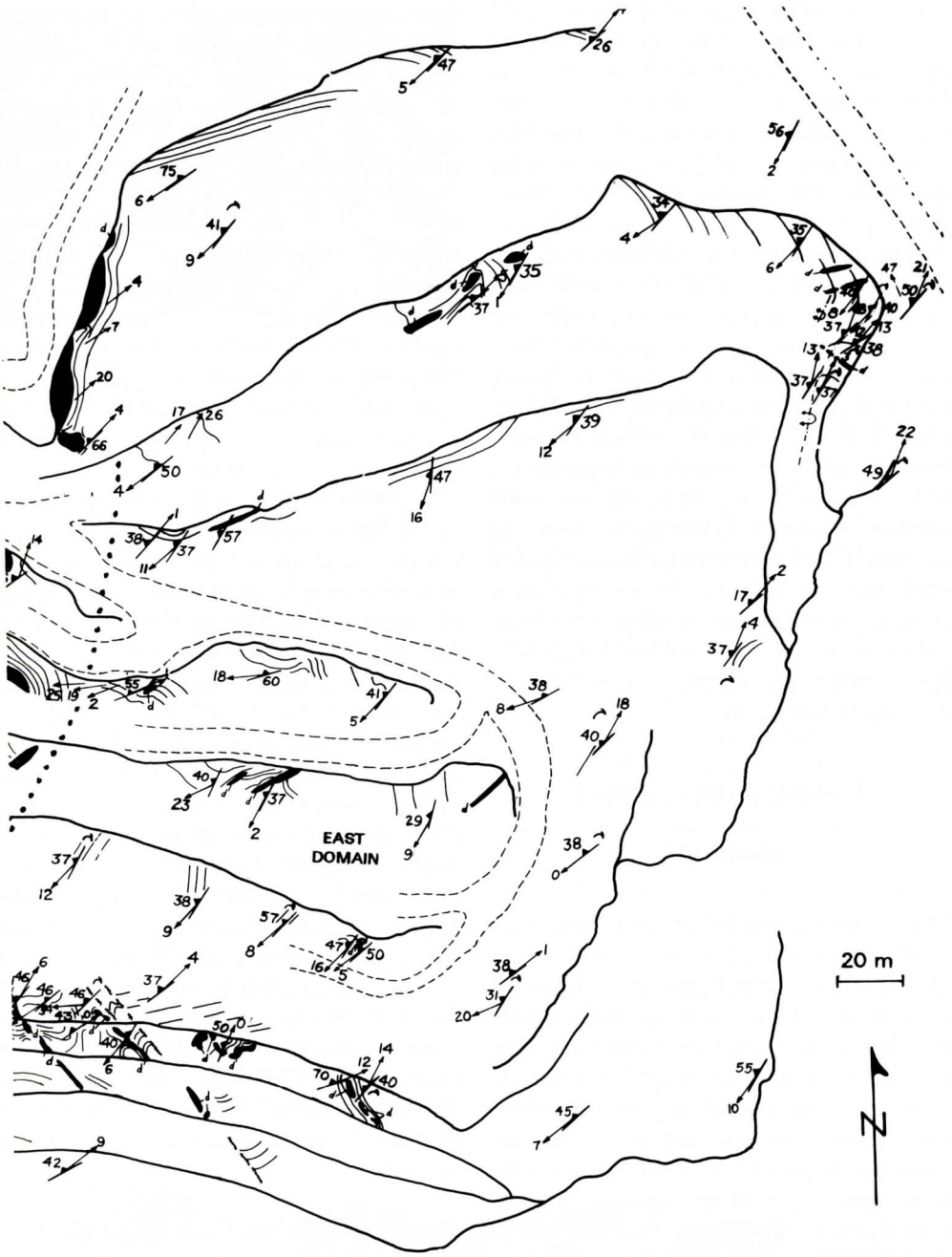

Figure 2. Schematic map of selected geologic features of quarry. Sketches of beds and dikes seen on the 6 vertical faces of the quarry are shown as plan views located at the base of each face. Structure domain boundaries, coarse dotted lines. Bed edges, light lines; dikes, d and shaded; strike and dip of axial-plane cleavage, line with filled triangle; bearing and plunge of bed-cleavage intersection lineations, arrow; shear surface, dashed wavy line; overturned fold, standard symbol; overturned beds, curved arrow. Note halves of map overlap in center.

light-gray felsic ash layers up to 15 cm thick.

A possible source of the ash is a volcanic ring complex centered about 3.5 km west of the quarry, marked by felsic lava domes, flows, necks, and dikes, with associated metagabbro bodies (Seiders, 1981). Flows and tuffs are interlayered with mudstones of the Tillery, indicating that volcanism was concurrent with sediment deposition. The volcanic center also is the suspected source of the several felsic dikes that played an important role in partitioning the deformation of the quarry rocks. Those dikes are subalkaline (Koeppen, in press), sparsely phyric metarhyolites and metadacites, similar to many rocks of the volcanic complex. Most of the dikes are approximately perpendicular to bedding in the enclosing mudstone; assuming original horizontality of beds, the dikes would have been intruded as near-vertical bodies. Because the dikes commonly contain microspherulites, indicators of quenching and crystallization at or very near the surface, it is inferred that dike intrusion occurred even before significant burial.

QUARRY STRUCTURES

General

The quarry consists of four levels in the main pit and two levels in the upper pit on the northeast side (Figure 2). In Figure 2, the structural sketch of the vertical working face of each bench has been rotated into plan view. The north and south walls are roughly perpendicular to strike and present approximately true cross sections; the east and west walls are approximately parallel to strike. Quarry walls display numerous small structural domains that are separated by faults or by shears developed along the contacts with dikes (Figure 2). Tightness of folds generally increases with proximity to these features, and disharmonic folding and structural discontinuities are characteristic features. Locally, nonfolded layers are flanked by folded layers in the face above or below, across detachments on bedding or cross-cutting shear surfaces. Some subdomains feature gentle folds of the mudstone; others have open to close folds (even tight, near isoclinal in rare instances) on scales from centimeters to tens of meters. Folds show various forms. Most common are folds with thickened hinges and thinned limbs (Class 3 of Ramsay, 1967). All folds are asymmetric to overturned southeastward, with northwest-dipping axial-planar cleavage. Overturning is not extreme: most overturned beds dip 61°-85° northwest. Typical asymmetric anticlines have thinned southeast limbs, but in zones with numerous faults or shear zones strongly asymmetric anticlines may have both limbs markedly thinned or their southeast limbs sheared out.

Northwest-dipping, penetrative cleavage is clearly visible in most of the quarry rocks, and it is present at microscopic scale in all of the rocks examined in thin section. As throughout the slate belt, the cleavage varies in morphology from planar, continuous type to rough or anastomosing, spaced type. The most typical form seen in the quarry rocks probably is slightly anastomosing. Apparent offsets of mudstone laminae of 0.05-0.20 cm along cleavage surfaces are common, and offsets up to 0.5 cm have been observed. In thin section, despite the jagged profiles of offset laminae or disharmonic microfolds with ragged crests (Figure 3), minute details of sedimentary fabric such as alternating thin laminae and micrograding within individual laminae are preserved. Only one cleavage is readily observable in the mudstone, but close inspection in a very few places beside dikes shows S-C shear fabric (Berthe and others, 1979); the intersection of the S and C surfaces makes a shallowly plunging lineation.

Relations of Folds, Cleavage, and Dikes

For purposes of description, the quarry has been divided into three domains on the basis of details of structural style (Figure 2); each has internal discontinuities that separate the smaller subdomains mentioned above.

In the west domain, gentle folds predomi-

Figure 3. Photomicrograph of mudstone showing folds of laminae and pressure shadows on axial-planar cleavage. Black grains are pyrite. Field of view 5 mm across.

nate, but cleavage dips change from steep at the west end of exposures to moderate and gentle across the remainder of the domain. Overturned beds, marked in Figure 2, occur just west of two zones of thin rhyolite dikes, interrupting the 140-m extent of otherwise gentle folds. Some dikes are loci of shear and local warping of beds in the adjacent mudstone, but along other dikes no shear or disruption of bedding is observed. Near the east border of the domain, the effect of dike presence is seen where a narrow shear zone separates gentle folds to the west from steeply dipping beds warped around two boudins of a sill-like rhyolite body. Most of the rhyolite dikes do not have easily discernible mesoscopic cleavage, but some in a group of five thin dikes (only three shown on Figure 2) on the second bench face at the west end are mildly to intensely sheared and display prominent biotitic cleavage. In the most conspicuously sheared of these dikes, the geometry of S-C fabric and of pressure shadows around biotite porphyroblasts indicates northwest-over-southeast dip-slip shear. Despite the obvious concentration of shear fabric in this dike, disruption of the adjacent mudstone is minor.

The central domain is dominated by the presence and structural effects of a large tabular rhyolite body that is variably discordant and concordant with respect to bedding in the enclosing mudstone (Figure 2). At its north end (in the topmost working face) this rhyolite basically is sill-like, stretched into three mostly concordant boudins. The lenticular pod at the south end of these boudins crosscuts beds, has flow banding parallel to its steep sides, and appears to be a feeder dike. Below, in the main pit, the rhyolite occurs in both a warped tabular body and disconnected pods resembling boudins (Figures 2 and 4). Relations of the pieces indicate an original body with two tabular tongues subjected to folding and boudinage. The boudins were rotated, with shear along the dike contacts and tight folding of adjacent mudstone at places. Where shear was localized between the dike pods, the mudstone cleavage tends to be subphyllitic to phyllitic. Along the west side of the easternmost rhyolite pod on level two (Figure 4), bedding and cleavage have been rotated into parallelism. On the east side of this pod, cleavage was warped around the rhyolite and into the neck between two incompletely separated boudins, indicating a buttress effect of the dike pods as cleavage formed, probably combined with additional boudinage during the folding and cleavage formation.

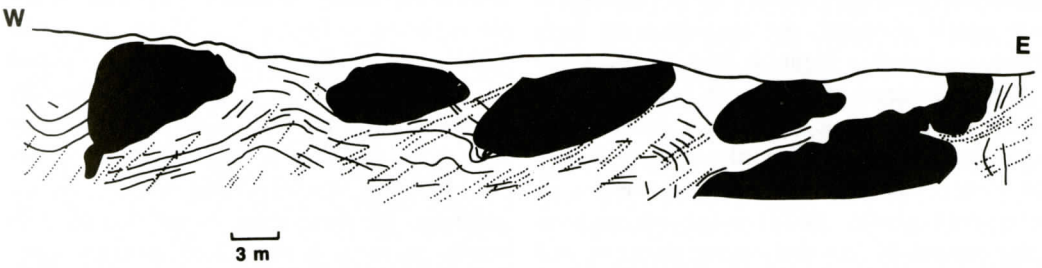

Figure 4. Sketch of boudinaged dike, middle bench, north wall of south pit. Bed edges, solid lines; cleavage, dotted lines; dikes, shaded.

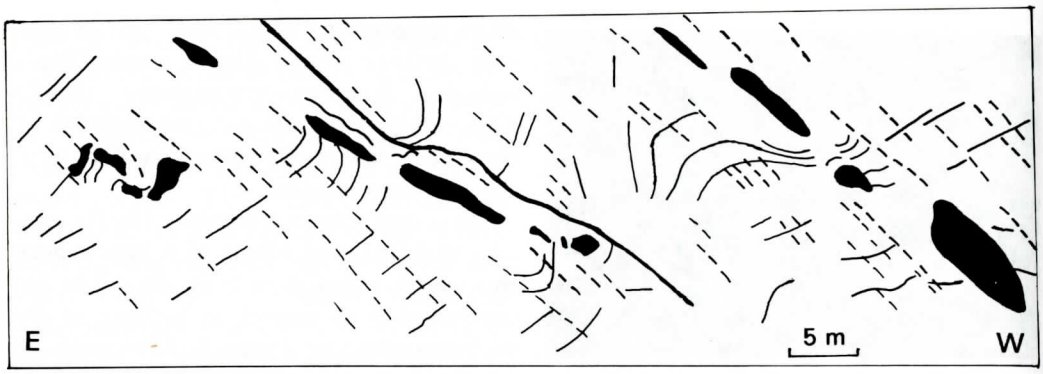

Figure 5. Tracing of photomosaic, showing structure and boudinaged dikes, south wall of south pit, east domain. Bed edges, thin solid lines; cleavage, dashed lines; dikes, shaded; shear surface, thick solid line.

The eastern domain (Figure 2) contains gentle to open folds in its western part; folds in the eastern part commonly are tighter and overturned eastward, especially in the vicinity of dikes and small shear zones. The eastern domain displays much greater variation (up to 60 degrees) in trends of bed-cleavage intersection lineations than the other domains. Some of this variation is related to changes in cleavage attitudes across zones of dikes and shears, and is inferred to result from post-cleavage rotations during shear late in the deformation event. The style of structure in the eastern domain is open folds with limbs thinned, cleavage of moderate westward dip, and tabular dikes stretched in boudins both along cleavage and at slight angles to cleavage, as shown in Figure 5. The east vergence of folds, the northwest dip of cleavage, and the en echelon dike boudin geometry indicate dominantly northwest-over-southeast rotation and shear.

Despite the shear and local dislocations along some dikes during deformation, stereograms and tabulated data for the three domains are nearly identical; the measurements have been combined in Figure 6. Bed data give reasonably coherent girdles, with beta-axes in a fairly tight grouping. Cleavage is similar in all domains; dips are all northwest and mostly moderate, with only a very few near vertical or extremely gentle. Bed-cleavage intersections also are nearly identical among domains, and indicate a pattern of folding with gentle plunges dominantly southwest but with some northeast plunges. We infer that both the folding and most of the late rotations of structures occurred on similar, shallowly plunging axes.

The many dikes in the quarry, in their own deformation and in their relations to folds and cleavage, provide a gauge of the variability of the deformation across small distances. Some dikes provided mechanical loci for sharp breaks in structural style and intensity. Most of the thin, tabular dikes are either parallel to cleavage in the surrounding mudstones, or within a few degrees of parallel. Many of these dikes display boudinage, with the boudins connected by a train of vein quartz. Separation of dike boudins ranges from boudins just touching to gaps of about 5 m. A single dike may display this range; some dikes are much more deformed than others. Where folds are least well developed and of low amplitude, as in the west end of the main pit, dikes display only minor boudinage and the boudins are barely separated. In contrast, the stretching in dikes along cleavage on axial planes of individual folds is especially noticeable. One such example is shown in Figure 7, a 25-cm thick dike with classic boudinage. The boudins are pulled out in blunt tails, in a geometry indicating northwest-over-southeast shear along the fold axial plane this dike occupies. Extension during boudinage was 60 percent or more. In rare instances, the shear sense manifested by dike boudin geometry is ambiguous, perhaps opposite to the northwest-over-southeast shear sense recorded generally throughout the quarry.

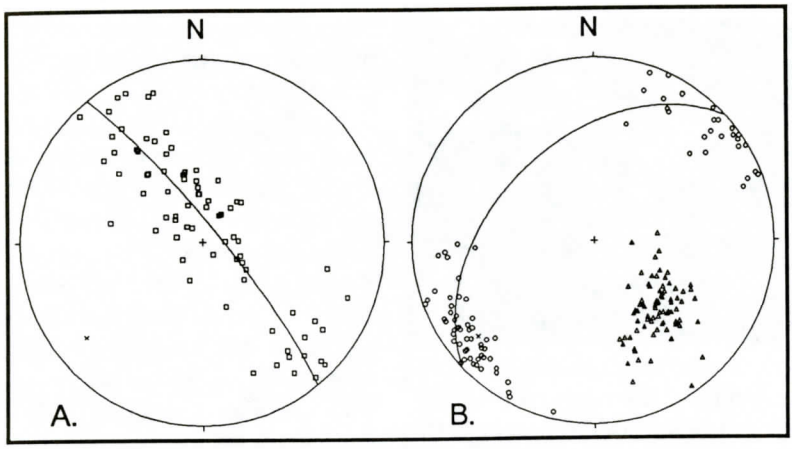

DOMAIN	BETA (n)	CLEAVAGE (n)	BED-CLV LIN (n)
West	S45°W10° (25)	N47°E44°NW (23)	S51°W6° (24)
Center	S54°W10° (22)	N47°E45°NW (26)	S51°W6° (24)
East	S52°W3° (30)	N47°E44°NW (32)	S54°W6° (35)

Figure 6. Stereograms for combined west, central, and east domains. A. Bedding plot: Squares, poles to bedding; solid line, best-fit girdle; x, beta axis. B. Cleavage plot: triangles, poles to cleavage; solid line, mean cleavage plane; circles, bed-cleavage intersection lineations; x, beta-axis. Statistical means, best-fit data, and number of measurements shown for the separate domains in table below stereograms.

Figure 7. Boudinaged dike near northeast corner of quarry. Prominent cleavage dips to left (northwest), generally parallel to dike in axial zone of fold. Face is about 9m high.

Observations in the quarry reveal only one generation of folds and cleavage. The cleavage is axial planar to folds at all scales (Figures 2, 3 and 8), indicating its relation to the folding event. Shear, dominantly northwest-over-southeast, was clearly a part of the deformation event. That rotational sense for the pervasive deformation is indicated in folds asymmetric or overturned to the southeast, and in shear fabrics developed on the axial-planar cleavage in mudstone and in similarly oriented cleavage in dikes. Metamorphic biotite growth on the cleavage in mudstone, and in a shear fabric in one dike (parallel to surrounding cleavage) evidently was part of the deformation. This is discussed in detail below.

MICA GROWTH IN RELATION TO CLEAVAGE

The linkage of the low-greenschist facies metamorphism and the penetrative deformation in the Carolina slate belt has been tacitly assumed in prior work (e.g., Noel and others, 1988). Potassium-argon dating of eight whole-rock samples from the Albemarle sequence containing white mica gave an average age of 483±15 Ma, interpreted as the time of cooling through white-mica argon-retention temperature after the metamorphic event (Kish and others, 1979). More recently, $^{40}Ar/^{39}Ar$ age spectra for two whole-rock samples of Tillery Formation collected about 45 km south of the Asheboro quarry were interpreted to indicate a minimum age of metamorphism of about 455

Figure 8. Photomicrograph of mudstone showing disharmonic folding of laminae, strong cleavage development, and strain shadows around biotite grains. Large biotite grains (1) are overgrowths and show ghost laminae; other biotite grains (2) are aligned (grown) on cleavage, separated by muscovite and quartz grown in strain shadows. Field of view 7 mm across.

Ma (Noel and others, 1988). These samples exhibited cleavage and much fine-grained white mica, but the whole-rock age could not directly be assigned to white mica that had grown on the cleavage because of the potential argon contributions of other mineral phases in the samples, and because some of white mica in the samples could have been of detrital or diagenetic origin. As discussed above, Asheboro quarry rocks provide evidence that the folds, faults, and cleavage are related and formed in a single event, associated with growth of metamorphic minerals like biotite and white mica, suitable for $^{40}Ar/^{39}Ar$ dating.

In the quarry mudstone, the prominent spaced cleavage, developed at grain scale, is marked by aligned fine-grained chlorite and white mica. The white mica generally is too fine grained to be separated for mineral age determination. Coarser-grained biotite is common in some parts of the mudstone. It occurs as scattered, megascopically visible (0.1-1.0 mm) porphyroblastic grains in the mudstone. There is no evidence for detrital or diagenetic biotite; most biotite grains show no relation to bedding, but some grains clearly overgrew laminae and are products of metamorphism. A good example is seen in Figure 8, where a large biotite grain displays ghost outlines of mildly warped mudstone laminae, and also shows that biotite growth was constrained at both ends by cleavage surfaces. That grain and most other biotite grains are associated with well-developed strain shadows parallel to cleavage. Figure 8 also shows biotite that formed on cleavage. The largest example involves three differently oriented grains separated by strain-shadow areas of quartz and white mica. Nearly all biotite grains observed had characteristics like these that indicate crystallization during (apparently late in) the deformation associated with cleavage formation. Rare examples of inclusion-free, sharp-edged biotite grains were found that warped cleavage and grew without strain shadows, suggesting that some biotite grew statically after deformation but before metamorphic temperatures had dissipated below the stability field of biotite.

Most of the felsic dikes do not have cleavage visible at mesoscopic scale. Except for three dikes at the west end of the quarry, they do not contain biotite and the chlorite formed in metamorphism occurs in ragged clumps and individual grains without conspicuous alignment. Where cleavage occurs, whether weakly or strongly developed, chlorite is aligned in single wavy surfaces and in zones of anastomosing surfaces. One of the dikes on the north wall of the main pit (central domain) shows little mesoscopic cleavage, but has fractures on which pyrite grew and was smeared out in subsequent shear on the fracture surfaces. In thin section, however, a faint cleavage is marked by aligned, very finely crystalline chlorite and minor paragonitic white mica. The paragonitic mica has very low potassium content and too little argon for dating. Very sparse porphyroblasts of white mica up to 1.0 mm across (Figure 9) crosscut the cleavage in a few places. They are clearly younger than the cleavage; some are internally strained, indicating that conditions for white mica growth occurred later than main cleavage formation, but while deformation was still occurring. These white mica porphyroblasts were sampled and dated. Adularia also was identified but was rare in occurrence, and material sufficient for dating

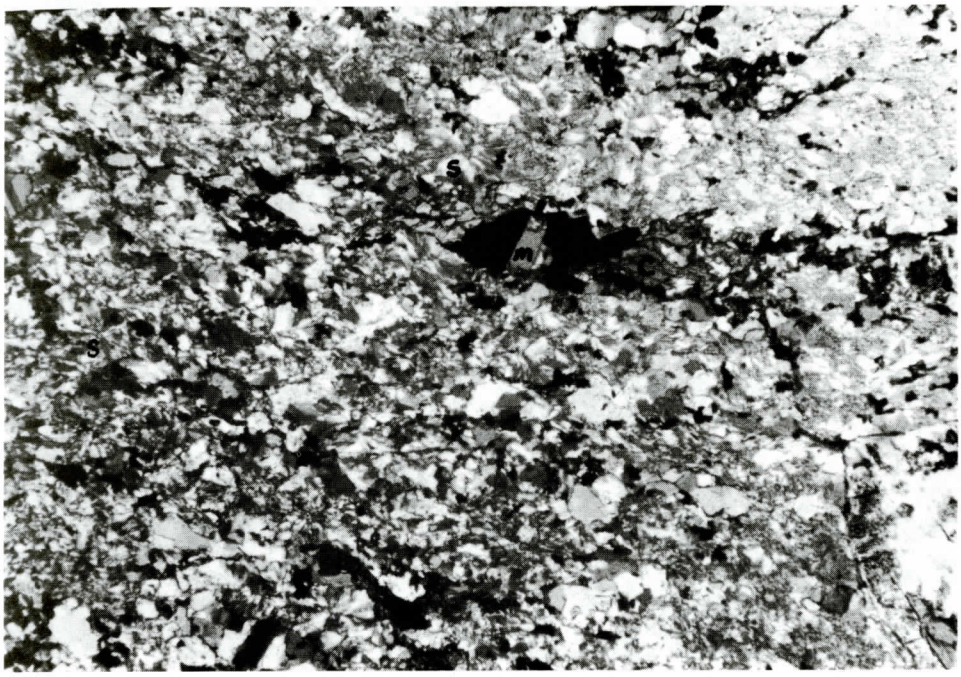

Figure 9. Photomicrograph of rhyolite dike (sample 88-11-15D), showing elongate pyrite (black) and calcite (c) grains grown along cleavage and euhedral muscovite (m) crystal grown still later across the pyrite grain. Radial texture marks spherulites (s). Field of view 5 mm across.

could not be collected.

Two of the biotite samples used for age determination come from different parts of the only dike to display a significant amount of biotite. That rhyodacite dike, one of the group of five sheared dikes at the west end of the quarry, is anomalous in comparison to the other felsic rocks of the quarry and surrounding area. Biotite is the principal potassic phase in the rock. One of the dated samples, from near one side of the dike, contains 5-10 percent finely crystalline biotite in clumps with some internal alignment of biotite grains and in individual grains defining a weakly developed cleavage. As in the mudstone, a few grains of biotite are not aligned with cleavage. They are larger and fresher looking than the biotite on cleavage, and do not have strain shadows. The presence of these biotites provides an additional indication that peak metamorphic temperatures persisted after the period of cleavage formation. Because biotite is not known to form below its closure temperature for argon diffusion, $^{40}Ar/^{39}Ar$ results of the biotite should provide a reliable indication of the minimum age of cleavage formation.

The other dated sample is from near the middle of that dike. It is from a strongly sheared zone that contains about 30 percent biotite, enough to make the dike brown rather than the usual gray to greenish gray. The fabric is characterized by bands of granulated quartz and feldspar with considerable calcite, alternating with bands consisting of biotite anastomosing around oval or round eyes of intensely saussuritized feldspar and calcite. The eyes have mesoscopic pressure-shadow tails and rotated orientations indicating west-over-east shear sense. The biotite is dominantly aligned to form cleavage or foliation (Figure 10) that is parallel to the sides of the tabular dike (C of an S-C shear fabric), and is very fine grained, probably due to comminution during the extreme shearing of the dike. Figure 10 also shows generally coarser grained biotite aligned on surfaces (S) oriented about 30 degrees to the

Figure 10. Photomicrograph of argon-dated rhyolite/rhyodacite dike (sample 88-11-15F) with unusual abundance of biotite marking S-C shear fabric (C surfaces trend horizontally across picture; S surfaces trend upward to right). Field of view 7 mm across.

main cleavage. Transition between the less foliated and the very sheared portions of the dike is gradual, through a zone in which biotite appears in increasing numbers of irregular planar clots marking ever better defined cleavage. It is clear that shearing and biotite-grade metamorphism were synchronous.

AGE DETERMINATION

Results

Three 125-150μm biotite samples, one from mudstone and two from the rhyodacite dike, and a white-mica porphyroblast from a rhyolite dike were analyzed by the $^{40}Ar/^{39}Ar$ age spectrum dating technique described in the Appendix. The argon isotopic data are presented in Table 1 and Figures 11 and 12.

The results from all three biotite samples are very similar; they exhibit a small disturbance in the low-temperature portions of the age spectra followed by an age plateau (Snee and others, 1988) containing 54 to 91 percent of the ^{39}Ar released. Samples 88-11-15A and 15F show slight age decreases in the highest temperature steps (the low age of the 1000°C step of sample 15E is due to electronic problems during the isotopic analysis). No age significance is attached to the low apparent ages of the low-temperature steps. This disturbance in the age spectra may be due to the presence of impurities in the samples, slight alteration of the biotites, or a later thermal event. As the low-temperature ages are not consistent between samples, a later thermal event is unlikely. The more likely cause is slight alteration of the biotites, although no evidence of this is observable in thin-section, or the presence of inclusions or impurities. The apparent K/Cl ratios of the low-temperature steps may be interpreted to represent the degassing of fluid or solid inclusions. No chlorine-derived argon was detectable in the plateau portions of the age spectra, which suggests that the source of the

Table 1. $^{40}Ar/^{39}Ar$ Analytical Data for Biotite and White Mica Samples 88-11-15A (mudstone), 88-11-15E (near side of dike), 88-11-15F (sheared dike), and 88-11-15D (rhyolite dike).

T °C	$^{40}Ar_R/^{39}Ar_K$ *	Apparent* * K/Cl	Percent ^{39}Ar	Radiogenic Yield (%)	$^{39}Ar_K$ (10-13 moles)	Apparent Age*** (Ma) and error
			88-11-15A Biotite			
J = 0.009320 ± 0.5%					Sample wt. = 0.0264g	
675	24.858	302	4.1	99.1	1.69	375.91 ± 1.34
750	30.524	.30	20.6	99.1	8.50	451.64 ± 0.30
825	30.454	****	21.6	99.5	8.92	450.73 ± 0.35
900	30.588	****	14.6	99.4	6.03	452.49 ± 0.82
1000	30.836	****	25.0	99.6	10.35	455.73 ± 0.35
1075	30.816	****	12.7	99.5	5.24	455.46 ± 0.38
1150	28.618	523	1.5	99.2	0.63	426.52 ± 4.48
					Total Gas Age =	450
			Plateau Age (54% of $^{39}Ar_K$ in 900°-1075°C steps) =			455.2 ± 2.3
			88-11-15E Biotite			
J = 0.009765 ± 0.5%					Sample wt. = 0.0997g	
650	27.277	2059	5.1	96.5	10.19	426.01 ± 0.46
750	29.376	****	26.5	99.9	53.32	454.98 ± 0.63
850	29.412	****	17.9	99.9	36.07	455.46 ± 1.23
950	29.414	****	23.0	99.4	46.26	455.48 ± 1.42
1000	29.128	****	17.1	99.9	34.49	451.58 ± 0.73
1050	29.566	13178	8.8	98.0	17.62	457.57 ± 0.31
1100	29.454	7258	1.6	98.5	3.21	456.04 ± 0.34
					Total Gas Age =	453
			Plateau Age (67% of $^{39}Ar_K$ in 750°-950°C steps) =			455.1 ± 2.3
			88-11-15F Biotite			
J = 0.009780 ± 0.5%					Sample wt. = 0.1000g	
675	23.351	38	2.6	97.3	4.87	371.07 ± 1.49
750	29.139	1862	5.8	99.5	10.95	452.35 ± 0.65
825	29.388	****	14.4	100.0	27.15	455.76 ± 1.38
900	29.443	****	16.8	99.8	31.74	456.51 ± 0.48
1000	29.432	****	20.7	100.0	39.10	456.36 ± 1.48
1100	29.566	****	33.5	100.0	63.32	458.20 ± 1.65
1175	29.489	****	5.4	99.4	10.22	457.14 ± 0.84
1250	29.087	1802	0.9	97.4	1.634	451.63 ± 2.10
					Total Gas Age =	454
			Plateau Age (90.7% of $^{39}Ar_K$ in 825°-1175°C) =			456.7 ± 2.3
			88-11-15D White Mica			
J = 0.009991 ± 0.25%					Sample wt. = 0.0109g	
950	27.913	1571	9.9	95.8	0.3404	443.75 ± 0.58
1000	27.948	33281	24.2	98.0	0.8333	444.25 ± 0.54
1030	27.820	2323	6.9	95.2	0.2385	442.44 ± 1.08
1060	27.864	2356	6.8	94.8	0.2333	443.06 ± 0.97
1090	27.973	2123	7.0	95.0	0.2407	444.60 ± 0.59
1120	27.957	1374	7.8	95.5	0.2696	444.37 ± 0.87
1150	28.253	22010	13.4	97.4	0.4604	448.54 ± 0.41
1180	28.341	3342	16.2	97.8	0.5603	449.78 ± 0.35
1210	28.453	2575	7.9	95.9	0.2717	451.35 ± 0.76
					Total Gas Age =	446
			Plateau age (62.5% of $^{39}Ar_K$ In 950°-1120°C) =			443.98 ± 1.39

* $^{40}Ar/^{39}Ar$ ratios represent radiogenic ^{40}Ar and potassium-derived ^{39}Ar after corrections for mass discrimination, the presence of atmospheric argon, and the production of interfering argon isotopes during neutron irradiation (Haugerud and Kunk, 1988; McDougall and Harrison, 1988; and Dalrymple and others, 1981). Argon blanks for biotite samples were in the 10^{-15} mole size range, were atmospheric in composition, and were not subtracted.

**Calculated as described in ArAr* (Haugerud and Kunk, 1988) from measured isotopic ratios.

***The analytical uncertainty of the age of individual temperature steps (1SD) is calculated from standard statistical methods on five sets of argon peak values measured over an interval of about 10 minutes by the method described in Haugerud and Kunk (1988). No error is calculated for the total gas ages. The uncertainty of the plateau age includes a 1SD uncertainty on the irradiation parameter J as described in Haugerud and Kunk (1988).

****Chlorine-derived ^{38}Ar was below the detection limit of the mass spectrometer (10^{-16} moles).

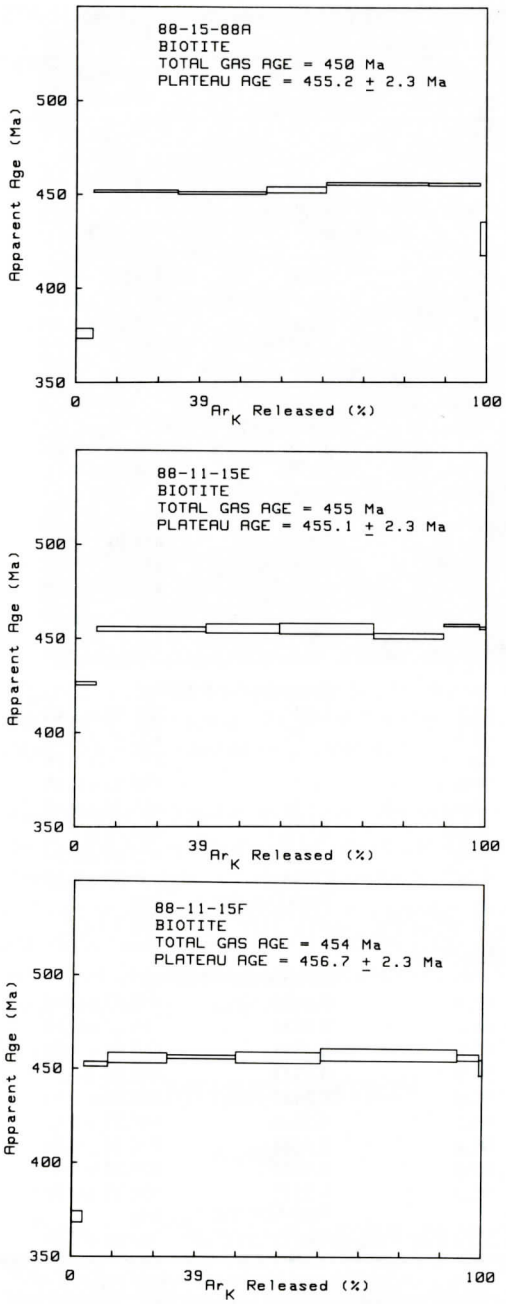

Figure 11. $^{40}Ar/^{39}Ar$ age spectra of biotite samples: 88-11-15A, mudstone; 88-11-15E, near side of biotitic rhyolite dike; 88-11-15F, biotite-rich, strongly sheared zone of rhyolite dike.

low age gas was depleted in that portion of the spectra.

The plateaux of the three biotite age spectra range from 456.7±2.3 Ma to 455.1±2.3 Ma and clearly are not statistically different from one another (error is one standard deviation of the mean and includes uncertainty in the irradiation parameter J). The highest temperature release steps of samples 15A and 15F are somewhat lower in apparent age than the plateau because of either a proportionally larger contamination of the gas by system blank at elevated temperatures, or the presence of impurities or alteration products within the analyzed samples. As with the low-temperature steps, comparison of K/Cl ratios of the high-temperature steps and the plateau steps again suggests that effects of impurities or alteration may be the cause of the low apparent ages.

The white-mica porphyroblast sample from a rhyolite dike also was analyzed using $^{40}Ar/^{39}Ar$ age spectrum dating techniques. The argon isotopic data for this sample (15D) are presented in Table 1 and Figure 12. Although this sample has a plateau age of 444±1 Ma containing 63 percent of the ^{39}Ar released, the age spectrum is slightly sigmoidal in shape and climbs in age in the upper three temperature steps (37 percent of the ^{39}Ar released) to a maximum age of 451 Ma. Calcium-derived ^{37}Ar was not detected in any of the temperature steps in the age spectrum, but small amounts of reactor-produced chlorine-derived ^{38}Ar were observed. K/Cl ratios of the individual steps of the age spectrum are not uniform. There are two K/Cl

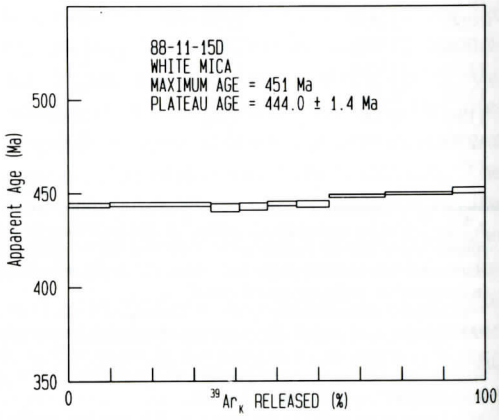

Figure 12. $^{40}Ar/^{39}Ar$ age spectrum of white-mica porphyroblast sample 88-11-15D from rhyolite dike.

spikes in the age spectrum data, at 1000°C and 1150°C. Both spikes are preceded by values that are slightly lower than those for steps after the spikes The first spike in K/Cl is in the second step, on the plateau portion of the age spectrum. The second K/Cl spike is in the first temperature step that climbs in age off of the plateau portion of the age spectrum. These variations in the K/Cl ratios probably reflect variations in chemical composition of the white mica associated with its crystallization history.

Interpretation

The mean of the three biotite plateau ages, 456±2 Ma, is interpreted as the time that the biotites cooled through their argon-retention temperature as metamorphic temperatures declined from their peak. It is possible that the biotites could contain unrecognized extraneous argon, but our results are virtually identical to those of Noel and others (1988) for whole-rock dating of similar samples of mudstone.

For a constant diffusion domain size, the closure temperature of biotite for argon diffusion is a function of cooling rate and composition. The closure temperature of annite-phlogopite solid-solution series for argon diffusion has been reported to be compositionally controlled, and dependent on the annite content of the mica (Giletti, 1974; Harrison and others, 1985; McDougal and Harrison, 1988). Closure temperature in the phlogopite-annite solid solution is inversely proportional to the annite molar content of the mica. Biotites 15A and 15F are Ann63 and Ann42, respectively, and have plateau ages that are the same within the limits of analytical precision. Assuming that the biotites do not contain extraneous argon, the occurrence of significantly different annite contents from samples that have had the same thermal history, and have virtually identical apparent ages, argues for fairly rapid cooling through their respective closure temperatures for argon diffusion. Model calculations of the closure temperature (Dodson, 1973) of samples 15A and 15F (assuming D_0=0.077 cm^2/sec., a=75 μm, and E=45 and 50 kcal/mole respectively; Harrison and others, 1985) suggests that they should differ by about 60°C in closure temperature for cooling rates of 1°C- 100°C/Ma. Using the difference in calculated closure temperatures together with the $^{40}Ar/^{39}Ar$ plateau age data, a cooling rate of about 10°C/Ma or higher is calculated. This suggestion is further supported by the agreement in age between our cleavage biotite samples (456±2 Ma) and the whole-rock $^{40}Ar/^{39}Ar$ ages (455 Ma) from samples taken 45 km to the south (Noel and others, 1988). The primary potassic phase in their samples is white mica that grew during cleavage formation. Although the closure temperatures of white micas is not well constrained, they are generally reported to have higher closure temperature than for biotites, assuming the same cooling rate. Again, a fairly rapid cooling rate would account for the similarity in age of these two very different types of samples.

The white-mica age spectrum results of sample 88-11-15D are somewhat more complex. The sample has a plateau age of 444±1 Ma, some 12 million years younger than the mean of the biotite results. Several other factors that are also important to the interpretation of these data are: 1) The white mica did not grow as part of the cleavage, but as porphyroblasts across the cleavage sometime after the formation of cleavage. 2) It is not uncommon for white mica to grow below its closure temperature for argon diffusion (McDougal and Harrison, 1988). 3) The high-temperature portion of the age spectrum increases in age to a maximum of 451 Ma, a value that is similar to our biotite age spectrum results, and the overall age spectrum is somewhat sigmoidal in shape.

Because the white-mica porphyroblasts clearly grew after the cleavage, the age of this white mica need not be related to the time of cleavage formation. It is possible from petrographic observations to say that some of the white mica is strained, but the timing of that strain is not constrained; it could relate to the minor post-cleavage shear and rotations, mentioned earlier, that occurred late in the end deformation.

An $^{40}Ar/^{39}Ar$ age spectrum for a single gen-

eration of white mica grown below its closure temperature presumably would be fairly flat. This is not the behavior seen for our sample of white mica. Instead, we have a spectrum that is flat over the first 63 percent of its argon release and then climbs in the last 37 percent to an age 7 million years older than the age plateau. Similar patterns have been seen in samples that contain more than one generation of white mica, the younger of which grew below argon closure temperatures in white mica. In cleaved rocks of the Martinsburg Formation, Wintsch and Kunk (1992) and Wintsch and others (in press) described rocks that contained three separate populations of white micas: detrital muscovite, authigenic phengite, and phengite on cleavage. $^{40}Ar/^{39}Ar$ spectra of their samples displayed a marked sigmoidal pattern with climbing ages in the low-temperature portions, followed by a nearly flat, plateau-like segment at intermediate temperatures, and climbing ages in the high-temperature portions. Their study of the Martinsburg samples suggests that the rocks contained two generations of white mica that grew below closure temperature and a detrital white mica, the age of which was not reset under the conditions of the later white-mica growth. Among their conclusions, they suggested that the nearly flat intermediate-temperature-of-release portion of the spectrum was simply a product of mixing of white-mica populations and did not have any geologic meaning. They also noted that the high release-temperature climb in the age spectrum was also a problem of mixing populations, and that the maximum age in their results represented a minimum age of the detrital component.

Our white mica-bearing sample differs from those of Wintsch and Kunk (1992) and Wintsch and others (in press) in several ways: It is an igneous rock with no mica that is older than the cleavage; the first, or cleavage generation of white mica is soda-rich paragonite with insufficient K to affect the argon age; and our age spectrum does not have a strong increase in age with increasing temperature of release in the low-temperature portion of the age spectrum. However, several similarities do exist. Our white-mica age spectrum is slightly sigmoidal, and the high release temperature portion of the age spectrum is marked by strongly climbing apparent ages that approach, but do not reach, those of the biotite samples. In addition, the variation in apparent K/Cl ratio in our white-mica age spectrum probably represents variations in its chemical composition that correspond to changes of physical environment during post-cleavage white-mica growth. If this is the case, the apparent plateau age of the white mica represents a mixed age and has no geologic meaning. If there were more than one time of porphyroblastic mica growth, the mixed age would involve a range of components from the earliest mica growth to the most recent growth, but we have no relevant information on this, other than a presumed tie, at the upper end, with the time of biotite growth.

A second possible interpretation of the difference in apparent plateau ages of the white mica and biotite, is the inclusion of extraneous argon in the biotite samples and that part of the white mica subject to argon release at high temperature. The presence of extraneous argon is not usually resolvable in biotite age spectra, but its effect would be to make the plateau age older than it should be. If extraneous argon is present in the only the upper temperature steps of the white mica, the plateau age would represent the minimum age for mica growth that accompanied cleavage formation. Arguments against this interpretation are: 1) The biotite plateau ages from two different lithologies are the same. If extraneous argon were present, variation in the apparent ages would be expected. 2) It would be unlikely for $^{40}Ar/^{39}Ar$ results from the whole-rock samples of Noel and others (1988), a third lithology from 45 km to south, to agree so well with the ages of our biotite samples.

In either case, the interpretation from a geological perspective is much the same. Cleavage in the Tillery Formation at the quarry is the product of a Late Ordovician metamorphic and structural event. If the biotite samples do not contain extraneous argon, they cooled rapidly from peak metamorphic conditions that accom-

panied cleavage formation through their closure temperatures at 456±2 Ma. If extraneous argon is present in the samples, the white-mica results suggest that the cleavage formed prior to 444±1 Ma. The fact that the white-mica results contain an age component (451 Ma) that is close to the biotite age (456±2 Ma) suggests that the latter age is close to the true age of mica growth and cleavage formation. It is possible that the 444±1 Ma age of the strained, post-cleavage white mica provides some indication of the duration of the tectonic event; however, based on the limited nature of the data that we present, this conclusion is quite speculative and can not meaningfully be expanded.

DISCUSSION

The Asheboro quarry shows structures (folds, shears, minor faults) that are consistently east vergent and associated with the formation of northwest-dipping cleavage axial-planar to the folds. Structural style across the quarry and most the slate belt varies; folds in one zone are gentle, and in another, tight and overturned. At the quarry scale, however, similarity of structural geometry of different domains suggests that kinematically the deformation overall was relatively homogeneous. The deformation sequence involved cleavage formation, folding on shallowly plunging axes, and shear associated with southeast-directed faulting. As deformation progressed, rotations of northwest-over-southeast sense overturned folds and rotated cleavage that probably originally was near vertical (it is parallel with dikes that are generally perpendicular to beds). The pattern of southeast-directed rotation and displacements is suggestive of thrusting of Tillery Formation mudstones. In the quarry we see only small-scale shears or faults and rotations that likely mark splays; if the inference of thrusting is correct, then the thrust decollement must be at some depth below the quarry, a decoupling surface beneath the zone of intensified deformation near the Tillery-Uwharrie contact. This structural array at the quarry appears to represent a single deformation episode, and is very similar to the structural configuration seen by the authors in reconnaissance across the Carolina slate belt.

Deformation was synchronous with conditions that allowed crystallization of white mica and biotite on cleavage and white mica as post-cleavage porphyroblasts. Biotite grew abundantly in one sheared dike with S-C fabric, along with unusual amounts of coarsely crystalline calcite; we infer this to mean that fluid flow was concentrated along the shear as metamorphic temperature was maintained. Biotite growth elsewhere was limited, but metamorphism at biotite grade (350-325°C with calcite present) is believed to have persisted past the end of compressional deformation, judging from rare grains of biotite (not dated) that grew without strain shadows. Similarly, muscovite porphyroblast growth seems to have occurred after cleavage formation, perhaps at temperatures below the 325-300°C range. Using the standard 30°C/km geothermal gradient, temperatures required for the observed mica growth would indicate crustal depth of about 10 km, although it probably was considerably less under elevated temperature conditions of orogenic deformation. The deformation involved both brittle (faults, block rotations) and ductile (folds, shear with intense biotite growth) elements, indicating conditions near the brittle-ductile transition, probably in the 6-8 km depth range. From that crustal level, only minor post-deformation uplift would have been necessary to reach the closure temperature of biotite, consistent with the span of ages given by our data.

ACKNOWLEDGMENTS

Martin Marietta Aggregates is gratefully acknowledged for its permission to study exposures in the quarry. Particular thanks are due to Mr. Harry Winchester, District Production Manager at the time of the study, for providing the aerial photograph and taking an interest in the work, and to Mr. John "Doc" Cook, Ashe-

boro Plant Manager at the time of the study, for assuring both daily access and safety guidance.

REFERENCES

Alexander, C.A., Jr., Mickelson, G.M., and Lanphere, M.A., 1978, MMhb-1: A new $^{40}Ar/^{39}Ar$ dating standard, in Zartman, R.E., ed.: Short papers of the Fourth International Conference, Geochronology, Cosmochronology, Isotope Geology, U.S. Geological Survey Open-file Report 78-701, p. 6-8.

Berthe, D., Choukroune, P., and Jegouzo, P., 1979, Orthogneiss, mylonite and non-coaxial deformation of granites: The example of the South Armorican shear zone: Journal of Structural Geology, v. 1, p. 31-42.

Butler, J.R., and Fullagar, P.D., 1978, Petrochemical and geochronological studies of plutonic rocks in the southern Appalachians: III. Leucocratic adamellites of the Charlotte belt near Salisbury, North Carolina: Geological Society of America Bulletin, v. 89, p. 460-466.

Butler, J.R., and Secor, D.T., Jr., 1991, The central Piedmont, in Horton, J.W., Jr. and Zullo, V.A., eds., The geology of the Carolinas: Carolina Geological Society, Knoxville, University of Tennessee Press, p. 59-78.

Conley, J.F., 1962a, Geology of the Albemarle Quadrangle, North Carolina: North Carolina Division of Mineral Resources Bulletin 75, 26 pp.

Conley, J.F., 1962b, Geology and mineral resources of Moore County, North Carolina: North Carolina Division of Mineral Resources Bulletin 76, 40 pp.

Conley, J.F., and Bain, G.L., 1965, Geology of the Carolina slate belt west of the Deep River-Wadesboro Triassic basin, North Carolina: Southeastern Geology, v. 6, p. 117-137.

Dalrymple, G.B., Alexander, C.A., Jr., Lanphere, M.A., and Kraker, G.P., 1981, Irradiation of samples for $^{40}Ar/^{39}Ar$ data using the Geological Survey TRIGA reactor: U.S. Geological Survey Professional Paper 1176, 55 pp.

Dodson, M.H., 1973, Closure temperature in cooling geochronological and petrological systems: Contributions to Mineralogy and Petrology, v. 40, p. 259-274.

Farrar, S.S., 1985, Tectonic evolution of the easternmost Piedmont, North Carolina: Geological Society of America Bulletin, v. 96, p. 362-380.

Gibson, G.G., Teeter, S.A., and Fedonkin, M.A., 1984, Ediacarian fossils from the Carolina slate belt, Stanly County, North Carolina: Geology, v. 12, p. 387-390.

Giletti, B.J., 1974, Studies in diffusion I: Argon in phlogopite mica, in Geochemical transport and kinetics, Hofmann, A.W., Giletti, B.J., Yoder, H.S., Jr., and Yund, R.A., eds., Carnegie Institution of Washington Publication 634, p. 107-115.

Glover, Lynn, III, and Sinha, A.K., 1973, The Virgilina deformation, a late Precambrian to early Cambrian(?) orogenic event in the central Piedmont of Virginia and North Carolina: American Journal of Science, v. 273-A, p. 234-251.

Glover, Lynn, III, Speer, J.A., Russell, G.S., and Farrar, S.S., 1983, Ages of regional metamorphism and ductile deformation in the central and southern Appalachians: Lithos, v. 16, p. 223-245.

Goldsmith, Richard, Milton, D.J., and Horton, J.W., Jr., 1988, Geologic map of the Charlotte 10 x 20 Quadrangle, North Carolina and South Carolina: U.S. Geological Survey Miscellaneous Investigations Series, Map I-1251-E, scale 1:250,000.

Harris, C.W., 1982, An unconformity in the Carolina slate belt of central North Carolina: New evidence for the areal extent of the ca. 600 Ma Virgilina deformation [M.S. thesis]: Blacksburg, Virginia, Virginia Polytechnic Institute and State University, 90 p.

Harris, C.W., and Glover, Lynn, III, 1985, The Virgilina deformation: Implications of stratigraphic correlation in the Carolina slate belt: Carolina Geological Society Field Trip Guidebook, 59 p.

Harris, C.W, and Glover, Lynn, III, 1988, The regional extent of the ca. 660 Ma Virgilina deformation: Implications for stratigraphic correlation in the Carolina terrane: Geological Society of America Bulletin, v. 100, p. 200-217.

Harrison, T.M., Duncan, I, and McDougall, I., 1985, Diffusion of ^{40}Ar in biotite: Temperature, pressure and compositional effects: Geochimica et Cosmochimica Acta, v. 49, p. 2461-2468.

Haugerud, R.A., and Kunk, M.J., 1988, ArAr*, a computer program for reduction of $^{40}Ar/^{39}Ar$ data: U.S. Geological Survey Open-file Report 88-216, 68 pp.

Kish, S.A., Butler, J.R., and Fullagar, P.D., 1979, The timing of metamorphism and deformation in the central and eastern Piedmont of North Carolina: Geological Society of America Abstracts with Programs, v. 11, p. 184-185.

Koeppen, R.P., in press, Geochemistry of felsic volcanic rocks of the Carolina slate belt: U.S. Geological Survey Bulletin.

McDougall, Ian, and Harrison, T.M., 1988, Geochronology and thermochronology by the $^{40}Ar/^{39}Ar$ method: Oxford University Press, New York, 212 pp.

Milton, D.J., 1984, Revision of the Albemarle Group, North Carolina: U.S. Geological Survey Bulletin 1537-A, p. 69-72.

Noel, J.R., Spariosu, D.J., and Dallmeyer, R.D., 1988, Paleomagnetism and $^{40}Ar/^{39}Ar$ ages from the Carolina slate belt, Albemarle, North Carolina: Implications for terrane amalgamation with North America: Geology, v. 16, p. 64-68.

North Carolina Geological Survey, 1985, Geologic map of North Carolina, Raleigh, N.C., scale 1:500,000.

Offield, T.W., 1994, Lithotectonic map and field data---reconnaissance geology of the Carolina slate belt and adjacent rocks from southern Virginia to central South Carolina: U.S. Geological Survey Open-File Report 94-420, 2 diskettes (map, text, data spreadsheet).

Ramsay, J.G., 1967, Folding and fracturing of rocks: New

York, McGraw-Hill Book Company, 568 p.

Seiders, V.M., 1981, Geologic map of the Asheboro, North Carolina and adjacent areas: U.S. Geological Survey Miscellaneous Investigations Map I-1314, scale 1:62,500.

Snee, L.W., Sutter, J.F., and Kelly, W.C., 1988, Thermochronology of economic mineral deposits: Dating the stages of mineralization at Panasqueira, Portugal by high precision $^{40}Ar/^{39}Ar$ age spectrum techniques on muscovite: Economic Geology, v. 83, p. 335-354.

Staudacher, Th., Jessberger, E.K., Dorflinger, D., and Kiko, J., 1978, A refined ultra high-vacuum furnace for rare gas analysis: Journal of Physics. E: Scientific Intruments, v. 11, p. 781-784.

Steiger, R.H., and Jager, E., 1977, Subcommission on geochronology: Convention on the use of decay constants in geo- and cosmochronology: Earth and Planetary Science Letters, v. 36, p. 359-362.

Stromquist, A.A., and Sundelius, H.W., 1975, Interpretive geologic map of the bedrock, showing radioactivity, and aeromagnetic map of the Salisbury, Southmont, Rockwell, and Gold Hill Quadrangles, Rowan and Davidson Counties, North Carolina: U.S. Geological Survey Miscellaneous Investigations Series Map I-888, scale 1:48,000.

Stuckey, J.L., 1928, The pyrophyllite deposits of North Carolina: North Carolina Department of Conservation and Development Bulletin 37, 62 p.

Wintsch, R.P., Kunk, M.J., and Epstein, J.B., in press, Alleghanian cleavage and Acadian diagenesis in the Martinsburg Formation, eastern Pennsylvania: $^{40}Ar/^{39}Ar$ whole-rock dating and geological constraints: American Journal of Science.

Wintsch, R.P., and Kunk, M.J., 1992, $^{40}Ar/^{39}Ar$ evidence for an Alleghanian age of slaty cleavage in the Martinsburg Formation, Lehigh Gap area, eastern Pennsylvania: Geological Society of America Abstracts with Programs, v. 24, p. A85.

Wright, J.E., and Seiders, V.M., 1980, Age of zircon from volcanic rocks of the central North Carolina Piedmont and tectonic implications for the Carolina volcanic slate belt: Geological Society of America Bulletin, v. 91, p. 287-294.

APPENDIX

The samples were processed using standard heavy liquid, magnetic separation, and paper shaking methods to a purity of greater than 99.5 percent. The samples were then encapsulated in tin foil, numbered, sealed under vacuum in fused silica vials, and placed in a watertight aluminum can in the U.S. Geological Survey TRIGA reactor (Dalrymple, and others, 1981) and rotated at one rpm as a portion of the ^{39}K in the sample was converted to ^{39}Ar. ^{39}Ar production was monitored using MMhb-1 hornblende (age 519.4 Ma; Alexander and others, 1978) irradiated with the samples. The irradiated samples were placed in the sidearm of a double vacuum, low blank furnace similar in design to that described by Staudacher and others (1978), and degassed in a stepwise fashion. The resulting aliquots of gas were then cleaned using Fe-V, Al-Zr, and Ti getters and analyzed for their argon isotopic composition in a VG mm1200b mass spectrometer operated under static conditions. For each analysis, five sets of the argon peaks were measured. These values were then linearly regressed. The resultant peak values and uncertainties were reduced using ArAr* (Haugerud and Kunk, 1988). Decay constants used were those recommended by Steiger and Jaeger (1981). Corrections for reactor-produced interfering argon isotopes were made using the values published by Dalrymple and others (1981).

SOUTHEASTERN GEOLOGY
V. 35, No.2, June1995, p. 79-92

GEOMORPHIC DEVELOPMENT AND PALEOENVIRONMENTS OF LATE PLEISTOCENE SAND HILLS, SOUTHEASTERN LOUISIANA

JOANN MOSSA

3141 Turlington Hall
Department of Geography
University of Florida
Gainesville, FL 32611

BOB J. MILLER (Deceased April 12, 1987)

Department of Agronomy, Louisiana Agricultural Experiment Station
Louisiana State University
Baton Rouge, LA 70893

ABSTRACT

Several conspicuous sand hills with a relief to 10 m parallel coastal plain valleys in southeastern Louisiana. Previous workers have interpreted these sand hills to be eolian dunes that migrated onto broad floodplain flats, and then based revisions of the regional geological history and paleoclimate on such inferences. Instead, stratigraphic and soils data, including the presence of gravel and lack of a basal unconformity, indicate that the sand hills sediments are dominantly fluvial. The sand hill morphology is strongly erosional in origin, reflecting later actions of streams and hillslope processes. Subsequent deposition of alluvium and colluvium buried the low-lying parts of the paleolandscape so that broad flats currently surround these erosional remnants of mixed-load fluvial systems.

INTRODUCTION

Although numerous investigations concern the Quaternary landscapes and associated deposits of Louisiana, many aspects of the Quaternary geomorphology and stratigraphy are unresolved. The paleoenvironmental origin of Late Pleistocene sand hills that form north-to-south oriented complexes paralleling modern river valleys in southeastern Louisiana (Figure 1) represents an important component of these unresolved problems. This is because the inferred eolian origin (Lambert, 1965; Cullinan, 1969; Otvos, 1971) has led to conclusions regarding the regional paleoclimate and revisions of the Pleistocene chronostratigraphy (Lambert, 1965; Otvos, 1971, 1975). The elongate hills are locally distinctive in slope and elevation with a maximum relief of approximately 10 m, lengths up to 700 m, and widths approaching 500 m. The sand hills occur to the east of the modern Comite, Amite, Tickfaw, and Natalbany Rivers and to the west of the Tangipahoa and possibly the Comite rivers as discontinuous complexes up to 25 km long (Figure 1). Ancestral coastal plain rivers (Lambert, 1965; Otvos, 1971) and margins of wetland lakes (Cullinan, 1969) were considered to be the source of the dune sands.

Lambert (1965) and Cullinan (1969) inferred that the hills were eolian dunes because of their oblong morphology and dominantly sandy texture. Lambert (1965) noted the presence of sixteen large hills in Livingston and Tangipahoa parishes (Figure 2) and deduced that the hills formed by eolian reworking of point bars. He assessed their age as late Wisconsinan based on their association with large meander scars entrenched in the Prairie surface, which he considered to be mid-Wisconsinan in age. Cullinan (1969) conducted a study of the geology of Washington and St. Tammany parishes to the east, but noted the presence of the two southernmost sand hills of the Tangipahoa complex in Tangipahoa Parish. He proposed that the hills were formed by eolian processes along the

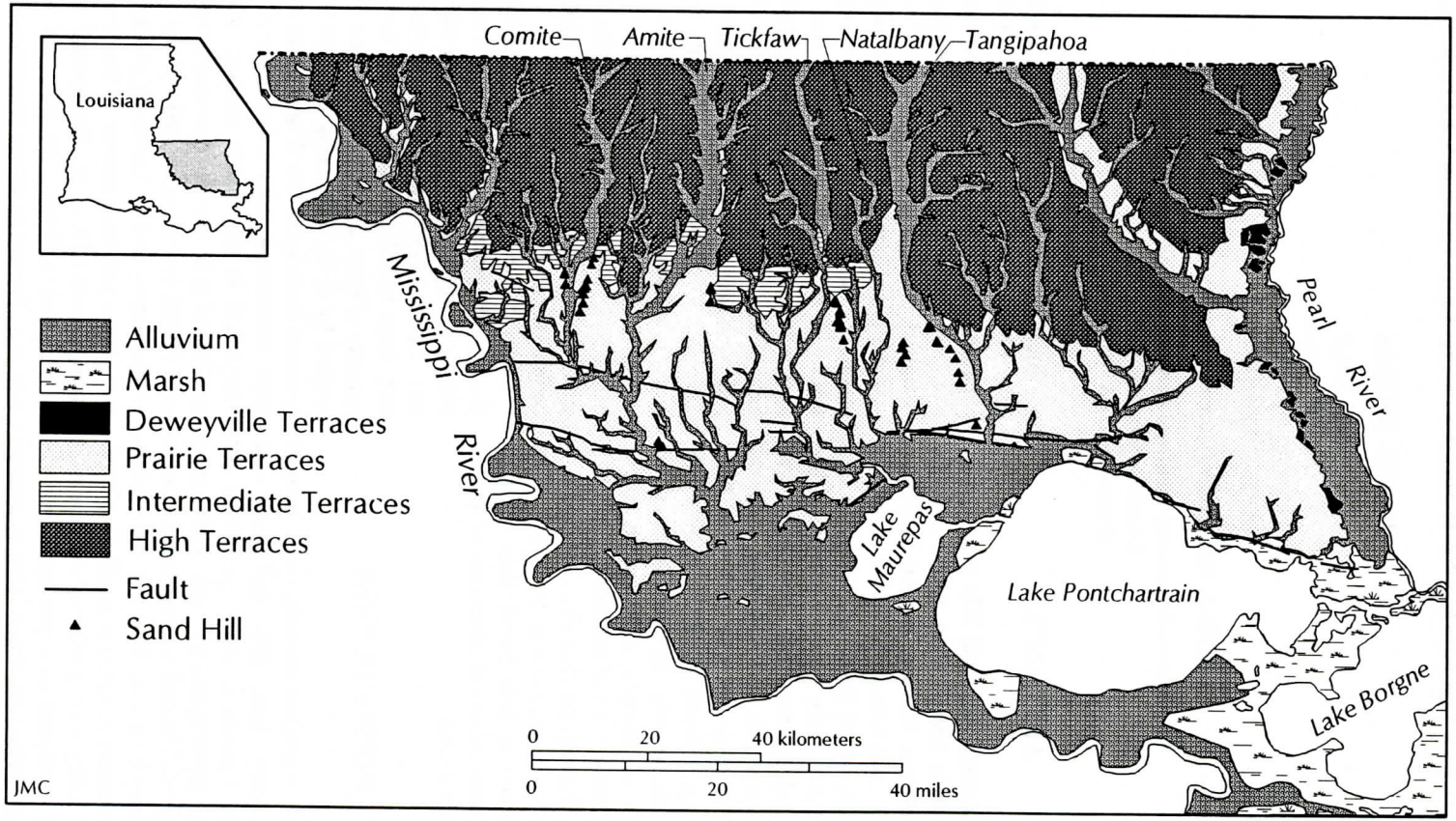

Figure 1. Geology of southeastern Louisiana showing the location of sand hill complexes with relief of three or more meters (source: Snead and McCulloh, 1984 and topographic maps).

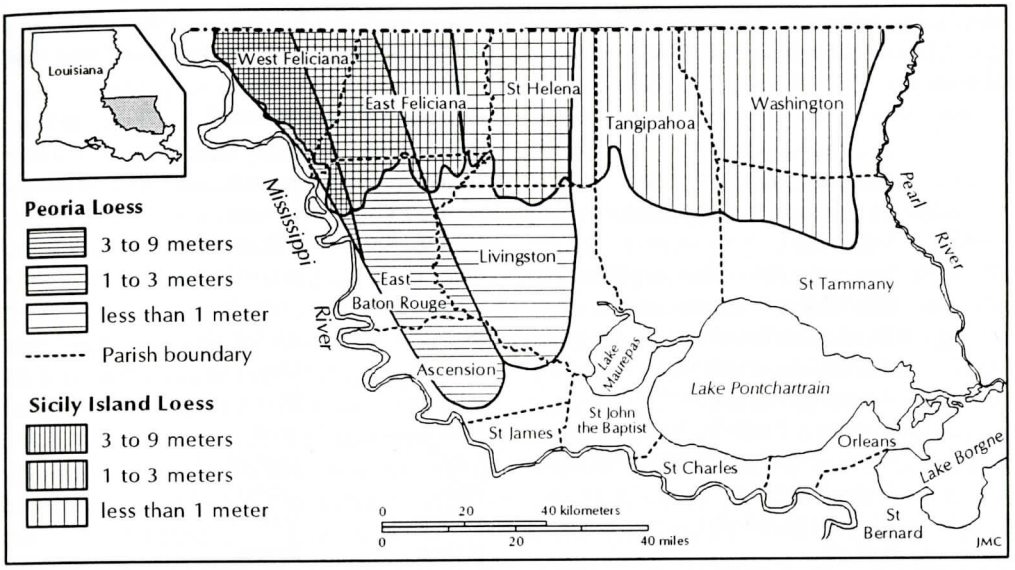

Figure 2. Distribution of the Peoria and Sicily Island Loess in southeastern Louisiana (source: Miller and others, 1986).

margins of an ancestral Lake Pontchartrain.

Of all prior studies, Otvos' (1971) was most in-depth, using sedimentologic data to infer an eolian origin for seventy sand mounds and hills in southeastern Louisiana. Evidence includes 2 to 13% of the quartz grains being rounded and well-rounded, medians being in the medium sand range ($0.26 \geq D_{50} \geq 0.33$ mm), and sorting being good after clay was removed from a number of samples. Similarities between sediments within the hills and the fluvial channel samples beneath were noted. For instance, he concluded that a buried sand unit, which was underlain by pebbly sands and overlain by floodplain silts, was most likely fluvial rather than eolian despite its good sorting and steep cross sets. Yet because of the morphology and the dominantly sandy nature of the sand hills, and the lack of other apparent explanations, it was concluded that these were eolian and thus younger than surrounding deposits. Considering the surrounding sediments to be Sangamonian, he estimated the age of the sand hills as early Wisconsinan.

The paleoenvironments and the role of eolian processes in Louisiana during the Quaternary is not well understood. It is possible that with differing environmental conditions during the Pleistocene, wind was a more important agent than at present. However, it would take a radically different wind and moisture regime to form dunes of such large size along humid coastal plain rivers given the scale of their source. Quaternary paleoecological studies are limited in number, geographic distribution, and temporal continuity (Delcourt and Delcourt, 1985; 1987) and are insufficient to evaluate the paleoclimate of this area. Additionally, other morphologic features, including the presence of several large meander scars which occur in the study area and elsewhere in Louisiana (Saucier and Fleetwood, 1970; Robertson, 1980; Alford and Holmes, 1985; Kesel, 1986) have been used to suggest the opposite—that river discharges were much larger at times during the Quaternary because of pluvial climates.

It is prudent to reassess the origin of these late Pleistocene sand hills in southeastern Louisiana, especially given that an eolian origin has significant ramifications regarding the environmental conditions and Quaternary paleoclimates in this region. This reassessment is based on geomorphic and stratigraphic aspects of soils and sediments of the sand hills and sur-

Table 1. Comparative differences between modern soils developed in Peoria and Sicily Island loesses in Louisiana. These comparisons are based between soils having similar landscape and internal soil drainage characteristics.

	Loess Parent Material	
Soil Characteristic	**Peoria**	**Sicily Island**
Solum thickness	least	greatest
Thickness of A + E horizons	least	greatest
Color (Hue)	least red	reddeet
Maximum clay content, arg illic horizon	least	greatest
Total clay content in solum	least	greatest
Weatherable minerals, non-clay fraction	greatest	least
Amount of smectite clay	greatest	least
Amount of micaceous clay	greatest	least
Amount of kaolinite clay	least	greatest
Interlaying/interstratification of clay	least	greatest
Fe-oxide content	least	greatest
CEC per unit of clay	greatest	least
Soil pH	highest	lowest
pH-dependent CEC and acidity	least	greatest
Extractable acidity ($BaCl_2$•TEA)	least	greatest
% Al saturation (effective CEC basis)	least	greatest
% base saturation (ef fective, NH_4OAc at pH 7.0, summation of cations)	greatest	least
Exchangeable Ca/Mg ratio	greatest	least
Total and extractable P	greatest	least

rounding areas, with most of the detailed field investigations being conducted along the Tangipahoa sand hill complex in Tangipahoa Parish (Figure 2). This site was chosen because the sand hills are numerous, show considerable variety in size and morphology, and were recently mapped in soil surveys.

REGIONAL GEOLOGY

Eolian deposits present in southeastern Louisiana include the Peoria and Sicily Island loesses (Miller and others, 1985) (Figure 2). Stratigraphic correlation up the Mississippi Valley and the decreasing thickness with distance from the valley shows the Mississippi River was the source of loess (Spicer, 1969; Miller and others, 1985). One reason why the Mississippi River was a source of loess during glaciations, but is not presently, is because there was a much larger sediment supply from glacial outwash from the continental interior (Saucier, 1967, 1968; Smith and Saucier, 1971; Autin and others, 1991). The large sediment supply promoted a dominantly braided pattern where the sediments of unvegetated bars were vulnerable to erosion from winds. Local coastal plain streams were not receiving sediment supply from glacial outwash, and extensive coring shows they have no effect on loess thickness in southern Louisiana (Figure 2) (Spicer, 1969; Miller and others, 1985). Close to the Mississippi valley, loess can serve as a stratigraphic marker for relative age assessments, but further it becomes less uniform by mixing with underlying sediments (Miller and others, 1988).

Ages of the Peoria Loess determined by radiocarbon and by thermoluminescence (TL) agree fairly well, placing this deposit between 20,000 and 9,000 years B.P. in the lower Mississippi valley (Pye and Johnson, 1988). Radiocarbon dates synthesized by Clark and others

(1989) for Peoria Loess range between 24,000 and 15,000 years B.P. The Sicily Island loess has been dated in nearby Vicksburg, Mississippi using TL as between 85,000 and 76,000 years B.P. (Pye and Johnson, 1988). Using amino acid racemization, it has been suggested that this loess is much older, either early Illinoian (Clark and others, 1989) or late Illinoian (Clark and others, 1990) and certainly greater than 125 ka. Possible ages of the loesses have also been discussed by others (Alford, 1990; McKay and Follmer,1985; Miller, 1991; Rutledge and others, 1990; Schumacher and others, 1987) with the scientific community being divided. Although agreement regarding the absolute ages of loess deposits would improve the chronostratigraphic framework of this study, it is not essential for later interpretations. Stratigraphic correlation, buried soils, and relative age assessments of surficial soils developed in loesses (Table 1) were used by Miller and others (1985) to map the distribution of the two major loesses. Maps based on such data (Figure 2) show that the Comite sand hill complex, which lies closest to the Mississippi valley, is only blanketed by Peoria loess. Thus, the sediments comprising the sand hills were likely deposited between these periods of loess deposition.

The sand hills occur at the highest elevations on the Prairie Terraces or Prairie Complex, following nomenclature of Snead and McCulloh (1984) and Autin and others (1991), respectively (Figure 1). These have traditionally been considered to be a single, merging river- and coast-parallel surface based on the initial work of Fisk (1938a, 1938b). Although much published information proposes otherwise, Snead and McCulloh (1984) describe that "Three levels are recognized; two along alluvial valleys, the lower coalescing with its broad coastwise expression; the third, still lower found intermittently gulfward". Drawing on the findings of various researchers (i.e. Doering, 1956; 1958; Smith and Russ, 1974) who worked in the Red River valley, Autin and others (1991) suggest that the Prairie Complex has at least two major chronostratigraphic components. Yet, while terrace sublevels have been mapped in southwestern Louisiana (Smith and Russ, 1974; Kesel, 1980-1982), similar observations have yet to be made or applied in southeastern Louisiana.

The presence of only the Peoria Loess and the minimal degree of soil development on the Prairie Terraces implies that the minimum age of the surface is Farmdalian (22-28 ka B.P) (Alford and others, 1983; Miller and others, 1985; Miller, 1991). The maximum age of the surface remains disputable, at least until some agreement is reached regarding the absolute ages of the Sicily Island loess. Integrating significant works in the region, Autin and others (1991) proposed a compromise--that this unit contains at least two major chronostratigraphic components, suggesting that both the Sangamon and Farmdale were important times for aggradational processes of the Prairie Terraces.

The Intermediate Terraces, the next highest morphostratigraphic surface mapped by the Louisiana Geological Survey (Snead and McCulloh, 1984), is even more controversial. The Intermediate Terraces or Intermediate Complex (Autin and others, 1991) covers a much smaller area (Figure 1) and has not been recognized by all investigators (Cullinan, 1969; Campbell, 1971). Local fieldwork shows that the upper component appears to dominantly colluvial in the study area, with soil development characteristics intermediate to the Prairie and older High Terraces (Mossa and Autin, 1989) or Upland Complex (Autin and others, 1991). Near the Mississippi valley, the Intermediate Terraces are blanketed both the Sicily Island and Peoria loesses (Miller and others, 1985; 1986), indicating the minimum age of this terrace complex is Sangamonian.

From the perspective of regional geology, there are at least two problems with the eolian dune hypothesis. First, the sand hills are large compared to existing sediment sources, with lengths and widths commonly more than twice that of modern point bars of local rivers. The sand hills are also proportionately higher in elevation and larger in surface area than dunes in the lower Mississippi valley (Saucier, 1978)

where the sand source and bar sizes were considerably greater. Additionally, there is no evidence, as in other locations where fluvial dunes have been observed (Franzmeier, 1970) that local streams have influenced the patterns and thickness of loess deposits. Because silt can be transported by wind at considerably lower velocities than medium sand, the lack of loess from streams that supposedly provided sufficient sediment sources for the formation of large dunes is also problematic.

GEOMORPHIC RELATIONSHIPS

Except for the Comite sand hill complex, which received the greatest amount of loess, most sand hills are mapped as well-drained Cahaba sandy loams (Typic Hapludults) with 3 to 6% slopes (McDaniel and others, 1990). The distribution of the Cahaba series illustrates parts of the Tangipahoa and Natalbany sand hill complexes (Figure 3). Topographic maps and soil surveys show the irregular size, morphology, and spacing of the largest sand hills, especially on the southern end of each the five major sand hill complexes. The Comite sand hill complex is only 4 km in length with low-relief, relatively small hills on both sides of the valley. The Amite sand hill complex is the longest, but consists of only four large hills, of which the two northernmost are separated from the two southernmost by about 25 km. These sand hills are all approximately 2 km to the east of the modern valley. As the other complexes, the 6.6 km-length Tickfaw sand hill diverges from the modern valley toward the south. The northern end of the complex is less than 1 km from the valley and the southern end is about 5 km from the valley. Individual hills are spaced 0.5 to 2 km apart. As shown in Figure 3, the Natalbany sand hill complex also diverges from the river toward the south, with the complex ranging from less than 1 km to about 4 km from the modern valley. Spacing of individual hills is about 0.5 to 2 km. The greatest density of sand hills lies in the 20 km-long Tangipahoa sand hill complex located to the west of the valley (Figure 3). Moving downvalley, the distance from the river increases from 1 to about 5 km, and the spacing between hills increases from less than 1 km to as much as 5 km apart.

Maps constructed with soil survey data in Tangipahoa Pariah show the distribution of soils developed on sandy late Pleistocene sediments, and the location and extent of sand and gravel pits (Figure 3). Cahaba soils develop on sand hills with slopes of 3 to 6%, and on low-relief, gently-sloping sand ridges of 1 to 3% (Figure 3). The low ridges are much more extensive geographically. Stratigraphic data, discussed later, supports that the Cahaba soils typically form in sediments of late Pleistocene paleochannels. We recognize that the same soil can cross several stratigraphic units, but suggest that a strong correlation exists between these soils and late Pleistocene fluvial deposits in the study area. Additionally, other predominantly sandy soils, such as the Stough, Myatt, and Prentiss, are most likely part of these paleochannel complexes. Collectively, these form a wide band toward the northern end of the sand hill complexes, between East Pontchatoula and Skulls Creek (Figure 3). Toward the southern end of the sand hill complexes, directly east and south of Hammond, the distribution of Cahaba and other sandy soils are less common. Unlike the northern end of the complexes, surficial sediments of the abandoned channels surrounding the sand hills and sand ridges are silt loams, likely transported by colluvial and alluvial processes. Because soil series are delineated based upon horizon characteristics such as texture, color and drainage, additional field work is suggested to assess relationships between stratigraphic units and soils.

While details of the ancestral courses and chronology are unclear, there was likely repeated shifting or avulsion of a river systems for the area of sandy late Pleistocene soils paralleling the modern channels to be so widespread. Although multiple channels may have been contemporaneous, the occurrence of fluvial sediments at different landscape positions suggests that different ages may be repre-

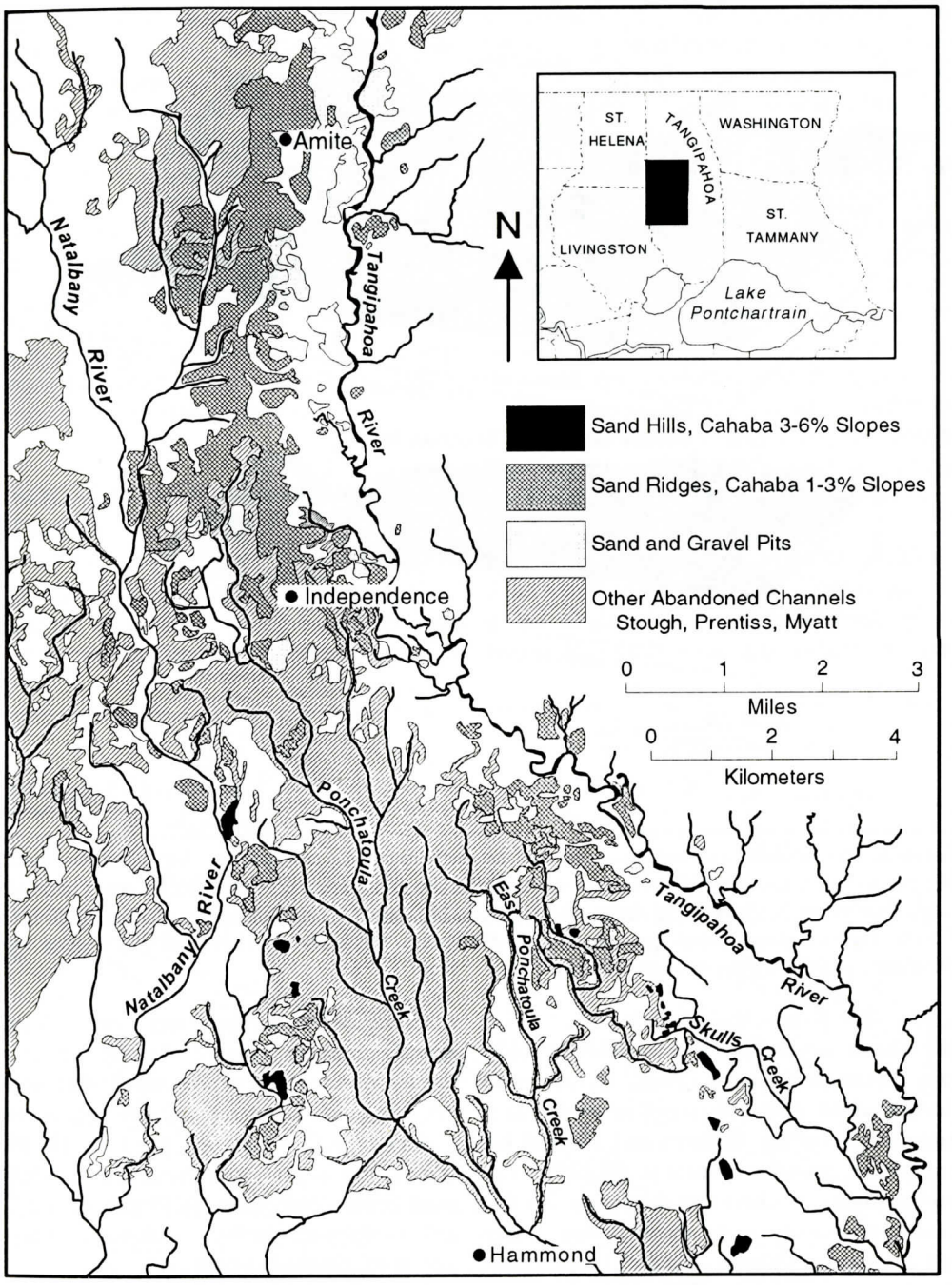

Figure 3. Sand hill complexes, associated soils, and sand and gravel mines in central Tangipahoa Parish (data from McDaniel and others, 1990). Sand hills are mapped as Cahaba, 3-6% slopes, and sand ridges as Cahaba, 1-3% slopes. Field study suggests these and other sandy soils developed on late Pleistocene sediments, including both mounds and depressions, often develop on sediments of late Pleistocene paleochannels.

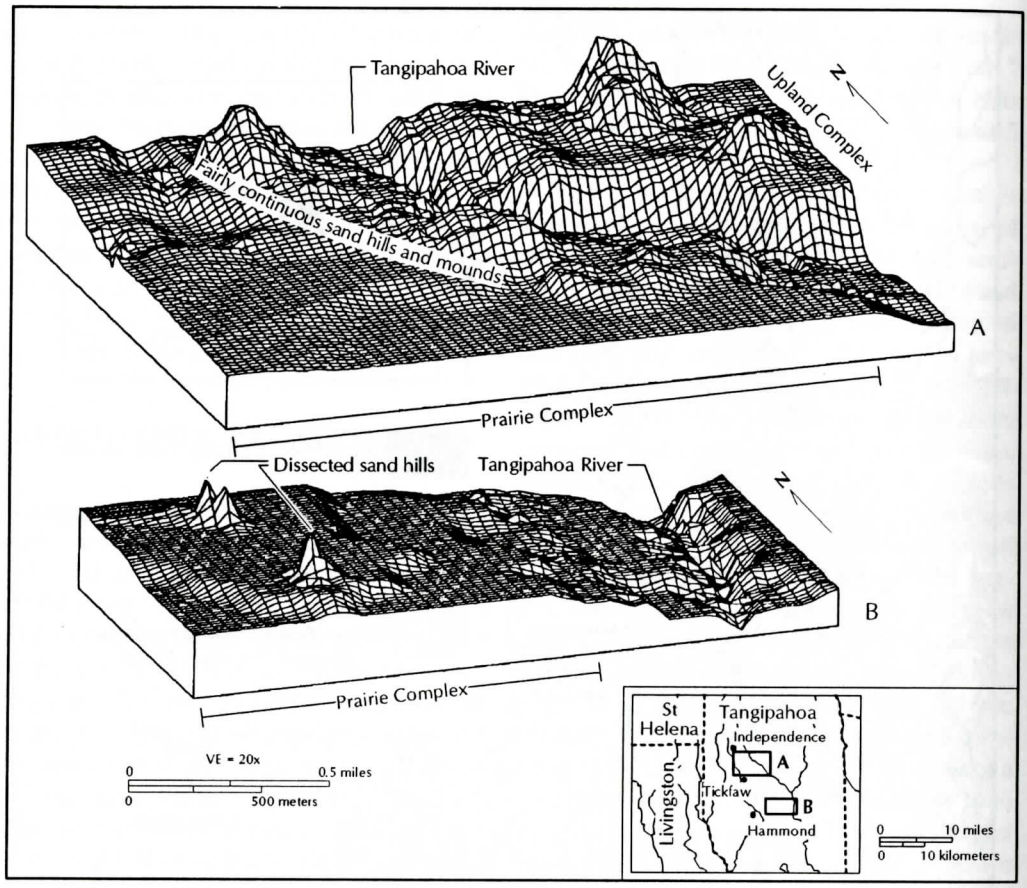

Figure 4. Three-dimensional landscape views of the northern (above) and southern (below) ends of the Tangipahoa sand hill complex. Near the northern end, the complex occurs near the valley along a hummocky ridge. Further south, the complex shows dissected sand hills about 5 km from the modern Tangipahoa River (source: Hammond and Robert quadrangles, 1:24,000 scale). The landscape to the east of the valley shows the older Upland Complex or High Terraces.

sented. We believe that Cahaba soils on 3 to 6% slopes generally are developed on older late Pleistocene river systems. Cahaba soils developed on 1 to 3% slopes in some cases, particularly on the northern end of sand hill complexes, are often similar in age to those on higher slopes but show less dissection. In other cases, particularly on the southern end of sand hill complexes, Cahaba soils on 1 to 3% slopes develop on younger late Pleistocene river systems than those on higher slopes. Other paleochannels are likely buried by younger sediments.

The distribution of sand and gravel pits (Pits-Arents complex) also provides near-surface evidence of the location and extent of abandoned channels (Figure 3). Because sand occurs in much greater proportions than gravel, yet is in much lower demand, most mines must extract gravel to stay in operation. Of those mines that occur away from the floodplain, most occur along pathways formed by the sand hill complexes, further confirming these as gravel-bearing paleochannels.

Three-dimensional landscape views show north-to-south variations in the spacing and morphology of the hills and ridges of the Tangipahoa sand hill complex (Figure 4). Near the northern end, but downvalley of where the sand hill complex is confined by Intermediate and

High Terraces, Cahaba and associated soil series occur on a long, fairly continuous, hummocky ridge that is higher in elevation than adjacent surfaces (Figure 4, top). In contrast, at the southern end of the complex, relief of these sand hills typically increases, slopes are greater, and the spacing is further apart and more irregular than on the northern end (Figure 4, bottom). Especially at this end, the irregular size, shape, and spacing suggest considerable erosional modification since deposition. Multiple morphologic surfaces are apparent, suggesting that multiple sublevels of the Prairie Complex occur in the study area.

SOIL-GEOMORPHIC AND SOIL-STRATIGRAPHIC RELATIONSHIPS

Stratigraphic investigations were concentrated in Tangipahoa Parish because several hills are present and the modern soil survey was recently completed. Crests, sideslopes, and toeslopes of several hills and lower relief ridges were bored with a truck-mounted Giddings hydraulic probe. Penetration varied from less than 2 to over 5 m and was limited by high water tables, particularly on the low landscape positions, and by tightly packed sedimentary textures including gravelly clays or sandy clays. Soil horizons and morphologic properties were classified in the field, and borings were then transported to the laboratory for detailed observation and particle size analyses. Sediment size mixtures were determined for each soil horizon and some lamellae within the C-horizon. Results presented are confined to two features, one toward the northern end and the other toward the southern end of the complex.

Two lines of soil-stratigraphic evidence observed frequently in the field refute the eolian origin of the sand hills. First, gravel occurs frequently near the surface in many

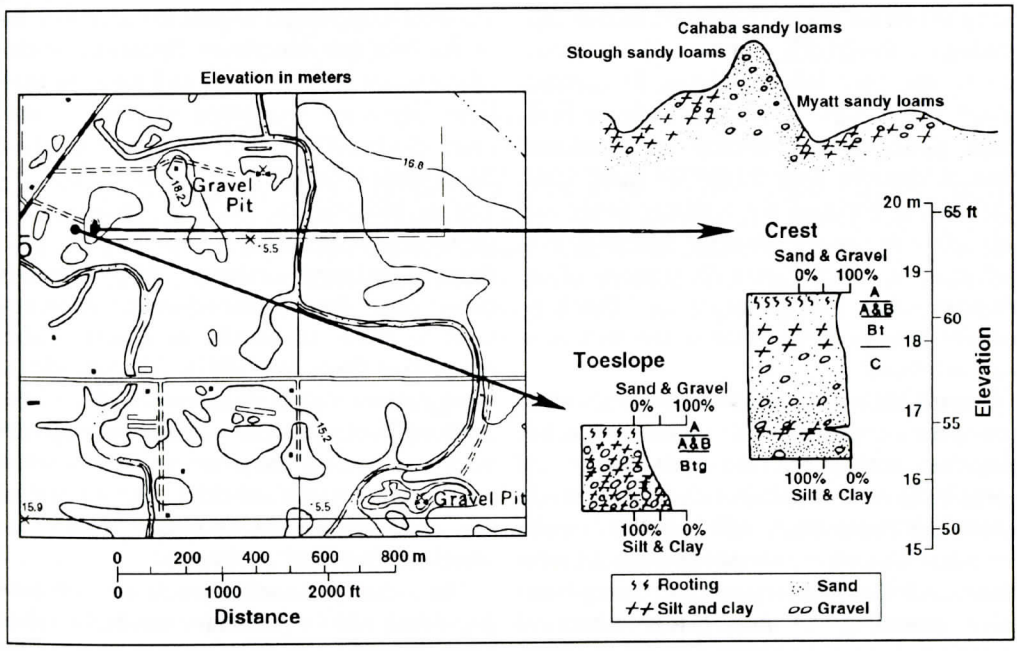

Figure 5. Stratigraphy of a 2.5 m-relief sand hill (30°33'28"N, 90°25'06" W) on the northern end of the Tangipahoa sand hill complex. The major soil horizons and a schematic diagram of the combined sand and gravel content vs. the combined silt and clay content are shown for borings acquired at various hillslope positions. Gravel occurs at shallow depths beneath the hillcrest. At toeslopes, gravel and clay content of soils increase (map source: Hammond quadrangle, 1:24,000 scale).

sand hills and, in fact, many of the hills are gravel mines. Because winds cannot transport large gravel, we doubt the eolian origin of these features. Second, no underlying change in lithology, weathering zone, buried soil, or other unconformity exists below the hills. Such a contact should exist if dunes were transported onto floodplain deposits. The fact that it does not suggests relatively continuous fluvial deposition.

Especially on the northern, low-relief end of the complex, gravel occurs close to the surface of many sand hills. Soils typically include the Cahaba, Stough (Fragiaquic Paleudults), Myatt (Typic Ochraquults) (McDaniel and others, 1990) sandy loams (Figs. 3 and 5). Cahaba soils, in terms of depositional environments, probably have developed on fluvial bars of late Pleistocene river systems. In borings of such hillcrests, several pebbles, up to 20 mm in diameter, occurred at depths less than 2 m from the surface. Also, the topographic map shows that hills of similar morphology nearby are being mined for gravel (Figure 5), further supporting the fluvial origin of the sediments comprising the sand hill complexes. In contrast, Myatt and Stough soils occur at lower landscape positions and develop on abandoned channel deposits with mixed sediment sizes. The surface horizons are typically sandy and subsurface horizons often show increasing clay and gravel content (Figure 5). Because of the abundant clay and gravel, it is difficult to acquire borings longer than a few meters at such locations.

Toward the southern, dissected, high-relief end of the complex, gravel is less common but may be encountered at depth. Sediments beneath the crest of an 8 m-relief hill are sandy loams and loamy sands with lamellae beneath the solum (Figure 6). Borings beneath the sideslope show that pebbles, with maximum diameters exceeding 16 mm (-4ϕ), occurs at elevations higher than the surrounding broad flats. Lower sideslope borings show that sand deposits extend at least 3 m lower than the broad flats. There is no evidence of a stratigraphic discontinuity, which should occur if, as proposed, dunes migrated onto broad floodplains adjacent to ancestral rivers. Toeslope borings show silt loams burying sandy clays, clay loams, or loamy sands with root traces and well-developed soil structure. The soil association is generally the Cahaba-Guyton-Abita (Figure 6). The Guyton silt loam (Typic Glossaqualfs) occurs in depressions and sediments are commonly sandy clay loams lower in the profile. The Abita silt loam (Glossaquic Paleudalfs) occurs on broad flats and has sandy sediments at depth (McDaniel and others, 1990). Both soils are developed on locally derived fine sediments that often blanket sandy stream deposits.

DISCUSSION

An alternative origin of sand hills hypothesizes deposition by mixed-load fluvial systems, later fluvial erosion, followed by alluvial and colluvial infilling. Both erosion and infilling are most pronounced toward the southern end of the sand hill complexes. Sediments within hillcrests are ancestral bars and those on toeslopes represent abandoned channels, sometimes blanketed with sheetwash and colluvium. As in modern coastal plain fluvial systems, the size of bed and bar materials decreases and depth-to-gravel increases downstream. Sand deposits are laterally extensive, likely related to the tendency for unconfined coastal plain systems to avulse repeatedly as observed elsewhere (i.e. Galloway, 1981). Alternatively, in some cases, multiple channels may have been contemporaneous. It is possible there may have been some eolian reworking of the sediments comprising the hills and ridges, but we suggest that wind was not the dominant agent in the creation of sand hill morphology.

The ancestral fluvial channels were contemporaneous with or post-dated the Sicily Island (early Wisconsinan to late Illinoian) loess but were abandoned before deposition of Peoria (late Wisconsinan) loess. The absence of an unconformity under the hills, and their relationships to surrounding sediments, especially

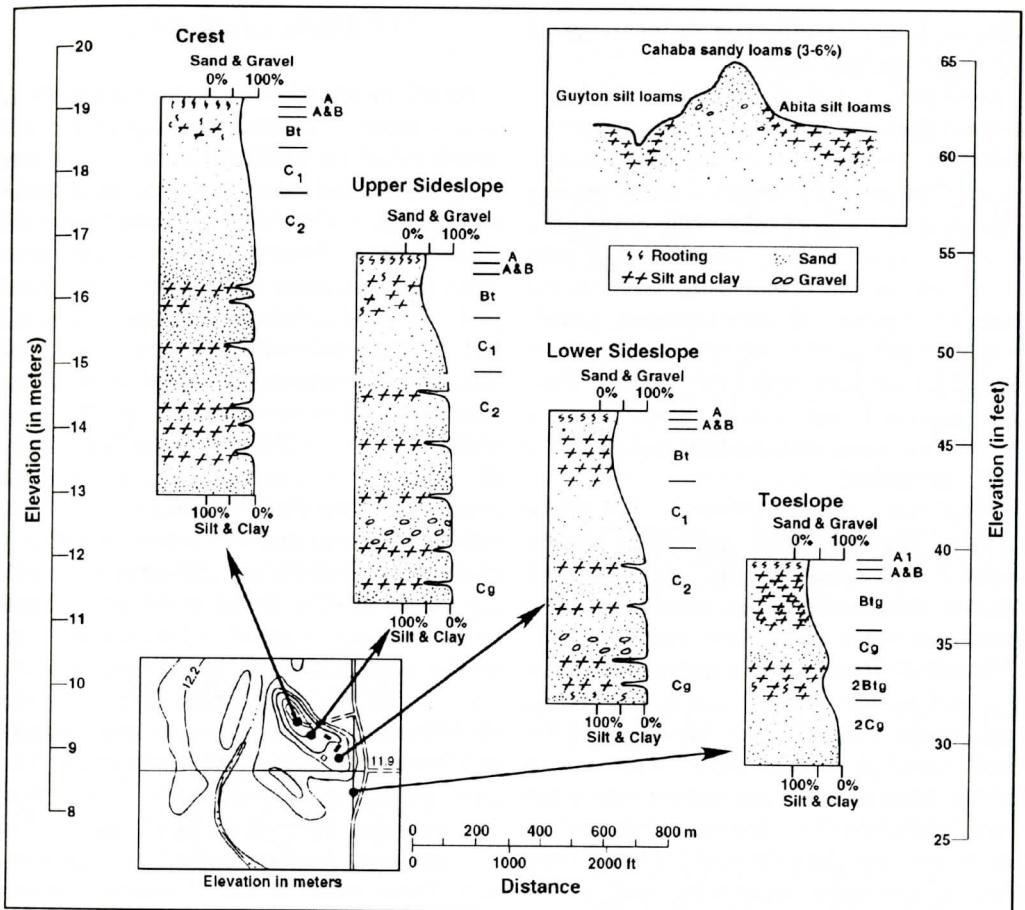

Figure 6. Stratigraphy of an 8 m-relief sand hill (30°30'23" N, 90°24' W) on the southern end of the Tangipahoa sand hill complex. The major soil horizons and a schematic diagram of the combined sand and gravel content vs. the combined silt and clay content are shown for borings acquired at various hillslope positions. Beneath the hillcrests, soils are sandy with gravel at higher elevations than the broad flats. Unconformities indicative of deposition onto a floodplain are not apparent (map source: Hammond quadrangle, 1:24,000 scale).

on the southern end of the complexes, suggests that they are presumably older, rather than younger, than the surrounding surface. This explanation also conforms with the typical scenario of landscape position in the region, where older deposits are generally higher and more dissected than younger deposits.

Fluvial erosion explains the high relief, large and irregular surface area, and irregular spacing of the hills. Multiple episodes of erosion and infilling explain the occurrence of sublevels of the Prairie Terraces in southeastern Louisiana (Figure 4). We suggest that the older and highest sublevel is a dissected alluvial surface that forms the sand hill complexes; remnants were preserved as the stream channels, possibly larger than present, began to migrate laterally and entrench. The pronounced relief of the sand hills, and the presence of other inliers of varying age in this area, suggests the importance of erosion in Quaternary landscape modification. The timing of the erosional modifications by streams likely occurred during environmental changes, including those associated with glacioeustastic processes. Given the extent of cut and fill in the region,

most erosional modification likely occurred before the late Wisconsinan.

Long-term, nearly continuous sheet erosion and hillslope processes also have influenced landscape development near the sand hill complexes. The soils developed on coarse-grained sediments of the sand hills likely erode more slowly by sheet erosion processes than soils developed on other sediments, such as the selectively preserved coarse-grained gravel-defended ridges (Brown, 1967). Especially toward the southern end of the complex, long-term colluvial and alluvial processes have infilled low areas near the hills and created a fairly flat surface.

There are several questions for future research, including what and where are the regional equivalents to the sand hills and whether this local erosion correlates with a larger and more significant erosional cycle. Comments on these matters are highly speculative and require detailed chronostratigraphic studies here and elsewhere. Elsewhere on the Gulf coastal plain, there are no features with similar relief although low-relief sandy ridges with Cahaba soils form less-dissected sand hill complexes near the Calcasieu River in southwestern Louisiana (Kilpatrick and others, 1980). Possible explanations of the high relief sand hill complexes in southeastern Louisiana may be related to local neotectonics such as the Wiggins uplift in southern Mississippi (Holdahl and Morrison, 1974), cut-and-fill cycles associated with changes in sediment supply such as loess deposition, and landscape modifications associated with changes in the course of the Mississippi River and its distributaries. On the south Atlantic coastal plain, sand hills of varying size and morphology also have been described (Thom, 1967; Daniels and others, 1969; Colquhoun and others, 1972), typically attributed to an eolian origin. Where their size is inconsistent with the scale of sediment source and where the base of the sand hills lacks a stratigraphic unconformity, cut-and-fill mechanisms may represent an alternative or additional explanation for sand hill formation.

CONCLUSIONS

Eolian origins for late Pleistocene sand hills in southeastern Louisiana initially were questioned based on evidence which shows that local streams did not influence loess distribution and are not a major sediment source for dune creation. Field evidence caused us to reject an eolian origin because of: 1) the occurrence of gravel in many of the hills, and 2) the lack of an unconformity at the base of the sand hills, which indicates that these were not transported onto an adjoining floodplain. The presence gravel mines along pathways formed by the sand hill complexes also contradicts an eolian origin. An alternative origin for the sand hills hypothesizes that they are erosional remnants of fluvial origin and older than surrounding sediments. The fluvial origin is supported by the presence of gravel and the relationships of the sand hills with surrounding deposits, such as abandoned channels. Their irregular distribution, inconsistent shape, and irregular size is attributed to erosional modification. The older relative age is suggested by relationships to surrounding deposits on the southern end of the complexes and their higher landscape position. These ancestral late Pleistocene mixed-load rivers were probably less entrenched multiple-channel systems or single-channel systems that experienced periodic avulsions.

Results of this study indicate that interpreting depositional environments exclusively from grain size, sorting, and morphology may sometimes be problematic. Such interpretations are particularly misleading when used to infer past climates and to propose modifications of the regional chronostratigraphy. Paleoclimatic reconstruction should ideally involve paleoecological approaches, as well as morphostratigraphic, lithostratigraphic, and pedostratigraphic approaches for interpreting depositional and erosional episodes and relationships. Further studies of the distribution and stratigraphy of erosional remnants or inliers may be prove useful for better understanding erosional aspects of Quaternary landscape modification in the coastal plain.

ACKNOWLEDGEMENTS

The lead author thanks reviewers Ray Daniels and Jim Richardson for their useful suggestions, and Whitney Autin and Harry Roberts of LSU for earlier comments. W.J. Day, formerly with the Department of Agronomy, Agricultural Center, LSU, assisted in the field and laboratory. The Louisiana Geological Survey and various USDA-SCS personnel provided logistical and technical support and preliminary soils maps during the fieldwork phase of research. Jan Coyne, Jeff Lower, and Mark McLean of the University of Florida assisted with figure preparation. I also am grateful for having had the opportunity to learn and interact with Bob Miller, a special person who could not participate in the final phases of this project because of his untimely death.

REFERENCES CITED

Alford, J.J., 1990, Quaternary aminostratigraphy of Mississippi Valley loess; Discussion: Geological Society of America Bulletin, v. 102, p. 1136.

Alford, J.J. and Holmes, J.C., 1985, Meander scars as evidence of major climate change in southwest Louisiana: Annals of the Association of American Geographers, v. 75, p. 395-403.

Alford, J.J., Kolb, C.R., and Holmes, J.C., 1983, Terrace stratigraphy in the Tunica Hills of Louisiana: Quaternary Research, v. 19, p. 55-63.

Autin, W.J., Burns, S.F., Miller, B.J., Saucier, R.T., and Snead, J.I., 1991, Quaternary geology of the Lower Mississippi Valley, p.p. 547-82 *in* Morrison, R.B., ed., Quaternary Non-glacial Geology, Conterminous U.S.: The Geology of North America, v. K-2, Geological Society of America, Boulder, Colorado.

Brown, B.W., 1967, A Pliocene Tennessee River hypothesis for Mississippi: Southeastern Geology, v. 8, p. 81-84.

Campbell, C.L., 1971, The gravel deposits of St. Helena and Tangipahoa Parishes, Louisiana (Ph.D. Dissertation): Tulane University, New Orleans, LA, 292 p.

Clark, P.U., Nelson, A.R., McCoy, W.D., Miller, B.B., Barnes, D.K., 1989, Quaternary aminostratigraphy of Mississippi Valley loess: Geological Society of America Bulletin, v. 101, p. 918-26.

Clark, P.U., McCoy, W.D., Oches, E.A., Nelson, A.R., and Miller, B.B., 1990, Quaternary aminostratigraphy of Mississippi Valley loess; Reply: Geological Society of America Bulletin, v. 102, p. 1136-8.

Colquhoun, D.J., Bond, T.A., and Chappel, D., 1972, Santee submergence, example of cyclic submerged and emerged sequences, *in*: Nelson, B.W., ed.: Environmental Framework of Coastal Plain Estuaries, Geological Society of America Memoir 133, Boulder, Colorado, p. 475-96.

Cullinan, T.A., 1969, Contributions to the geology of Washington and St. Tammany Parishes, Louisiana (Ph.D. Dissertation): Tulane University, New Orleans, 287 p.

Daniels, R.B., Gamble, E.E., and Buol, S.W., 1969, Eolian sands associated with coastal plain river valleys: Some problems in their age and source: Southeastern Geology, v. 11, p. 97-110.

Delcourt, H.R., and Delcourt, P.A, 1985, Quaternary palynology and vegetational history of the Southeastern United States, p. 1-37 *in* Bryant, V.M., Jr., and Holloway, R.G., eds., Pollen Records of Late-Quaternary North American Sediments, American Association of Stratigraphic Palynologists Foundation.

Delcourt, P.A., and Delcourt, H.R., 1987, Long-term Forest Dynamics of the Temperate Zone: A Case Study of Late-Quaternary Forests in Eastern North America, Ecological Studies Analysis and Synthesis, v. 63, Springer-Verlag, New York, 439 p.

Doering, J.A., 1956, Review of the Quaternary surface formations of the Gulf Coast region: American Association of Petroleum Geologists Bulletin, v. 40, p. 1816-1862.

Doering, J.A., 1958, Citronelle age problem: American Association of Petroleum Geologists Bulletin, v. 42, p. 764-786.

Fisk, H.N., 1938a, Geology of Grant and LaSalle Parishes: Louisiana Department of Conservation, Geological Bulletin 10, 246 p.

Fisk, H.N., 1938b, Pleistocene exposures in western Florida Parishes, Louisiana, p. 3-26 *in* Fisk, H.N., ed., Contributions to the Pleistocene History of the Florida Parishes of Louisiana: Louisiana Department of Conservation, Geological Bulletin 12.

Franzmeier, D.P., 1970, Particle size sorting of proglacial eolian materials: Soil Science Society of America Proceedings, v. 34, p. 920-4.

Galloway, W.E., 1981, Depositional architecture of Cenozoic Gulf coastal plain fluvial systems, *in* Ethridge, F.G. and Flores, R.M., eds., Recent and Ancient Nonmarine Depositional Environments: Models for Exploration, SEPM Special Publication 31, p. 127-55.

Holdahl, S.R., and Morrison, N.L., 1974, Regional investigation of vertical crustal movements in the U.S., using precise relevelings and mareography data: Tectonophysics, v. 23, p. 373-90.

Kesel, R.H., 1980-1982, Unpublished maps of the Quaternary terraces west of the Mississippi River: Alexandria, Lake Charles, Port Arthur, Natchez, and New Orleans quadrangles, Louisiana Geological Survey open file, scale 1:250,000.

Kesel, R.H., 1986, Some preliminary notes on the palaeohydrology of the lower Mississippi River during the Holocene and late Pleistocene, p. 366-76 *in* Ritchie, W., Stone, J.C., and Mather, A.S., eds., Essays for Professor

R.E.H. Mellor, University of Aberdeen, Aberdeen, Scotland.

Kilpatrick, W.W., McDaniel, D.M., Vidrine, J.K., and Roy, A.J., 1980, Soil Survey of Allen Parish, U.S. Department of Agriculture, Fort Worth, Texas, 110 p. and 58 sheets.

Lambert, E.H., Jr., 1965, Sand mounds of Livingston and Tangipahoa Parishes, Louisiana (abstr.): Geological Society of America Special Paper No. 82, p. 303.

McDaniel, D.M., Daugereaux, D., Stephens, W., Fleming, B., and Seeling, P., 1990, Soil Survey of Tangipahoa Parish, U.S. Department of Agriculture, Fort Worth, Texas, 142 p. and 64 sheets.

McKay, E.D., and Follmer, L.R., 1985, A correlation of lower Mississippi Valley loesses to the glaciated midwest: Geological Society of America, Abstracts with Programs, v. 17, p. 167.

Miller, B.J., 1991, Pedology, *in* Chapter 18: Quaternary geology of the lower Mississippi Valley, *in* Morrison, R.B., ed., Quaternary nonglacial geology; Conterminous United States: Boulder, Colorado, Geological Society of America, The Geology of North America, v. K-2, p. 564-73.

Miller, B.J., Day, W.J., and Schumacher, B.A., 1986, Loesses and loess-derived soils in the lower Mississippi Valley, Guidebook for Soils-Geomorphology Tour, American Society of Agronomy, 144 p.

Miller, B.J., Lewis, G.C., Alford, J.J., and Day, W.J., 1985, Loesses in Louisiana and at Vicksburg, Mississippi: Friends of the Pleistocene Field Trip Guidebook, South-Central Cell, 126 p.

Miller, B.J., Schumacher, B.A., Lewis, G.C., Rehage, J.A., and Spicer, B.E., 1988, Basal mixing zones in loesses of Louisiana and Idaho: II. Formation, spatial distribution, and stratigraphic implications: Soil Science Society of America Journal, v. 52, p. 759-64.

Mossa, J. and Autin, W.J., eds., 1989, Quaternary Geomorphology and Stratigraphy of the Florida Parishes, southeastern Louisiana: Louisiana Geological Survey, Field Trip Guidebook Number 5, 98 p.

Otvos, E.G., Jr., 1971, Relict eolian dunes and the age of the "Prairie" coastwise terrace, southeastern Louisiana: Geological Society of America Bulletin, v. 82, p. 1753-8.

Pye, K., and Johnson, R., 1988, Stratigraphy, geochemistry, and thermoluminescence ages of Lower Mississippi Valley loess: Earth Surface Processes and Landforms, v. 13, p. 103-124.

Robertson, G.A., 1981, Quaternary discharges of the lower Red River in Bossier, Webster, and Bienville Parishes, Louisiana (M.S. Thesis): Louisiana State University, 72 p.

Rutledge, E.M., West, L.T., and Guccione, M.J., 1990, Loess deposits of northeast Arkansas, p. 57-98 *in* Guccione, M.J., and Rutledge, E.M., eds., Field guide to the Mississippi Alluvial Valley, Northeast Arkansas and Southeast Missouri: Friends of the Pleistocene Field Trip Guidebook, South-Central Cell, 346 p.

Saucier, R.T., 1978, Sand dunes and related eolian features of the lower Mississippi alluvial valley, p. 23-40 *in* Hilliard, S.B., ed., Man and Environment in the Lower Mississippi Valley: Geoscience and Man, v. 19, 165 p.

Saucier, R.T., 1967, Geological investigation of the Bouef-Tensas Basin, Lower Mississippi Valley: United States Army Corps of Engineers Waterways Experiment Station Technical Report 3-757, Vicksburg, MS, scale 1:62,500.

Saucier, R.T., 1968, A new chronology for braided stream surface formation in the Lower Mississippi Valley: Southeastern Geology, v. 9, p. 65-76.

Saucier, R.T. and Fleetwood, A.R., 1970, Origin and chronologic significance of Late Quaternary terraces, Ouachita River, Arkansas and Louisiana: Geological Society of America Bulletin, v. 81, p. 869-90.

Schumacher, B.A., Miller, B.J., and Day, W.J., 1987, A chronotoposequence of soils developed in loess in central Louisiana: Soil Science Society of America Journal, v. 51, p. 1005-10.

Smith, F.L., and Russ, D.P., 1974, Geological investigation of the Lower Red River-Atchafalaya basin area: U.S. Army Corps of Engineers Waterways Experiment Station Technical Report S-74-5, Vicksburg, Mississippi.

Smith, F.L. and Saucier, R.T., 1971, Geological investigation of the Western Lowlands areas, Lower Mississippi Valley: United States Army Corps of Engineers Waterways Experiment Station Technical Report S-71-5, Vicksburg, MS.

Snead, J.I., and McCulloh, R.P., comps., 1984, Geologic Map of Louisiana:Louisiana Geological Survey, scale 1:500,000.

Spicer, B.E., 1969, Characteristics of the loess deposits and soils in East and West Feliciana Parishes, Louisiana (M.S. Thesis): Louisiana State University, Baton Rouge, 69 p.

Thom, B.J., 1967, Coastal and fluvial landforms, Horry and Marion counties, South Carolina: Louisiana State University Press, Coastal Studies Series No. 19, 75 p.

SOUTHEASTERN GEOLOGY
V. 35, No.2, June 1995, p. 93-119

GEOCHEMISTRY OF GROUND WATER FROM THE CASTLE HAYNE AQUIFER IN NORTHEASTERN NORTH CAROLINA

LYNN C. SUTTON[1] AND TERRI L. WOODS

Department of Geology
East Carolina University
Greenville, NC 27858-4353

ABSTRACT

Twenty-nine wells were sampled and older data collected by Federal and State government agencies were evaluated, in order to characterize the chemistry of ground water in the Castle Hayne aquifer and to determine the major geochemical processes controlling the observed water chemistry. The Eocene Castle Hayne aquifer of northeastern North Carolina consists of calcitic limestone with lesser amounts of dolomite, calcareous sands, and minor amounts of clay. Samples collected in 1993 were analyzed for eight major species (Ca^{2+}, Mg^{2+}, Na^{+}, K^{+}, Cl^{-}, SO_4^{2-}, SiO_2, and alkalinity), 22 trace metals, O_2, pH, Eh, NO_3^{-}, NO_2^{-}, PO_4^{3-}, NH_4^{+}, F^{-}, Br^{-}, and HS^{-} TDS ranged from 310 to 10,900 ppm. A geochemical modeling program, maps of ion concentrations, and Piper diagrams were used to analyze the data. Water from the Lower Castle Hayne and the eastern-most wells in the Upper Castle Hayne are all alkali- and chloride-rich and appear to be dominated by mixing with salt water. Waters from western wells of the Upper Castle Hayne are calcium- and bicarbonate-rich due to dissolution of aquifer carbonates. These waters may also be affected by reactions involving soil salts and fertilizers. Waters from the Upper Castle Hayne affected by pumping around the Texasgulf phosphate mine are dominated by mixed cations and bicarbonate. Water from one Upper Castle Hayne well is alkali- and bicarbonate-rich, possibly due to cation exchange and local recharge through overlying pocosins.

1. Present Address: Geophex, Ltd., 605 Mercury St., Raleigh, NC 27603-2343

INTRODUCTION

Geologic and Hydrologic Framework

The Eocene Castle Hayne aquifer, with withdrawals of 146 million gallons per day (mgd; 6395 L/s), is the most productive and most extensively developed aquifer in eastern North Carolina (Lyke and Treece, 1988) (Figure 1). From the zero isopach at its western margin, it dips and thickens eastward; the unit underlies almost the entire North Carolina Coastal Plain. The average thickness is 600 feet (183 m), and the top of the aquifer ranges from 0 to 1100 feet (335 m) below sea level (Sherwani, 1980). Limestone (composed of calcite and lesser amounts of dolomite) dominates the Upper Castle Hayne, and the Lower Castle Hayne consists of calcareous sands interbedded with limestone (Figure 2) (Gamus, 1972). Minor amounts of clay are dispersed throughout the Castle Hayne Formation (Lyke and Treece, 1988; Moran, 1989). Other minerals include calcium phosphates, glaucony, zeolite, microcrystalline quartz, pyrite, hematite, and limonite (Moran, 1989; Otte, 1981). Otte (1986) proposed that the Castle Hayne sediments were deposited in a coastal embayment.

Gamus (1972) divided the Castle Hayne aquifer system into three hydrologic units: the Upper Castle Hayne (UCH), the Lower Castle Hayne (LCH), and the Beaufort, but more recent descriptions by Winner and Coble (1989) and Giese and others (1991) have considered the Beaufort as a separate aquifer. The lithology of the Beaufort unit differs significantly from that of the Castle Hayne; it is dominated by fine glauconitic sand (Gamus, 1972).

As described by Giese and others (1991), the

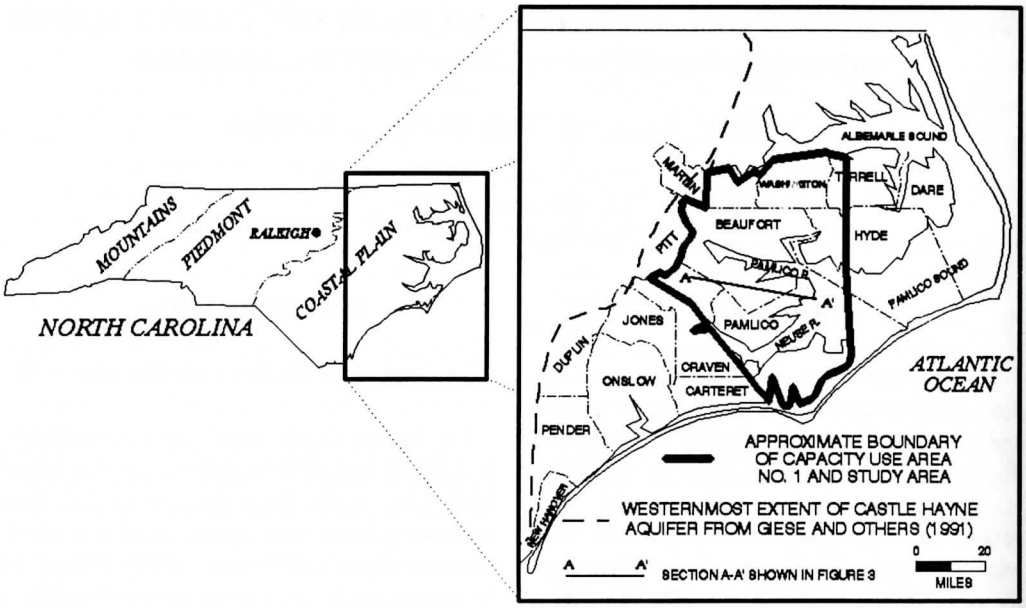

Figure 1. Location map of the study area showing the western-most extent of the Castle Hayne aquifer (Giese and others, 1991) and the location of Capacity Use Area No. 1.

System	Series	Stratigraphic Units	Hydrogeologic Units		Description
Quaternary	Recent Pleistocene	Undifferentiated Unnamed Unit	Post-Miocene Unit		Sand, silt, shells, and some clay
Tertiary	Miocene	Yorktown Formation	Yorktown Unit		Interbedded sand and clay with some shell beds
		Pungo River Formation	Pungo River Unit		Phosphate and quartz sand, silt, clay, and limestone
	Eocene	Castle Hayne Limestone	Castle Hayne Aquifer System	Upper Castle Hayne Unit	Permeable and porous shell limestone
				Lower Castle Hayne Unit	Shell limestone interbedded with calcareous sands
	Paleocene	Beaufort Formation		Beaufort Unit	Fine glauconitic sand, silty and clayey in part
Cretaceous	Upper Cretaceous	Peedee Formation	Peedee Unit		Sand interbedded with clay and silt
		Black Creek Formation	Black Creek Unit		Laminated clay with interbedded sand
		Cape Fear Formation	Upper Cape Fear Unit		Alternating beds of sand and clay
			Lower Cape Fear Unit		Fine sand
	Lower Cretaceous	Unnamed Formation	Lower Cretaceous Unit		Sand, shale, gravel and limestone
Basement					

Figure 2. Stratigraphic and hydrogeologic subdivisions of sedimentary units in the Coastal Plain of eastern North Carolina [modified from Gamus (1972) and Lloyd and Daniel (1988)].

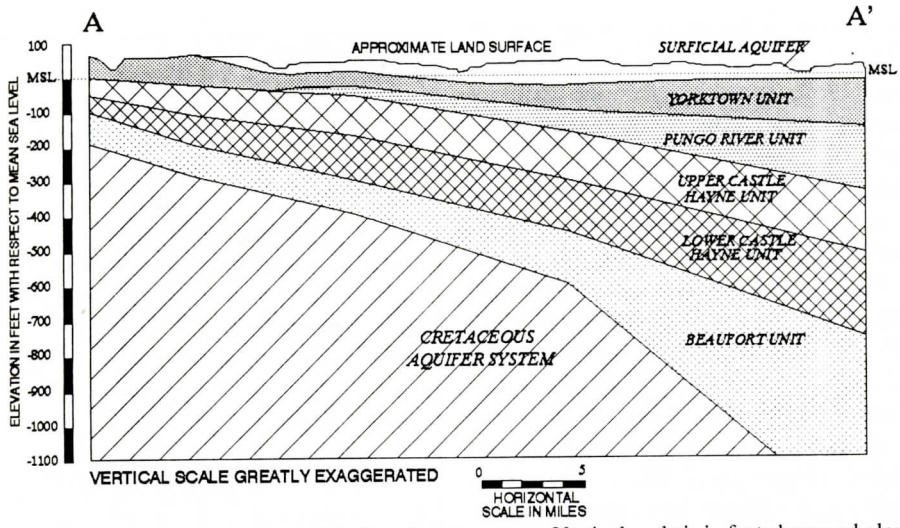

Figure 3. Hydrogeologic cross section of the Pamlico River area. Vertical scale is in feet above or below mean sea level (MSL). Horizontal scales are in miles. The location of the cross section is shown on Figure 1. (Modified from Reynolds, 1992).

hydrology of the Castle Hayne aquifer is influenced by several hydrologic units (Figure 3). The surficial aquifer affects recharge via leakage into the Castle Hayne aquifer. The Yorktown Formation is an aquifer itself but, together with the Pungo River Formation, the two units act as an aquitard above the Castle Hayne. The Beaufort hydrologic unit is a source of ground water moving upward into the Castle Hayne. In some portions of the Coastal Plain southwest of the New River the Castle Hayne is underlain by the youngest of the Cretaceous aquifers, the Peedee (Giese and others, 1991). This unit may also be a source of ground water moving upward into the Castle Hayne.

In 1971 the North Carolina Board of Water and Air Resources, Texasgulf Sulfur, and the NC Phosphate Corporation published a report estimating that 89% of the water pumped from the Castle Hayne aquifer is derived from the UCH (Joint Study, 1971).

Direct recharge to the Castle Hayne aquifer (i.e., water that does not move through confining units) takes place only in areas where the Castle Hayne crops out or is overlain only by permeable sandy materials. Most of these areas are on pocosins, or perched swamps. One inch (2.54 cm) of water, or less, per year moves down from the surficial aquifer into the deeper confined aquifers. Sherwani (1980) estimates that direct recharge to the aquifer is 20 mgd

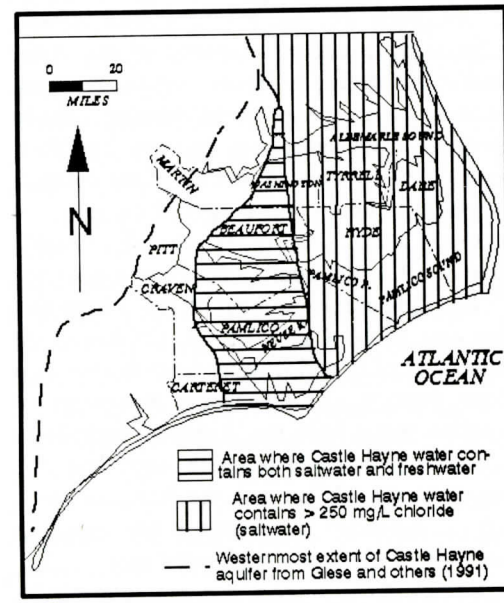

Figure 4. Map showing regions in the study area in which water from the Castle Hayne aquifer is fresh, contains greater than 250 milligrams per liter chloride, and contains both freshwater and saltwater (from Harned and others, 1989).

(876 L/s) north of the Pamlico River and 45 mgd (1971 L/s) south of the Pamlico River. DeWiest (1969) suggested that the recharge area covers approximately 290 square miles (750 km^2).

In the Castle Hayne Aquifer freshwater mixes with water of a dissolved salt composition similar to seawater (Harned and others, 1989) (Figure 4). Subsequent to initiation of pumping at the Texasgulf phosphate mine in 1965 (Figure 5), "the chloride content of the Upper Castle Hayne aquifer in the mine area was about 30 ppm, that of the Lower Castle Hayne 200 ppm, and of the Beaufort formation 3000 ppm" (Sherwani, 1980; p. 48). More recent chemical analyses have shown that the chloride content has increased and that the greatest concentrations occur near the center of pumping (NCDNER, 1976). Following their study of water chemistry at Cherry Point Marine Corps Air Station [about 15 miles (24 km) northwest of Morehead City; Figure 5], Lloyd and Daniel (1988) concluded that recent increases in chloride concentration are probably due to upward movement of water from the deeper parts of the Castle Hayne aquifer induced by excessive pumping of the upper aquifer. According to Heath (personal communication, 1992), the increased chloride is due to upconing from underlying aquifers, but Sherwani (1980) contended that all of the chloride increase cannot be due to upward migration of brackish water. He proposed five possible sources of water-quality deterioration in the UCH: (1) lateral movement of water from farther east in the Castle Hayne, (2) downward movement of brackish water from the Pamlico River estuary, (3) downward movement of brackish water from the Yorktown hydrologic unit, (4) upconing of brackish water from the Lower Castle Hayne and the Beaufort units, and (5) westward movement of the seawater-freshwater interface in the coastal area.

Because these sources can not currently be differentiated, and because all most probably originated as seawater of various ages or in marine formations, all such salty intermixed water will be referred to as "saline formation water" for the remainder of this report. Studies which are currently in progress employing strontium isotopes may allow us to differentiate these sources.

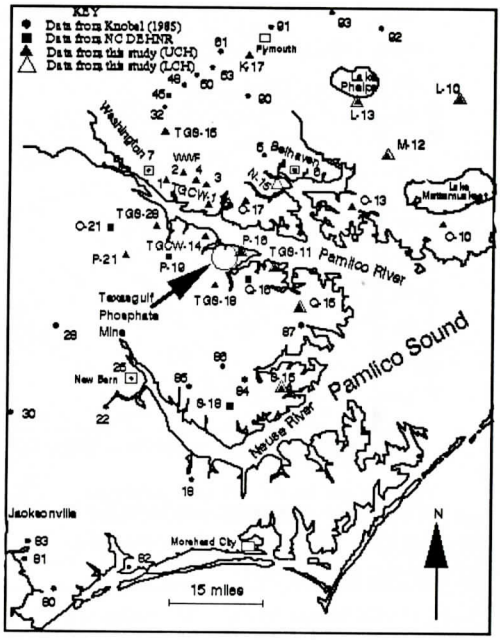

Figure 5. Locations of wells yielding water samples which provided data for Knobel (1985,●), NCDE-HNR (■), and this 1993 study (Δ and ▲). Locations at which wells from both the UCH and LCH were pumped are indicated by a closed triangle inside an open triangle. Open squares (□) indicate the locations of towns. A dot (•) inside an open square indicates that a sample was taken from a municipal well. The location of the Texasgulf phosphate mine is indicated by a large circle near the center of the map.

Previous Studies of Water Chemistry in the Castle Hayne

Chemical analyses of water from the Castle Hayne aquifer are available but there has been no thorough investigation of its chemistry or geochemistry in any region. According to Giese and others (1987), Castle Hayne water is hard (120-180 mg/L as $CaCO_3$) to very hard (>180 mg/L as $CaCO_3$). Hardness is attributed to Ca^{2+} and Mg^{2+} dissolved from limestone and dolomite (Wilder and others, 1978). The hard-

ness is lower near recharge areas and increases with residence time in the aquifer (Giese and others, 1987). Lloyd and Daniel (1988) found that Castle Hayne water has a median dissolved-solids concentration of 300 mg/L and a median pH of 7.25.

High concentrations of dissolved iron typify the aquifer. In recharge areas, iron concentrations often exceed the State drinking water standard of 0.3 mg/L (Giese and others, 1987). For example, water from wells at Cherry Point has a median iron concentration of 0.78 mg/L (Lloyd and Daniel, 1988). As soon as water enters the Castle Hayne aquifer, dissolved iron starts to precipitate. Wilder and others (1978) proposed that the iron concentration in the water is highest near recharge areas because the water has not been in the aquifer long enough for significant iron to precipitate (Wilder and others, 1978).

Wilder and others (1978) reported that silica usually ranges from 20-40 mg/L but occasionally approaches 80 mg/L. High concentrations of manganese (median concentration of 0.08 mg/L) and boron (0.12 mg/L) have also been found at Cherry Point, and chloride was observed to increase from 10 mg/L in 1942 to more than 40 mg/L in 1986 (Lloyd and Daniel, 1988).

Table 1 lists chemical analyses of water samples from the study area collected by the North Carolina Department of Environment, Health, and Natural Resources (NCDEHNR, 1981-1992) that were available to the authors at the time this manuscript was written. Table 2 shows data compiled by Knobel (1985) from the WATSTORE data base of the United States Geological Survey (USGS). This compilation includes only analyses for which electrical neutrality balanced within 5% for samples with TDS > 5 milliequivalents per liter, and within 10% for samples with TDS < 5 milliequivalents per liter.

In Knobel (1985) most of the wells are described as sampling the Castle Hayne Formation with no indication as to whether they penetrate the upper or lower aquifer. Because the UCH contains good-quality water, but the LCH water is relatively brackish (Sherwani, 1980), most of these analyses are probably from the UCH. Many of these samples were analyzed between 1952 and 1965 for a limited number of constituents, utilizing unspecified procedures, from wells for which construction information and depths are unknown.

Knobel (1985) contains many more analyses than are included in Table 2. Analyses for wells from outside the study area are not listed. Many of the analyses reported in Knobel (1985) from wells which were geographically very close to each other were chemically very similar. In this case, only the one well with concentrations nearest the average is reported. When analyses of the same well water sampled at different times were available, only the most recent analysis was listed in Table 2. More than 30 analyses were available for closely spaced wells along a transect from southwest to northeast across Martin County (32-61; Figure 5). Six wells were chosen at reasonable intervals along this transect to give good geographic coverage of the area. In a few cases, because of the probability that some wells may have penetrated the LCH, an analysis was rejected if it had much higher TDS, Cl^-, SO_4^{2-}, etc. than surrounding wells.

The major objective of the current study was to characterize the chemical composition of water from the Castle Hayne aquifer in Capacity Use Area No. 1 (Figure 1) using up-to-date procedures and analytical methods, and clearly distinguishing between samples from the UCH and LCH. [A capacity use area is an area where the use of water resources exceeds, or threatens to exceed, the renewal or replenishment of the resource to the extent that regulation is needed (NCDNER, 1974).] The second objective was to investigate the geochemical processes controlling the water chemistry. Analysis of water chemistry and interpretation of geochemical processes were addressed through a specific set of subobjectives that included determination of the: (1) concentrations of major and trace inorganic constituents, (2) speciation and behavior of inorganic constituents, (3) origin of inorganic constituents, and (4) minerals that are dissolving

Table 1. Representative analysis of important components in Castle Hayne ground water (NCDEHNR, 1978-1992).

WELL IDENTIFIER	Ca^{2+} mg/L	Mg^{2+} mg/L	Na^{+} mg/L	K^{+} mg/L	ALK as HCO_3^- mg/L	SO_4^{2-} mg/L	Cl^- mg/L	SiO_2 mg/L	NO_3^- mg/L	PO_4^{3-} mg/L	F^- mg/L	pH
O-17 (u)	84	23	33	10	390	0	42	29		0.06	0.600	8.2
O-17 (u)	87	22	28	11	390	0	39		0.66	0.06	0.600	7.50
P-21 (u)	63	4	11	1	250	0	6	22	0.44	0.86	0.200	7.50
O-10 (u)					530	26	1,500		<0.044	0.12		8.00
O-10 (u)					540	100	1,700	17	<0.044	0.031	1.200	7.70
L-13 (u)					700	74	26	16	<0.044	0.18		8.3
M-12 (u)	19	33	440	28	640	130	5 10	15	<0.044		1.5	8
M-12 (u)					580	120	620				1.5	7.9
P-16 (u)	64	23	2 1	13	380	5	25	24	0.35	0.9	0.6	7.6
P-16 (u)	52	26	16	11	350	7	16	18	0.44	0.9	0.5	8.1
P-19 (u)	28	4	25	2	90	39	14	11	0.35	0.55	<0.1	5.8
Q-16 (u)	40	31	43	500	356	14	12	22	<0.22	<0.15	0.7	7.5
Q-16 (u)	34	22	40	15	330	<5	20	11	0.26	1.4 1	0.7	8
Q-16 (u)	41	26	56	17	360	7	34	16	0.35	0.34	0.8	8.1
O-21 (u)					230	<5	5	30	<0.044	0.5		7.5
O-21 (u)					220	<5	5		<0.044	0.55		7.8
S-18 (u)	52	31	12	16	364	1	6	49			0.6	7.7
M-12 (l)	150	130	2,800	93	46	440	4,700	3	0.044	0.06 1	0.500	8.9
P-16 (l)	67	50	240	22	440	5	330	23	0.09	0.46	0.700	7.5
P-16 (l)	65	6	19	3	240	5	28	12	<0.044	0.37	1.3	8.1
Q-16 (l)	32	38	230	380	464	15	170	16	<0.22	<0.15	1.3	7.8
Q-16 (l)	18	28	200	24	410	17	200	6	0.22	0.34	1.3	8.6
Q-16 (l)	6	32	220	40	410	10	200	3	0.26	0.43	1.3	9

The letters in parentheses in the first column indicate whether the sample was taken from the Upper or Lower Castle Hayne aquifer.

and/or precipitating along the flow path.

The chemical analyses were also used to study the: (1) differences between the UCH aquifer and the LCH aquifer and (2) regional variability in the UCH and LCH aquifers.

STUDY AREA

Water samples from 29 wells in Capacity Use Area No. 1 (Figures 1 and 5) were collected. Texasgulf, the City of Washington, and the NCDEHNR provided access to the wells sampled. Data previously collected from wells in the area by the USGS and NCDEHNR were also evaluated, and representative analyses were included on many of the figures to follow. The Capacity Use Area includes Beaufort, Pamlico, and Washington counties, and parts of Carteret, Craven, Hyde, Martin, and Tyrrell counties (NCDNER, 1976). Within this area, a permit must be obtained from the state to withdraw over 100,000 gpd (4.4 L/s) of ground water or surface water. Seventeen of the sampled wells have an open interval in the UCH, eight in the LCH, and four are open to both intervals. The locations of all wells providing data for this study are shown on Figure 5. USGS data are indicated with filled circles, NCDEHNR data with closed squares, and data from this study with closed triangles (UCH) and open triangles (LCH).

PROCEDURES

Sampling Procedures

Wells were sampled in accordance with guidelines for the USGS pilot National Water-Quality Assessment Program (Hardy and others, 1989). Detailed sampling and analytical procedures are described in report # 70131 of the Water Resources Research Institute of the University of North Carolina (Sutton and Woods, 1994). Wells were purged a minimum of three well volumes to insure that the sample collected was representative of the water in the aquifer and not of the stagnant water in the well. Either a Myers jet pump or Myers sub-

Table 2. Representative analyses of important components in Castle Hayne ground water [from Knobel (1985).]

WELL IDENTIFIER	Ca^{2+} mg/L	Mg^{2+} mg/L	Na^{+} mg/L	K^{+} mg/L	ALK as HCO_3^{-} mg/L	Cl^{-} mg/L	SO_4^{2-} mg/L	SiO_2 mg/L	NO_3^{-} mg/L	PO_4^{3-} mg/L	F^{-} mg/L	pH
5	49	28	38	24	400	19	0.5	52	1.5		0.6	7.7
6	36	28	188	23	451	185	17	45	0.2	0.06	0.8	7.8
7	65	4			216	5	11	27	0.1			7.1
18	74	6	18	5	292	7	8	34	0.3		0.2	7.4
22	62	4	6	1	203	6	8	12	0.3		0.2	7.4
25	82	2			249	8	8	17			0.1	7.3
28	65	3			209	4	0.5	20	0.1		0.1	7.2
30	69	4	5	3	242	6	1	24	0.4			7.3
32	70	29			360	10	4					8.7
45	78	15			284	8	6					
48	50	47			391	13	8					
50	78	18			276	13	12					
53	58	20			284	9	1					7.6
61	75	24			356	12	3					7.2
80	73	2	9	1	234	9	8	17		0.3	0.1	7.3
81	69	2	6	1	222	7	4	19			0.2	7.2
82	69	2	10	1	226	15	2	25	0.1	0.4	0.2	7.2
83	64	2			200	6	3	16	0.1		0.3	7.1
84	42	51	15	14	410	12	2	59		0.1	0.8	7.8
85	52	12	7	3	224	7	1	78			0.6	7.7
86	42	32	7	7	295	6	1	61			0.6	7.7
87	21	34	134	22	532	19	44	54			0.9	8.2
90	66	30	19	14	396	8	1	50	0.3		0.5	7.7
91	35	45	101	22	322	169	12	36	0.2		0.6	8.5
92	40	50	555	50	604	758	64	40	0.4		0.9	8.1
93	20	24	320	30	606	234	33	34	0.5	0.1	1.1	8.2

mersible pump was used to purge the wells (Table 3). Wells purged with the jet pump were sampled with a Waterra inertial pump; those purged with the submersible were sampled with the same pump.

In wells at least six inches (15.2 cm) in diameter, chemical stability was monitored with a Hydrolab Surveyor II (an in-situ device to determine chemical parameters) placed five feet (1.5 m) below the pump intake; it measured pH, temperature, dissolved oxygen, conductivity, oxidation-reduction potential, and salinity. Temperature, pH, and Eh were also determined before sampling by placing a thermometer and pH and Eh probes in water from the well which was routed into the bottom of a one-liter, plastic beaker. The water flowed out through a tube near the top of the beaker, providing constant circulation.

Samples were collected after the well and the Waterra or submersible pumps were sufficiently purged and chemical stability had been reached. Samples were collected through tygon tubing connected to the outlet of the sampling pump. Unfiltered samples were collected for analysis of silica, fluoride, and dissolved oxygen. Other samples were collected after passing the water through an in-line filter (0.45 μm) and discarding the first 200 mL of water. Concentrated nitric acid was used to preserve 125 mL of sample to analyze for cations by inductively-coupled argon plasma-emission spectrometry (ICAPES). A 125-mL sample was collected to analyze for fluoride, chloride, bromide, nitrite, nitrate, phosphate, and sulfate using high performance liquid chromatography (HPLC). 25 mL of sample for sulfide analysis were added to a bottle containing 25 mL of sulfide anti-oxidant buffer (SAOB; Orion Research Inc., 1989). A 250-mL sample was collected and later frozen to analyze for ammonia, nitrite, nitrate, and phosphate using a spectrophotometer. Samples were placed in an ice chest after collection. Duplicate 50-mL samples collected for alkalinity determination were titrated immediately using a Hach digital titrator. Water samples for dissolved oxygen determinations were placed in an ice chest to be analyzed by the Winkler method (Strickland and Parsons, 1972) while purging the next well.

Table 3. Sample device used at each site.

Well	Sampling Method
K-17 a-5 (u)	Submersible
L-10 a-3 (u)	Jet pump purged, sampled with Waterra alone
L-10 a-5 (l)	Jet pump with Waterra beneath it
L-13 i-1 (u)	Jet pump with Waterra beneath it
L-13 i-5 (l)	Jet pump with Waterra beneath it
M-12 l-1 (u)	Submersible
M-12 l-4 (l)	(May) Jet pump with Waterra beneath it
M-12 l-4 (l)	(July) Submersible
N-15 y-5 (l)	Jet pump with Waterra beneath it
O-10 w-3 (u)	Jet pump with Waterra beneath it
O-13 f-1 (u)	(May) Jet pump with Waterra beneath it
O-13 f-1 (u)	(July) Submersible
O-17 i-2 (u)	Jet pump purged, sampled with Waterra alone
P-16 o-3 (u)	Submersible
P-16 o-4 (u)	Submersible
P-21 k-6 (u)	Jet pump with Waterra beneath it
Q-15 u-3 (u)	Jet pump with Waterra beneath it
Q-15 u-5 (l)	Submersible
S-15 y-3 (l)	Jet pump with Waterra beneath it
S-15 y-4 (u)	Jet pump with Waterra beneath it
TG CW-11A (u)	Jet pump purged,sampled with Waterra alone
TG CW-14 (u)	Outside spigot at private residence
TG S-11 (u)	Pump house spigot at private residence
TG S-11A (l)	Purged with air compressor, sampled with Waterra
TG S-15 (u)	Jet pump purged, sampled with Waterra alone
TG S-18 (u)	Purged with air compressor, sampled with Waterra
TG S-28 (u)	Sampled with both Waterra and air compressor
WWF-1 (b)	Jet pump with Waterra beneath it
WWF-2 (b)	Submersible
WWF-3 (b)	Submersible
WWF-4 (b)	Submersible

To evaluate analytical and sampling error, duplicate samples were collected at approximately every third well during the entire study.

Five of the sampled wells were part of the Texasgulf monitoring network. Two of these, equipped with permanent pumps, were sampled from a spigot (Table 3). After purging (the water was run for about five minutes) a specially designed fitting was attached to the spigot allowing the water to flow through the tygon tubing. The sampling procedure then continued in the same manner as for previous wells. Due to permanent fittings on top of the other wells (TGS-11A, TGS-18, TGS-28), they had to be pumped using an air compressor. Compressed air was introduced into the top of a drop pipe, which penetrated well below the surface of the water (probably as much as 40 feet (12 m) in some cases). Air pumped down the well pushed water out of a hole in the side of the casing near the top of the well. This configuration produced a flow rate of approximately 60 gpm (3.8 L/s), so the wells were purged up to ten well volumes. After purging, the Waterra pump was inserted through the drop pipe and the samples were collected as previously described. Analyses of well waters collected in this manner showed anomalous results for alkalinity, dissolved oxygen, pH, and Eh.

Laboratory Procedures

High Performance Liquid Chromatography

Samples for HPLC were analyzed within 24 hours on a Waters ion chromatograph with a conductivity detector in the Trace Element Laboratory at the East Carolina University School of Medicine. Before any of the samples were analyzed, the linearity of the chromatograph was checked using different concentrations of chloride (2 - 800 ppm) and sulfate (4 - 1600 ppm). A correlation coefficient of 0.99 was calculated. Samples with high chloride concentrations were analyzed twice, once undiluted and once diluted 1:10. Because the concentrations of nitrate, nitrite, and phosphate were expected to be near the detection limits, these anions were also determined by spectrophotometry. Fluoride concentrations were checked by ion selective electrode.

Chloride concentrations determined by HPLC were usually higher than those determined by titration, and for five wells there was a substantial difference (15-105%). This discrepancy was not noticed until two months after completion of HPLC analyses, so samples that had been frozen since collection were reanalyzed by Mohr titration, except for those with concentrations too low to titrate accurately (<36 ppm). Examination of chromatograms and data did not reveal the source of the error. However, for a few of the samples analyzed later in the study, standard peaks collected following sample analysis seemed to be slightly broader than initial standard peaks. Representatives of the chromatograph manufacturer suggested that concentrations may have been too high.

Spectrophotometry

Samples for silica analysis were kept refrig-

erated and analyzed within a week of collection by the molybdosilicate method (Stainton and others, 1974). Five standards were used each week [100, 200, 300, 400, and 500 µg/L (made from Fisher silica reference solution)] and a correlation coefficient of at least 0.998 was obtained each time. All samples were diluted 1:100 before analysis.

Nitrate, nitrite, phosphate, and ammonia from frozen samples were slowly thawed in a cold room 18 hours before analysis. Nitrate was reduced to nitrite with cadmium powder, and a solution of sulfanilamide and N-(1-naphthyl) ethylene-diamine dihydrochloride was added as the color agent (American Public Health Association, 1992). The same color reagent was added to untreated samples to determine the amount of nitrite only; this concentration was subtracted from the total nitrate + nitrite concentration to determine the concentration of nitrate. Potassium nitrate and sodium nitrite standards of 0.5, 1.0, 2.0, 3.0, and 5.0 micromolar were used. Phosphate was determined as phosphomolybdate using ascorbic acid as a reductant (American Public Health Association, 1992). Ammonia concentrations were determined by the phenolhypochlorite method (Solorzano, 1969).

Ion Selective Electrode

Sulfide samples were analyzed within a week of collection. The samples had very low levels of sulfide and could not be directly titrated with lead perchlorate; therefore, three sulfide standards were prepared periodically using reagent grade $Na_2S{\cdot}9H_2O$ and distilled, deaerated water. These standards were titrated with lead perchlorate to determine their concentrations and were then used to generate a calibration curve. The standards had concentrations such as 701, 71, and 7.1 ppm sulfide. Using a pH meter and an Orion Ag^+/S^{2-} electrode, the concentration of sulfide in the samples was determined by comparing the potential generated by the samples with the prepared calibration curve.

An Orion combination fluoride electrode was used to measure fluoride concentration. Samples were compared to working standards of 1.9 and 0.19 ppm F^- made from a stock solution of 0.4199 g NaF/L.

ICAPES

Inductively-coupled argon-plasma emission spectrometry (ICAPES) analyses were performed for 28 major and trace ions: aluminum, arsenic, beryllium, cadmium, calcium, chromium, cobalt, copper, iron, lead, lithium, magnesium, manganese, molybdenum, nickel, phosphorous, potassium, selenium, silica, silver, sodium, thallium, tin, titanium, uranium, vanadium, yttrium, and zinc. The samples were digested with nitric and hydrochloric acids before analysis. Only nine cations were found to have usable, reproducible concentration data (Tables 4 and 5).

Chloride Titration

To check the chloride concentrations determined by chromatography, samples containing more than 36 ppm chloride were titrated with $AgNO_3$ (Strickland and Parsons, 1972). Chloride standards of 5887, 3007, 973, 498, 264, and 116 ppm chloride were titrated using the same method applied to the samples.

RESULTS

Summaries of the concentrations of major and minor components determined for samples collected in 1993 are given in Tables 4 and 5. L-10 a-3, L-10 a-5, and TGCW-11A were the only sites at which the electrical neutrality was not balanced within 10%. Wells O-13 f-1 and M-12 l-4 were analyzed on two different dates so they are listed twice in these tables. Chloride concentrations for well waters containing less than 36 ppm chloride were determined by HPLC, whereas, more concentrated waters were analyzed by $AgNO_3$ titration.

Statistical Analysis of Results

Relative standard deviations (Rel.Std.Dev. in Tables 4 and 5; given as%) for all compo-

nents were calculated from pairs of duplicate analyses (except for chloride analyses of waters with greater than 36 ppm chloride). Wells for which duplicate samples were analyzed are indicated with an asterisk in Table 4, and the average concentration of the two is reported. The relative standard deviation was calculated by determining the standard deviation for each pair of duplicate analyses, dividing that number by the average concentration of the component in the sample, multiplying by 100, and then calculating the average relative standard deviation using all pairs of duplicate analyses. The relative standard deviation for each component determined the number of significant figures reported in the tables.

Only one analysis was replicated for waters with low chloride concentration (TGS-11); therefore, the relative standard deviation (2%) for chloride in these dilute samples (< 36 ppm, analyzed by HPLC) is based on a single duplicate analysis. For waters with higher chloride concentrations (analyzed by $AgNO_3$ titration) titrations of standards yielded concentrations which differed from the known concentrations by an average of 3.5% with a range of 0.02-8.95%. A value of 4% is, therefore, used in Table 4 to approximate the relative standard deviation of the chloride analyses.

The relative standard deviation reported for sulfide in Table 5 is an estimate. For samples containing greater than 0.5 ppm sulfide, the manufacturer of the Ag^+/S^{2-} electrode reports a relative standard deviation of 4 %. The precision of the method decreases, however, for samples of lower concentration; therefore, a value of 10% was applied to the sulfide analyses reported.

Accuracies of the ICAPES analyses are expressed as% recovery of the cations in a NIST-certified standard. Percent recoveries for Al, Ca, Fe, Li, Mg, Mn, Na, and Zn were 100, 100, 74, 85, 100, 97, 96,and 100, respectively. Percent recovery was not calculated for K, which was absent from the standard.

Results of previous analyses [NCDEHNR and USGS (Knobel, 1985); (Tables 1 and 2)] agree well with those from the 1993 study.

Comparison of Concentrations of Ions in Upper Castle Hayne and Lower Castle Hayne

The ranges in concentrations of aqueous species for the UCH and LCH, and any seemingly anomalous values, are listed in Table 6. Much

Table 4. Concentration of major components in Castle Hayne ground water. (Chloride by titration unless <36 ppm. Values <36 ppm were determined by chromatography.)

WELL IDENTIFIER	TEMP. (°C)	pH	Eh mv	TDS ppm	HCO_3^- ppm	Cl^- ppm	SO_4^{2-} ppm	Na^+ ppm	K^+ ppm	Ca^{2+} ppm	SiO_2 ppm	Mg^{2+} ppm
K-17 a-5 (u)	18	7.39	-60	970	395	243	37	164	23	49	17.6	37
L-10 a-3 (u)*	22	7.37	-130	4690	600	1770	340	1690	82	54	14.8	127
L-10 a-5 (l)	21	7.31	-140	8650	498	3630	790	3130	124	129	10.6	318
L-13 i-1 (u)	18	8.05	-160	1290	783	55	90	305	22	7	16.3	12
L-13 i-5 (l)	20	7.67	-160	1830	642	510	90	470	36	20	17.7	38
M-12 l-1 (u)*	20	7.44	-130	2090	688	520	180	560	39	21	16.8	41
M-12 l-4 (l)	20	7.33	-140	10,900	468	5500	1600	3190	103	131	17.3	251
M-12 l-4(l)*	22	7.03	-160	10,600	468	5100	1100	3360	121	140	17.8	273
N-15 y-5 (l)*	20	7.46	-110	2090	517	760	120	550	37	30	17.4	49
O-10 w-3 (u)	20	7.38	-140	3730	574	1790	160	980	54	41	18.1	96
O-13 f-1 (u)*	20	7.67	-140	1700	570	470	110	450	27	18	20.2	25
O-13 f-1 (u)*	20	7.57	-120	1720	556	470	110	480	29	19	19.5	28
O-17 i-2 (u)*	18	7.15	-40	620	393	54	0	28	11	74	32.2	25
P-16 o-3 (l)*	21	7.23	-60	1380	478	380	14	323	26	71	25.3	52
P-16 o-4 (u)	20	7.18	-60	590	407	35	0	19	13	57	31.0	28
P-21 k-6 (u)	16	7.27	0	370	242	7	0	10	1	77	22.8	4
Q-15 u-3 (u)	20	7.41	-110	950	503	134	35	170	18	29	26.4	32
Q-15 u-5 (l)*	20	7.49	-120	3660	542	1390	610	920	40	41	20.3	80
S-15 y-3 (l)	22	6.89	-100	2440	453	1030	140	560	31	84	26.0	96
S-15 y-4 (u)	19	7.17	-80	640	444	27	0	22	12	63	27.8	38
TGCW11A (u)*	18	7.09	-50	530	371	9	0	11	4	81	37.1	9
TGCW14 (u)	23	7.27	-100	380	264	6	0	8	1	69	20.8	5
TG S-11 (u)*	20	7.21	-110	610	415	24	0	39	16	51	29.3	30
TG S-11A (l)	22	7.29	-130	4900	532	2260	380	1470	58	57	18.5	102
TG S-15 (u)	17	6.92	10	520	346	13	0	15	2	82	37.4	7
TG S-18 (u)	22	7.41	-100	490	329	5	0	43	13	49	29.1	19
TG S-28 (u)	18	7.03	-70	530	361	7	0	10	4	103	32.6	6
WWF #1 (b)	17	7.34	-60	310	215	7	1	6	1	59	17.3	1
WWF #2 (b)	17	7.34	-30	360	249	4	0	10	1	63	27.8	3
WWF #3 (b)	17	7.30	-50	380	273	8	0	7	2	62	21.2	4
WWF #4 (b)	17	7.20	-60	390	273	5	0	9	2	65	32.3	4
Rel. Std. Dev.					1	4	10	2	3	3	1	4

Table 5. Minor and trace element analyses of Castle Hayne ground water. A dashed line was used when the accurate concentration of iron was not known, due to particulates in some of the samples. (ND = not determined)

WELL IDENTIFIER	Br^- ppm	F^- ppm	S^{2-} ppm	NH_4^+ ppm	NO_3^- ppm	PO_4^{3-} ppm	Al ppm	Fe ppm	Li^+ ppm	Mn ppm	Zn ppm
K-17 a-5 (u)	0	0.55	0.12	0.92	<0.001	0.009	0.03	0.21	0.03	<0.01	0.06
L-10 a-3 (u)	3	1.33	ND	6.62	0.001	0.012	0.07	--------	0.08	0.05	0.01
L-10 a-5 (l)	8	1.17	0.06	7.89	<0.001	0.016	0.03	--------	0.11	0.02	0.01
L-13 i-1 (u)	0	1.96	ND	1.04	0.001	0.064	0.09	0.32	0.02	0.01	0.01
L-13 i-5 (l)	7	1.29	ND	1.49	0.001	0.017	0.09	0.26	0.03	0.01	<0.01
M-12 l-1 (u)	3	3.20	1.6	2.28	0.004	0.009	0.02	0.19	0.05	0.01	0.01
M-12 l-4 (l)	5	1.31	ND	5.07	0.003	<0.001	0.03	--------	0.09	0.07	<0.01
M-12 l-4 (l)	4	1.35	2.4	5.42	0.006	0.003	0.09	0.67	0.10	0.01	0.21
N-15 y-5 (l)	5	1.19	0.02	0.80	0.002	0.015	0.06	--------	0.04	0.02	0.02
O-10 w-3 (u)	9	1.20	ND	3.99	0.002	0.023	0.11	0.82	0.06	0.05	<0.01
O-13 f-1 (u)	3	1.49	0.06	1.03	0.002	0.039	0.09	--------	0.03	0.03	0.02
O-13 f-1 (u)	2	1.52	0.47	1.44	0.004	0.012	0.01	0.15	0.03	<0.01	0.02
O-17 i-2 (u)	0	0.60	0.01	0.88	0.002	0.004	0.03	0.78	0.03	0.03	0.01
P-16 o-3 (l)	4	0.75	7.1	1.18	0.001	0.015	0.02	0.25	0.03	<0.01	0.09
P-16 o-4 (u)	0	0.58	0.03	0.93	<0.001	0.028	<0.01	0.22	0.01	<0.01	0.03
P-21 k-6 (u)	0	0.27	0.01	0.15	0.002	0.086	0.17	4.80	0.01	0.09	0.01
Q-15 u-3 (u)	0	1.11	2.6	0.77	0.000	0.040	0.02	0.19	0.02	0.01	<0.01
Q-15 u-5 (l)	16	1.65	1.1	0.90	0.002	0.017	0.03	0.29	0.04	0.01	0.06
S-15 y-3 (l)	0	0.75	2.6	1.12	0.004	0.003	0.22	0.40	0.03	<0.01	<0.01
S-15 y-4 (u)	0	0.56	0.57	0.58	0.000	0.006	0.02	0.19	0.01	0.01	<0.01
TG CW-11A (u)	0	0.61	5.8	0.79	0.002	0.023	0.01	0.48	0.03	0.01	0.01
TG CW-14 (u)	0	0.29	0.02	0.25	0.001	0.004	0.01	0.71	0.01	0.01	0.16
TG S-11 (u)	0	0.70	0.28	0.98	0.002	0.004	<0.01	1.08	0.02	0.01	<0.01
TG S-11A (l)	23	1.71	0.01	1.19	0.005	0.003	0.10	0.43	0.06	0.02	1.88
TG S-15 (u)	0	0.19	0.02	0.48	0.006	0.042	0.05	--------	0.04	0.34	0.02
TG S-18 (u)	0	1.01	0.04	0.76	0.005	0.003	0.16	0.23	0.02	<0.01	1.51
TG S-28 (u)	0	0.23	0.01	0.38	0.002	0.004	0.06	3.30	0.03	0.15	1.04
WWF#1 (b)	0	0.15	ND	0.06	<0.001	0.076	0.04	2.90	0.01	0.08	0.01
WWF #2 (b)	0	0.19	0.00	0.21	0.003	0.025	0.07	2.90	0.02	0.13	0.06
WWF #3 (b)	0	0.40	0.00	0.34	0.001	0.037	<0.01	1.20	0.02	0.06	0.09
WWF #4 (b)	0	0.27	0.01	0.33	<0.001	0.025	0.05	1.10	0.03	0.07	0.16
Rel. Std. Dev.	11	1	10	3	19	15	100	9	3	12	18

of this information will be discussed in more detail in a later section but a brief summary of important results follows.

TDS, chloride, and sulfate concentrations in the LCH are generally higher than those in the UCH at the same well site, and chloride is the major contributor to the TDS in the LCH. Alkalinity in the UCH generally increases from west to east but no geographic trend for the LCH is obvious. In the northeastern portion of the study area, the UCH wells have higher fluoride concentrations than those in the LCH. The high chloride-sulfate wells at the M-12 location have higher fluoride concentrations than surrounding wells. Bromide was found in all LCH wells, except for S-15 y-4, and in four of the eastern UCH wells. Bromide concentrations in LCH wells were always higher than those in UCH wells at the same location.

LCH wells always have higher concentrations of sodium, potassium, magnesium, and calcium than UCH wells at the same location. The eastern wells in the UCH were generally lower in silica than western wells, but there was no consistent relationship between silica concentrations of the UCH and LCH at the same location.

Improper filtration procedures at some wells (L-10 a-3, L-10 a-5, TGS-15, N-15 y-5, and the first samples taken at O-13 f-1 and M-12 l-4) allowed steel particulates from the well casing to pass through, so Fe concentrations are not given for these wells in Table 5. The reported manganese concentrations for these samples are also suspect. Iron was analyzed by ICAPES and the recovery was only 74% compared to 85 - 100% for all other cations. Within analytical error, the iron concentrations are similar in the UCH and LCH wells.

Of the minor cations (excluding Fe and Mn) analyzed by ICAPES, only Al, Li, and Zn gave usable, reproducible results. Where there was a significant difference between the concentrations of these cations in UCH and LCH wells, the UCH had lower concentrations than the LCH. Li in the UCH appears to increase from southwest to northeast and is higher in the LCH than in the UCH. The concentration of Al may increase outwards in all directions from the region south of Belhaven. No clear trend in Zn concentrations was observed.

Where wells penetrated both units the ammonia concentrations in the LCH were always higher than those of the UCH. No nitrite was found in the samples, and the patterns of nitrate

Table 6. Concentration ranges of aqueous species

Ion or other diss. spec.	Range in concentration (ppm unless noted)		Wells with anomalously low or high concentrations			
	UCH	LCH	LOW		HIGH	
			Well	Conc	Well	Conc
TDS	320 - 3730	1380-10600				
Cl^-	4 - 1790	380 - 5100	L-13 (U)	55	TGS-11aL	2260
			L-13 (L)	510	M-12 (L)	5100
$SO_4^=$	0 - 340	14 - 1100			TGS-11aL	380
					M-12 (L)	1100
					Q-15(L)	610
Alk	215 - 783	453 - 642			L-13 (U)	783
F^-	0.15-3.20	0.75-1.71			M-12 (L)	1.35
					M-12 (U)	3.20
Na^+	6 - 1690	323 - 3360			TGS-11aL	1470
					Q-15(L)	920
K^+	1 - 82	26 - 124				
Ca^{2+}	7 - 103	20 - 140				
Mg^{2+}	1 - 127	37 - 318				
Hard	69 - 658	204 - 1632				
SiO_2	11 - 26	15 - 38				
Iron	0.15-4.8	0.25-0.67				
NH_4^+	0.06-6.62	0.80-7.89				
NO_3^-	0 - 0.006	0 - 0.006				
PO_4^{3-}	0.003-.086	.003-.017				
S^{2-}	0 - 5.8	0.007-7.1			TGCW11aU	5.8
					P-16 (L)	7.1
pH	6.92-8.05	6.89-7.67				
Eh-mV	2 to -160	-60 to-160				

Alk = alkalinity as ppm HCO_3^- U = UCH sample L = LCH sample
[Hard = hardness, mg equivalent $CaCO_3$/L = 2.497(Ca, mg/L) + 4.118(Mg, mg/L) (American Public Health Association, 1992)]

and phosphate distribution were unclear, although phosphate concentrations appeared to be higher in the UCH. No consistent difference was seen in the sulfide values of the UCH and LCH.

Dissolved oxygen, detected in seven samples, ranged from 0.032 - 1.000 mg/L, but problems with sampling procedures at four wells suggest the values greater than 0.06 mg/L were inaccurate. The average pH for both the UCH and LCH was 7.30 with no consistent relationship observed between UCH and LCH wells at the same location. Eh values for the UCH are generally more positive than those for the LCH, suggesting that the UCH waters are more oxidizing.

DISCUSSION

Recharge Area and Rainfall Composition

Direct recharge to the Castle Hayne takes place only in areas where the Castle Hayne crops out, or is overlain only by permeable sandy materials (Figure 6). In these localities the aquifer is essentially unconfined. The major source of direct recharge to the Castle Hayne is rainfall. Estimates of the chemical composition of average rainfall in eastern North Carolina are given in Table 7. Recharge also occurs by leakage from overlying and underlying units and depends on the vertical hydraulic conductivity of the confining units and the head differences of the aquifers separated by the confining layers (Giese and others, 1991).

Methodology

Location of wells penetrating the UCH and LCH sampled in 1993 for this study are shown on Figure 5. Contour maps were drawn to reveal geographic trends in the concentrations of many aqueous species. Chemical data from the USGS (Knobel, 1985) and NCDEHNR are

included on maps showing concentrations of Ca^{2+}, Mg^{2+}, Na^{+}, SO_4^{2-}, HCO_3^{-}, and Cl^{-} in the UCH. For the USGS data only two samples were clearly distinguished as coming from the LCH; however, because water quality of the LCH is so much poorer than that of the UCH, it was assumed that the remainder of the analyses were for well waters of the UCH.

The four wells from the Washington well field (WWF) were included on the UCH maps because most of their water is derived from the UCH. Warner (1993) performed two aquifer tests on one well located south of WWF-1 and WWF-2 in the Washington well field. During the first test, the well was open to the entire Castle Hayne. For the second test, the portion of the well penetrating the LCH was filled with sand and sealed. Analysis of test results indicated that 70% of the water from this well comes from the UCH.

The computer program PHREEQE (Parkhurst and others, 1980) was used to determine the chemical speciation of solutes and to determine the saturation state of various mineral phases. Forty-two common carbonates, sulfates, hydroxides, oxides, sulfides, phosphates, and framework and layer silicates were examined. Calcite, dolomite, chalcedony, quartz, gibbsite, kaolinite, albite, microcline, muscovite, Ca-montmorillonite, illite, hematite, and goethite were saturated in many of the ground waters sampled. Siderite, chlorite, alunite, talc, and pyrite were saturated in a few samples. Solutions were undersaturated with respect to amorphous silica.

Figure 6. Region of direct recharge to the Castle Hayne aquifer [modified from DeWiest (1969)].

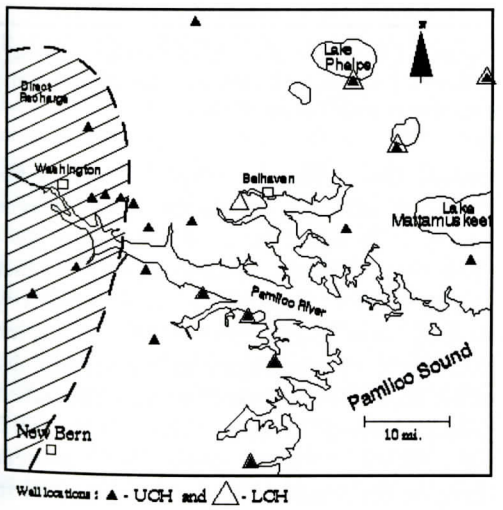

Table 7. Average chemical composition of rainfall in the recharge area of the Castle Hayne aquifer.

Ion	Concentration (ppm)	Ion	Concentration (ppm)
Na^{+}	0.27[3] - 1[2]	Cl^{-}	2[2,4]
K^{+}	0.1[1] - 0.2[2]	SO_4^{2-}	1.6 - 2[5]
Mg^{2+}	0.15[1]	NO_3^{-}	0.4 - 4[3,5,6]
Ca^{2+}	0.08[3] - 0.65[1]	NH_4^{+}	0.21 - 0.61[3,6]

1 from Gambell and Fisher 1966
2 from Junge and Werby 1958
3 from Willey and Kiefer 1993
4 from Willey and Kiefer 1990
5 from Willey et al. 1988
6 from D. Daniels, pers. comm.

Major Constituents

Calcium and Magnesium

Calcium is the most abundant cation in the dilute Ca-HCO_3 waters from the UCH in the western part of the study area (Figure 7). Local rainfall (0.08 - 0.65 ppm calcium; Table 7) is not a significant source of calcium; however, calcite and dolomite are major constituents of the aquifer, and most of the calcium is derived from limestone dissolution. No clear pattern of variation in the concentration of Ca^{2+} in the LCH emerged, but intermixing of saline formation water is probably significant in eastern wells.

Magnesium shows a general increase from west to east in the UCH (Figure 8), with a low in the region near Belhaven and Lake Phelps. The highest magnesium concentrations are found in the northeast in the LCH, but lack of data in the west makes it difficult to determine the trend. Local rainfall contains an average of 0.15 ppm of magnesium (Table 7), so it is not a significant contributor to magnesium concen-

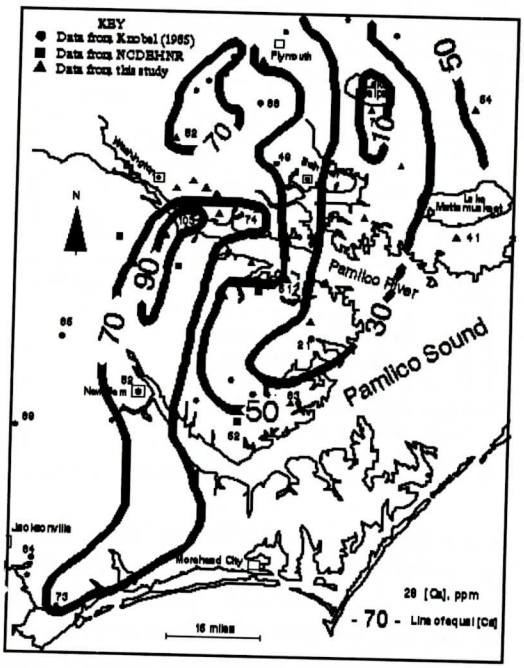

Figure 7. Concentrations of calcium (ppm) in waters of the Upper Castle Hayne.

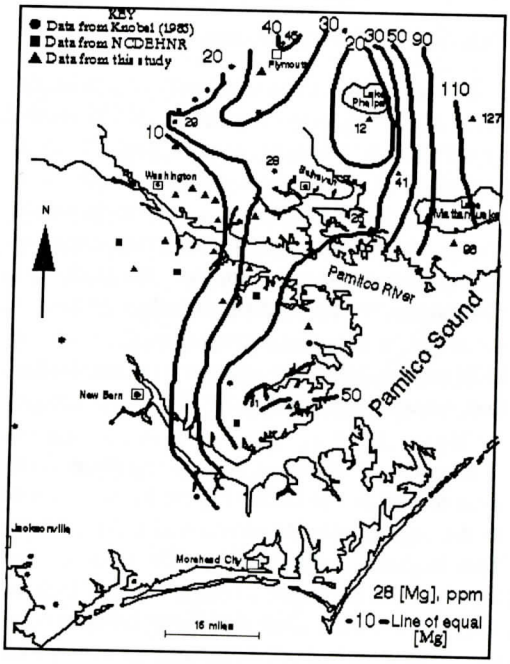

Figure 8. Concentrations of magnesium (ppm) in waters of the Upper Castle Hayne.

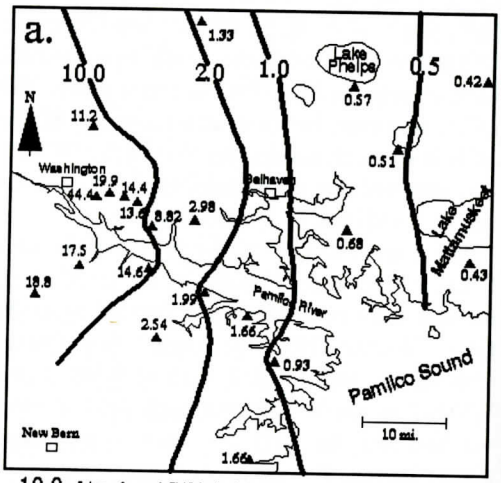

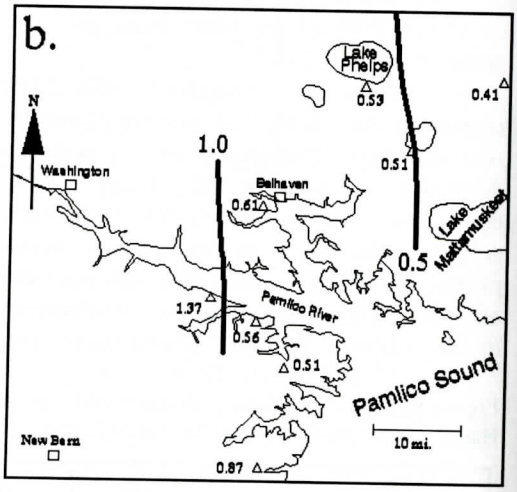

Figure 9. Distribution of the ratios of calcium to magnesium (by weight) in waters from the Upper (a) and Lower (b) Castle Hayne.

tration. Dissolution of dolomite and magnesium-rich calcite found in the Castle Hayne aquifer is an important contributor of magnesium, but Ca^{2+}/Mg^{2+} ratios suggest another source as well. Maps of Ca^{2+}/Mg^{2+} ratios (by weight) show high values to the west which decrease to the east (Figure 9). The mineralogy of the aquifer is dominated by calcite; abundant dolomite, where it occurs, could only lower the ratio to 1.65. The diagrams show a clear decrease in the ratio to values as low as 0.41 in

the eastern portion of the study area. The Ca^{2+}/Mg^{2+} ratio in average seawater is 0.32.

According to Sprinkle (1989), Mg^{2+} concentrations in the Floridan aquifer (which is primarily limestone) may equal or exceed Ca^{2+} concentrations in areas where brackish or saline waters are present; therefore, data presented here suggest mixing with saline formation water. Near Lake Phelps, where the Ca^{2+} and Mg^{2+} concentrations are anomalously low (Figures 7 and 8), the Ca^{2+}/Mg^{2+} ratio is similar to others in the area (Figure 9). This suggests that the process which is diluting Ca^{2+} and Mg^{2+} concentrations at this site is not affecting the proportions of Ca^{2+} and Mg^{2+}.

Bicarbonate

Bicarbonate is one of the principal anions found in the UCH. The predominance of Ca^{2+} and HCO_3^- ions in wells from the western part of the study area suggests that the bicarbonate is largely due to limestone dissolution, which is enhanced by the presence of dissolved CO_2 in recharge water. Alkalinities measured in this area are typical of waters whose composition is dominated by $CaCO_3$ dissolution (Sprinkle, 1989; Trainer and Heath, 1976). Carbonate buffering maintains the pH of the ground water between 6.9 and 8.1, and HCO_3^- is the predominant carbonate species in this range. Alkalinity in the UCH generally increases from west to east (Figure 10a).

Water from the area near Lake Phelps, typified by data collected at the L-13 site, has very high alkalinities (UCH=783 ppm and LCH=642 ppm; Figure 10) and low calcium and magnesium concentrations. The high HCO_3^- concentrations are balanced by Na^+. Similar high HCO_3^--low Ca^{2+} water was found where the Floridan aquifer is overgrown by hardwood and pine forests. Following traditional thinking that the source of bicarbonate in sodium-bicarbonate ground water is oxidation of organic materials (Chapelle, 1983), Sprinkle (1989) suggested that decaying forest litter produces waters high in soluble organic acid anions. He theorized that these organic acid anions would be titrated in addition to inorganic carbon species, thus giving higher alkalinities. Trainer and Heath (1976) also found that high concentrations of organic matter in soils resulted in a relatively high alkalinity in soil water. The high alkalinities in the area of Lake Phelps may be due to recharge through organics in overlying swamps and pocosins. The dominance of Na^+ over Ca^{2+} and Mg^{2+} may be a result of ion exchange of $2Na^+$ in clay min-

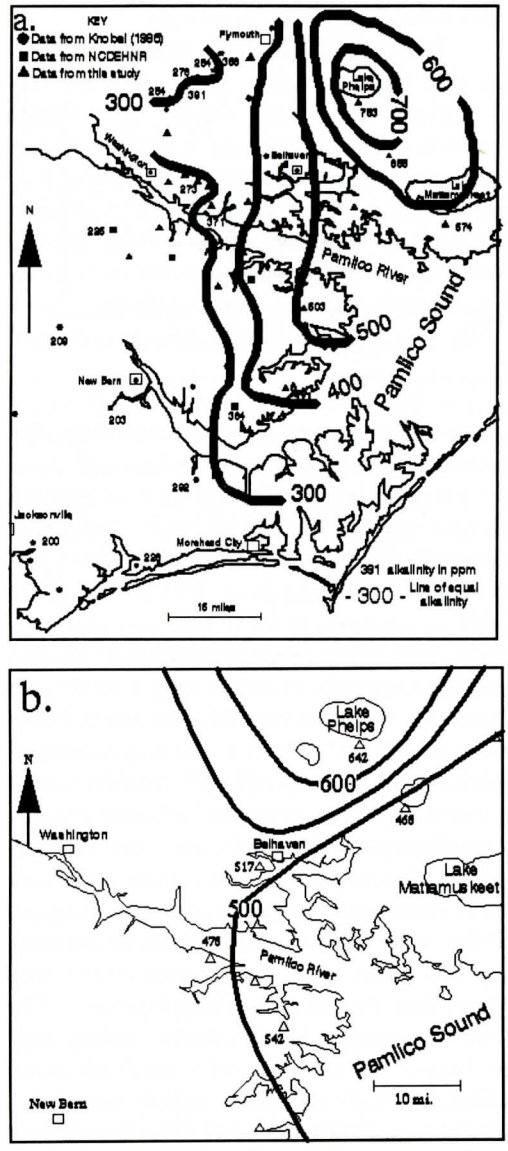

Figure 10. Alkalinity (in ppm of HCO_3^-) in ground waters of the Upper (a) and Lower (b) Castle Hayne.

erals for Ca^{2+} and Mg^{2+} in solution.

Besides L-13 i-1, TGS-28 has an alkalinity (361 ppm) which is higher than the surrounding wells and which is probably inaccurate. This number is not listed in Table 6 nor was it considered in the contouring of Figure 10a. TGS-28 was sampled with an air compressor (the footvalve came off the Waterra sampling pump and was lost in the well) yielding a sample of questionable reliability.

The saturation index of a mineral is defined as

$$\text{saturation index} = \log (IAP/K_T)$$

where IAP is the ion activity product of the dissolved components in the solution, and K_T is the solubility product of the solid or gaseous phase at the specified temperature. The calcite saturation index ranged from -0.20 to 0.11 in the UCH aquifer and from -0.25 to 0.11 in the LCH. A saturation index of zero indicates saturation but because of the possibility of CO_2 outgassing and errors in determination of pH and alkalinity, Sprinkle (1989) considered that a saturation index of -0.2 to +0.2 is indicative of calcite saturation in the Floridan aquifer.

According to this criterion, all waters in this study, except for S-15 y-3, are saturated with calcite. The negative values of the saturation index occurred at the eastern and western edges of the study area. The low values to the west suggest waters are less saturated in the area where direct recharge occurs (Figure 6). The lower saturation index observed to the east may be related to intrusion of saline formation water. Although S-15 y-3 is slightly undersaturated with calcite (-0.25), its UCH counterpart S-15 y-4 is saturated (0.03).

The saturation index of dolomite ranged from -1.60 to 0.78 in the UCH and from -0.12 to 0.99 in the LCH. Sprinkle (1989) considered that a saturation index of -0.4 to +0.4 indicates saturation. The degree of dolomite supersaturation was generally higher in the LCH than in the UCH at a given sample location. The saturation index of dolomite increases from west to east in the UCH, but no clear pattern emerged for the LCH. Dolomite was oversaturated (>0.4) in the northeastern part of the study area in both Castle Hayne aquifers. Sprinkle (1989) stated that apparent oversaturation of dolomite in the Floridan aquifer could be due to (1) errors in pH and alkalinity measurements, (2) local mixing of chemically different waters, (3) local occurrence of more soluble dolomites, or (4) inhibition of dolomite crystallization due to kinetic effects. In Castle Hayne waters Mg^{2+} concentration increases downgradient where dolomite is saturated or over-saturated. Perhaps Mg^{2+} is being introduced from saline formation water, and the accompanying increase in sulfate inhibits dolomite precipitation (Baker and Kastner, 1981).

Sulfate

Sulfate concentration increases from west to east in both the UCH and the LCH (Figure 11). Average rainfall in eastern North Carolina contains approximately 1.6-2 ppm of SO_4^{2-} (Table 7), but no SO_4^{2-} was found in water in the area where direct recharge occurs (Figure 6); therefore, the SO_4^{2-} is apparently being removed from solution by processes that have not yet been identified.

No sulfate minerals have been reported in mineralogical studies of the Castle Hayne. Figure 12 shows a gypsum trend and a seawater trend on a graph of SO_4^{2-} concentration versus SO_4^{2-}/ Cl^- ratio. These trends may be used to identify the sources of SO_4^{2-} in a water sample. Points A and B represent the SO_4^{2-} and Cl^- concentrations found in dilute ground water, with point B representing a more mineralized starting point. Analyses that plot near line A-C or B-D indicate that gypsum is the primary source of SO_4^{2-}, and analyses that plot along line A-E or B-E represent a mixing trend with seawater (E). The water samples from the Castle Hayne aquifer fall along the seawater trend, which indicates that seawater is the primary source of SO_4^{2-}. The upwards shift from the seawater ratio could be due to analytical problems experienced with the chromatograph.

Gypsum is undersaturated over the entire study area, but the saturation index increases from west to east. The gypsum saturation trend appears to be very similar to the dolomite satu-

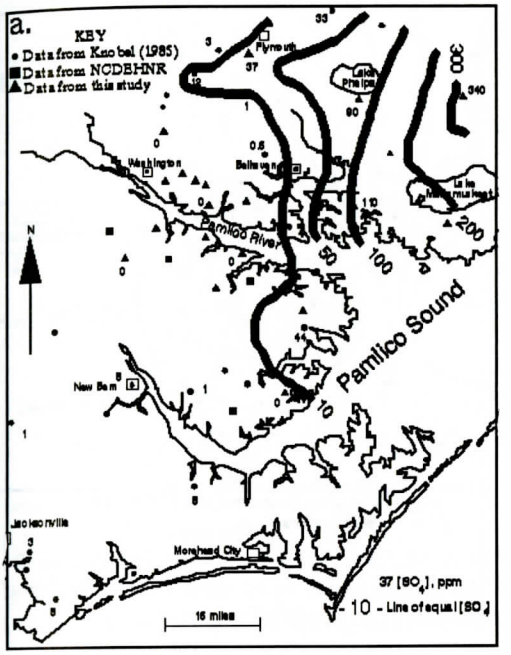

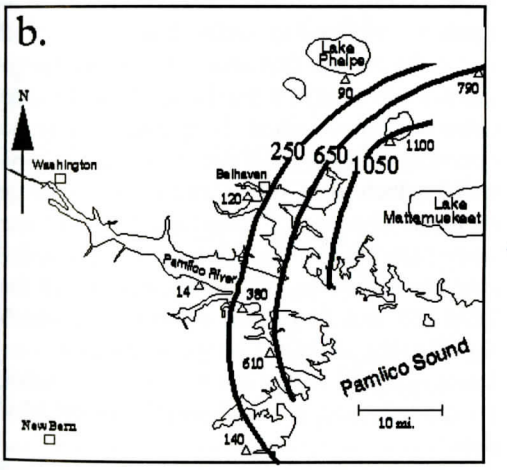

Figure 11. Sulfate concentrations in ground waters of the Upper (a) and Lower (b) Castle Hayne. The drinking water limit for the state of North Carolina is 250 ppm (NCDEHNR, 1989).

ration trend and probably changes as a result of intrusion of saline formation water rich in SO_4^{2-}.

Chloride

The chloride contents of some waters from UCH wells in the western region (Figure 13a) appear to have been acquired in the subsurface

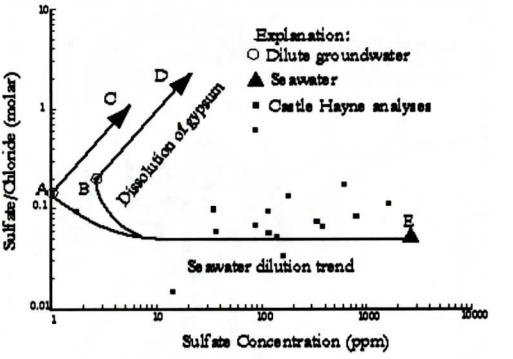

Figure 12. Molar ratios of sulfate to chloride plotted versus sulfate concentrations (ppm) for average dilute ground waters, seawater, and water from the Castle Hayne. Lines on the graph indicate the chemical evolution of ground waters in which gypsum is dissolving (A-C and B-D) or seawater is intermixing (A-E and B-E) [modified from Rightmire and others, 1974].

because the chloride content of local rainfall is only about 2 ppm (Table 7). Transpiration and evaporation are very active within capillary fringes above the water table (Nesbitt and Cramer, 1993). Soil and ground waters may become concentrated during dry seasons (July to September) and cause chloride to reach levels where it is adsorbed or exchanged onto organic materials or minerals. Data from Trainer and Heath (1976) suggest that a tenfold increase in the concentration of chloride in ground water is easily and routinely reached in most eastern North American ground waters during the dry seasons.

Chloride is the dominant anion in the LCH (Figure 13b), and dominates the anion concentration of the UCH in the easternmost region. Chloride concentrations increase from west to east in both units, and the contour patterns are very similar to those of sulfate. The source of chloride in the LCH and the eastern wells in the UCH is probably saline formation water, as the Castle Hayne Formation does not contain sufficient Cl-rich minerals to account for such high chloride concentrations by dissolution. Seawater trapped when these marine sediments were deposited, or during the sea level fluctuations of the Pleistocene, has probably since

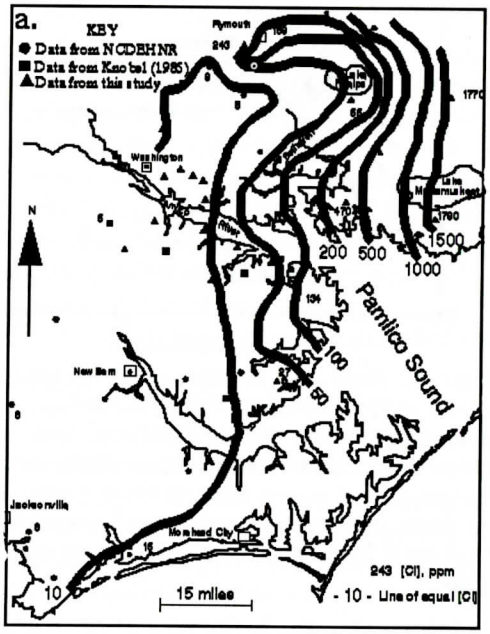

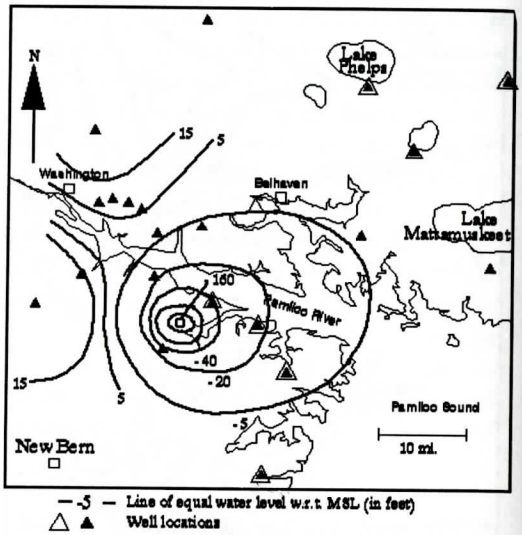

Figure 14. Observed potentiometric surface of the Castle Hayne aquifer in the vicinity of the Texasgulf phosphate mine [modified from Reynolds (1992)].

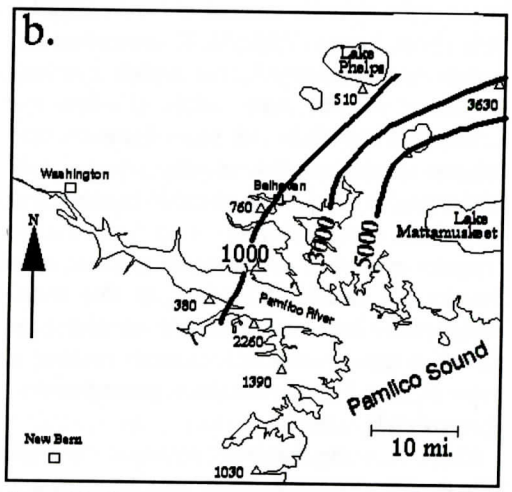

Figure 13. Chloride concentrations in ground waters of the Upper (a) and Lower (b) Castle Hayne. The drinking water limit for the state of North Carolina is 250 ppm (NCDEHNR, 1989).

been flushed out with freshwater. In the area around the Texasgulf phosphate mine, the chloride content has increased due to the lateral encroachment of chloride-rich water from beneath Pamlico Sound, and upconing of saline formation water from underlying units (Reynolds, 1992).

TGS-11A in the LCH has an anomalously high chloride concentration (2260 ppm) compared to surrounding wells. This site is well within the cone of depression created by pumpage at the Texasgulf mine (Figure 14). The high chloride concentration is probably due to upconing of saline water from underlying units, which is a direct result of the large removals of water by Texasgulf. The L-13 site (near Lake Phelps) has anomalously low chloride concentrations in both the UCH and the LCH (55 and 510 ppm, respectively) which significantly affect the shape of the contours. Local recharge at this site may be responsible for the reduction in the concentration of chloride.

Sodium and Potassium

Sodium concentrations increase from west to east in the UCH and the LCH; the greatest concentrations are in the northeast section of the study area (Figure 15). Potassium exhibits the same trend as sodium. Potassium and sodium concentrations in the western part of the study area are low but still too high to be due solely to rainfall (Table 7). The high concentrations can perhaps be explained by cation exchange of $2K^+$ and $2Na^+$ in clay minerals for Ca^{2+} in solu-

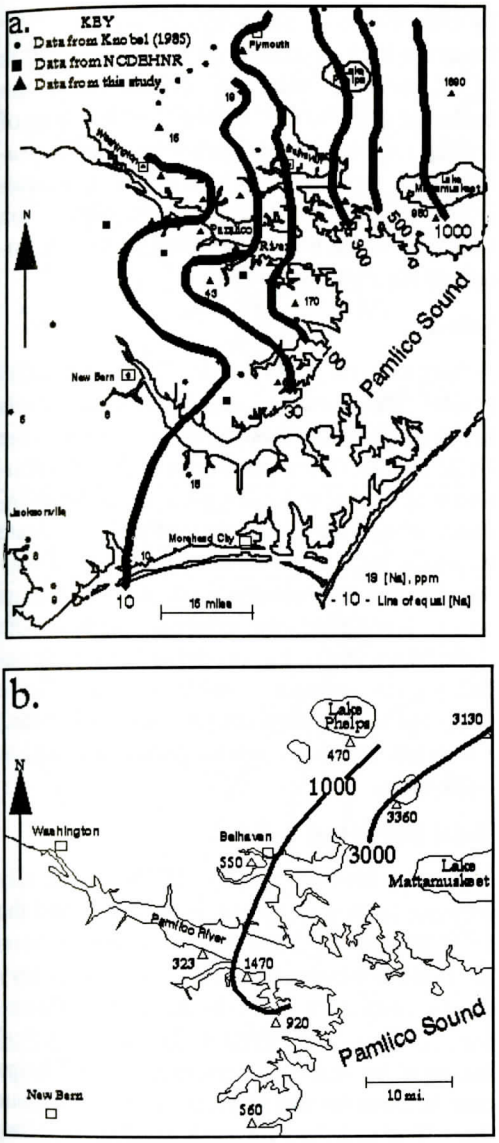

Figure 15. Sodium concentrations in ground waters of the Upper (a) and Lower (b) Castle Hayne.

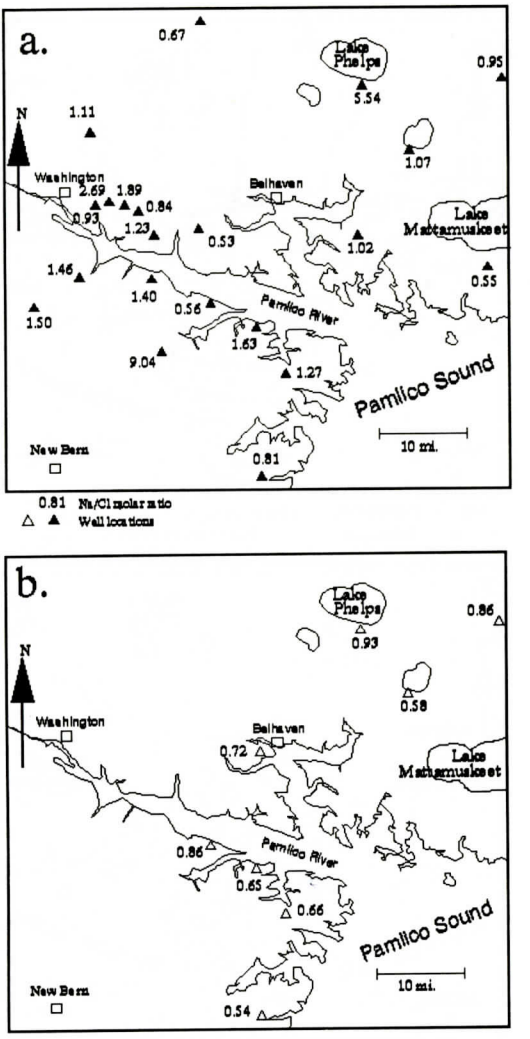

Figure 16. Molar ratios of Na^+/Cl^- in ground waters of the Upper (a) and Lower (b) Castle Hayne. The molar ratio for seawater is 0.86.

tion, or by leaching of K^+ and Na^+ from fertilizers applied to soils. The controlling process could not be determined from the information available. In the eastern part of the study area, the increase in K^+ and Na^+ is probably due to mixing with saline formation water.

The Na^+/Cl^- molar ratios (Figure 16) range from 0.53 - 9.04 and 0.54 - 0.93 for the UCH and LCH, respectively. Ratios much higher than the seawater value (0.86), which occur in areas where clay minerals are known to be present, were used as evidence for exchange of $2Na^+$ for Ca^{2+} by Sprinkle (1989) in his study of the Paleogene Floridan aquifer system. Evaporated precipitation recharging the system may also have caused the elevated ratios. In LCH wells, the Na^+/Cl^- ratios are less than those in the UCH and all but one are less than or equal to the seawater ratio. The K^+/Cl^- molar ratio of seawater is 0.02. UCH ratios approach this value in the easternmost wells, and all LCH

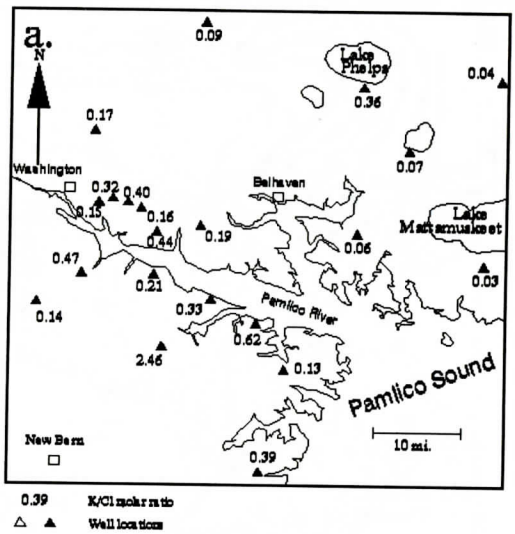

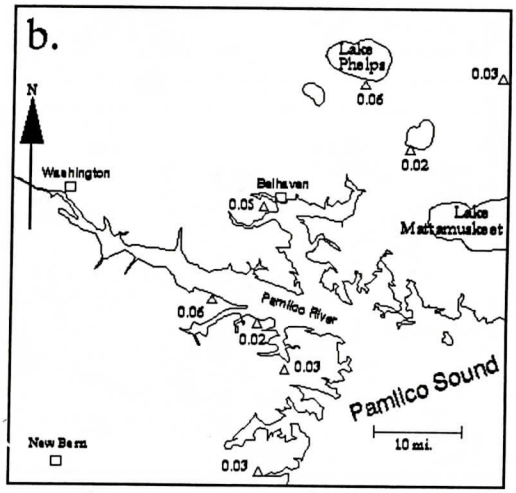

Figure 17. Molar ratios of K^+/Cl^- in ground waters of the Upper (a) and Lower (b) Castle Hayne. The molar ratio for seawater is 0.02.

waters approximate this ratio (Figure 17). Evidently the potassium and chloride in these wells are contributed mostly by saline formation water. The molar ratio of K^+/Cl^- for rainwater in the inland United States is 0.44 (Faure, 1991) and for eastern North Carolina is 0.11 (Willey and Kiefer, 1993); most western wells in the UCH have ratios in this range. The concentrations, however, are higher than those in rainwater, indicating that some K^+/Cl^- ratios in the Castle Hayne aquifer may have originated by evaporation of rainwater. Where the K^+/Cl^- ratios are high, K^+ could come from dissolution of K^+-bearing minerals (glauconite), ion exchange ($2K^+$ for Ca^{2+} or Mg^{2+}), or leaching of fertilizers. Sodium and potassium concentrations both increase from west to east while calcium seems to decrease; therefore, ion exchange could be an important process influencing the water chemistry.

Silica

Northeastern wells in the UCH and LCH aquifers are generally lower in silica than wells to the southwest, although distinct trends in the UCH and LCH are not evident. The distribution may be due to local variations in the abundance of opaline silica, chalcedony, or silicate minerals, such as glauconite or zeolite. It may also be due to recharge from overlying units which contain silicate minerals, such as the surficial aquifer or the overlying Miocene confining units. Another possible source might be some types of vegetation (grasses, reeds, etc.) which are very high in amorphous SiO_2 and/or cristobalite.

Total Dissolved Solids

Total dissolved solids (TDS) generally increase from west to east in the UCH and the LCH (Figure 18); the highest concentrations are in the northeast. The contour pattern is very similar to that for chloride and sulfate. Pumping at Texasgulf (Figure 14) and vertical recharge by dilute waters near Lake Phelps may account for the deflections in the contour lines. The eastward increase in TDS is apparently due to the increased intermixing of saline formation water. The TDS of average seawater is 34,500 ppm.

Minor Constituents

Fluoride

Fluoride concentrations generally increase from west to east in the UCH (Figure 19a) and UCH wells have higher concentrations than LCH wells in the northeast (Figure 19b). At M-12 locally high fluoride is evident in both Cas-

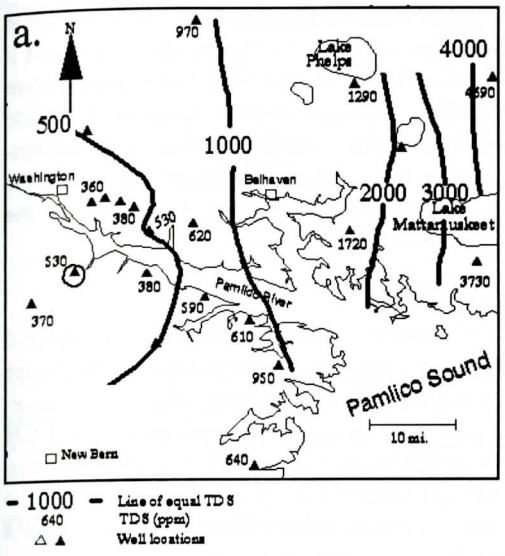

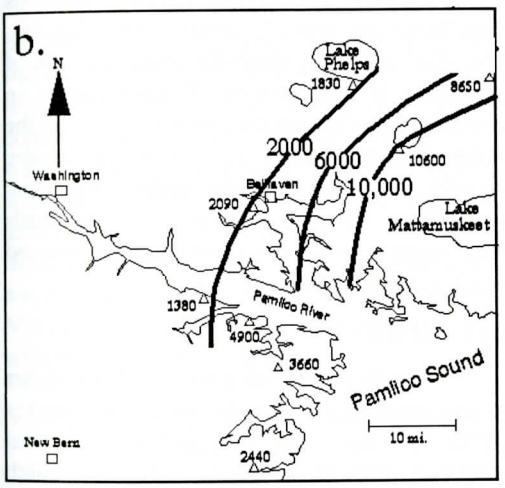

Figure 18. Total dissolved solids (TDS) in ground waters of the Upper (a) and Lower (b) Castle Hayne. TDS was calculated by summing the concentrations of all dissolved species. The national drinking water standard is 500 ppm.

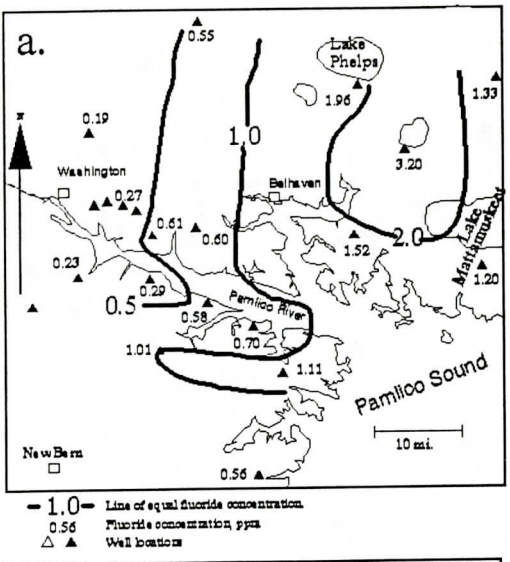

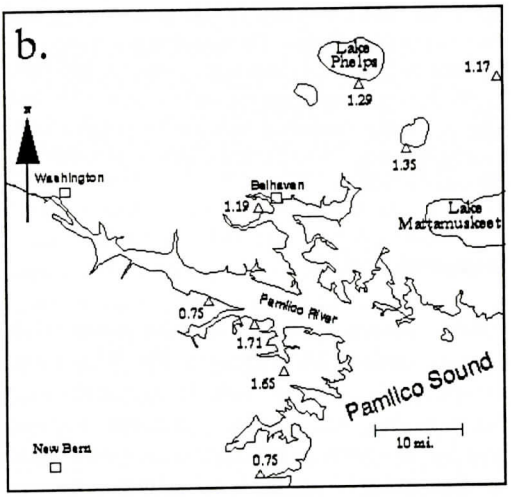

Figure 19. Fluoride concentrations in ground waters of the Upper (a) and Lower (b) Castle Hayne. The drinking water limit for the state of North Carolina is 2.0 ppm (NCDEHNR, 1989).

tle Hayne aquifers (UCH=3.20, LCH=1.35). Intermixing of saline formation waters, presumably of seawater origin, is not a likely cause of the increase observed from west to east because the F^-/Cl^- ratios of well waters are all higher than that of seawater. Also, some fluoride concentrations are higher than those of average seawater (1.6 ppm F^-). The occurrence of fluorine-bearing minerals in the Castle Hayne has not been adequately quantified, but in the region south of the study area the formation may contain as much as 5% phosphorite (Moran, 1989). Minerals within the aquifer may, therefore, be the source of fluoride. Also, to the east the aquifer is overlain by the Miocene Pungo River Formation, which is rich in carbonate fluor-apatite (Riggs, 1979, 1984). Perhaps ground water picks up fluoride from the overlying Pungo River Formation or from minerals within the aquifer, although no mechanism for this is apparent.

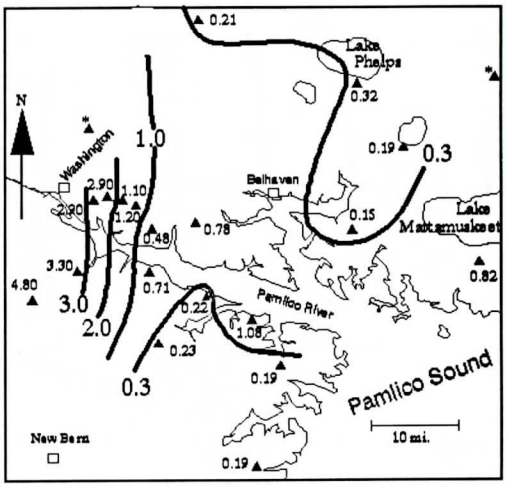

Figure 20. Iron concentrations in ground waters of the Upper Castle Hayne. The drinking water limit for the state of North Carolina is 0.3 ppm (NCDEHNR, 1989). Values determined for wells with an "* "were ignored during contouring because the samples were improperly filtered and particulates were visible in the sample bottles.

Iron and Sulfide

Iron concentrations are highest in the western wells of the UCH (Figure 20). Wilder and others (1978) suggest high concentrations occur in this area of direct recharge, because iron has not been in the aquifer long enough to oxidize and precipitate. A more likely explanation is that concentrations are higher due to the weathering of iron-bearing minerals in the surficial aquifer by more acidic (possibly organic-rich) water which has not been significantly neutralized by reaction with carbonate aquifer minerals. Ground water in the UCH is, in fact, generally more acidic in the western wells.

Small concentrations of sulfide were found; concentrations in the western wells in the UCH were generally lower than in eastern wells, except for one well located southeast of the Washington well field (TGCW-11A; 5.8 ppm). There was no apparent trend in the LCH wells. Measurable amounts of HS^- suggest the occurrence of microbial oxidation of organic material and sulfate reduction in the aquifer. Pyrite is found in the Castle Hayne formation, and it is possible that the iron which enters the system from the recharge area combines with sulfide to form pyrite, although pyrite is undersaturated in most waters. It is more likely that the pyrite formed during early diagenesis of the Castle Hayne.

Ammonia

Ammonia concentrations show a general increase from west to east in both Castle Hayne units (Table 5). At locations where wells penetrated both units, concentrations in the LCH exceeded those in the UCH. Concentrations in average seawater do not exceed 0.04 ppm, so intermixing of saline formation water is not a likely source of the ammonia unless it contains significant amounts of organic matter. A possible explanation for the high concentrations of ammonia is deamination of amino acids in organic matter within the aquifer itself or in the saline formation water which intrudes into the aquifer to the east. Under certain anaerobic conditions, the deamination of amino acids may occur releasing ammonia into the ground water (Drever, 1988).

pH and Eh

UCH wells in the east generally have higher pH values than those in the west. This trend is probably related to two factors: 1) local recharge through overlying pocosins which appears to be more abundant in the region around Lake Phelps, and 2) progressive down-gradient neutralization of acidic recharge water by reaction with aquifer carbonates.

As pointed out by Stumm and Morgan (1981) and Drever (1988), many, and perhaps most, measurements of Eh in natural waters using platinum electrodes represent mixed potentials not appropriate for quantitative interpretation. Such measurements can, however, be useful for identifying redox zones. Eh values generally become more negative from west to east in UCH wells; LCH wells in the northeastern portion of the study area had the most negative potentials. Vertical recharge through

Table 8. North Carolina drinking water standard (NCDEHNR, 1989).

Constituent	Standard (mg/L)	Constituent	Standard (mg/L)
arsenic	0.05	manganese	0.05
cadmium	0.005	nickel	0.15
chloride	250.0	nitrate	10.0
chromium	0.05	nitrite	1.0
copper	1.0	pH	6.5-8.5
dissolved solids (total)	500	selenium	0.01
fluoride	2.0	silver	0.05
iron	0.3	sulfate	250.0
lead	0.05	zinc	5.0

overlying organic-rich surface deposits might yield waters with lower redox potentials, as would flow of ground water downgradient away from an atmospheric source of oxygen.

Other Minor Constituents

Bromide found in Castle Hayne waters may be of marine origin as concentrations generally increase as chloride increases (Cl-Br correlation coefficient = 0.47). The higher phosphate concentrations in UCH wells than in LCH wells at the same site are perhaps due to leakage from overlying phosphate-bearing strata, although studies of the Castle Hayne south of the study area indicate that phosphorite layers are more abundant in the UCH (Moran, 1989). Manganese concentrations vary proportionally with those of iron (r = 0.86).

Comparison of Analyses with Drinking Water Standards

Table 8 presents the North Carolina drinking water standards for constituents analyzed in this study. LCH wells and many UCH wells (except for those in the west) exceeded the chloride limit of 250 ppm (Figure 13). One well in the UCH (L-10 a-3) and half of the LCH wells exceeded the limit (250 ppm) for sulfate (Figure 11). M-12 l-1, an UCH well, was the only one to exceed the limit for fluoride (Figure 19). Most wells in the UCH were above the limit for iron, especially in the western portion of the study area (Figure 20). Several UCH wells (located in the extreme east and west) were above the limit for manganese. None of the LCH wells were above this limit.

Hydrochemical Facies

Piper diagrams (1944) were used to delineate hydrochemical facies of samples collected for the present study (Figure 21). Figure 22 is a map of the distribution of hydrochemical facies for waters from the UCH. The LCH wells are all alkali-rich (3) and chloride-rich (C).

In the UCH, the wells to the far west are calcium-rich (1) and bicarbonate-rich (A), suggesting that dissolution of limestone controls their chemistry. In the region affected by the cone of depression generated by pumping at Texasgulf (Figure 14), most of the waters are composed of a mixture of cations. The northeasternmost wells in the UCH become alkali-rich (3) and chloride-rich (C), just like waters in the LCH. This probably reflects the mixing of fresh ground water and saline formation water. L-13 i-1 is alkali-rich (3) and bicarbonate-rich (A) because local recharge apparently dilutes chloride, adds bicarbonate due to its high organic content, and enhances alkalies due to cation exchange.

Trapp and Meisler (1992) studied the regional aquifer system underlying the Northern Atlantic Coastal Plain and found that the hydrochemical facies of each aquifer follows a general down-dip sequence from (1) water of variable composition, to (2) calcium and magnesium bicarbonate water, to (3) sodium bicarbonate water, to (4) sodium chloride water. In this study, there is not a clear sodium bicarbonate facies (3A) except at location L-13 i-1 (discussed previously). Instead, there is a mixed cation bicarbonate facies (4A) which may originate from perturbation due to pumping at Texasgulf.

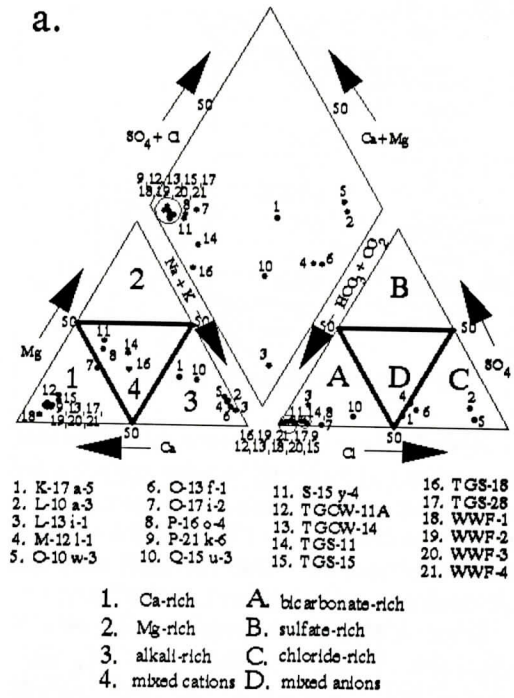

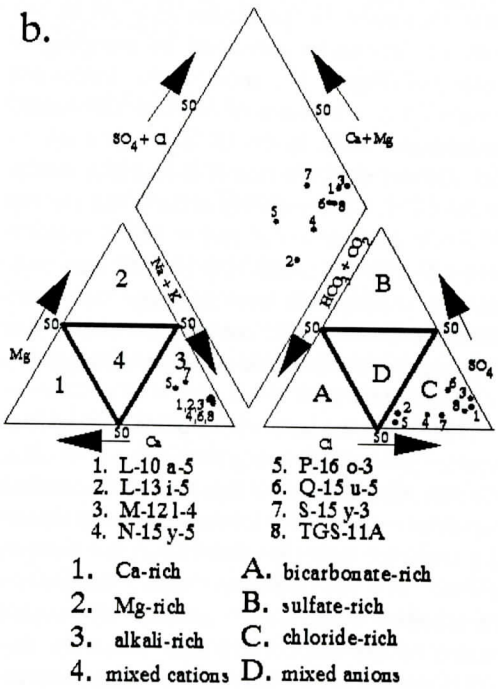

Figure 21. Piper diagrams for ground waters of the Upper (a) and Lower (b) Castle Hayne.

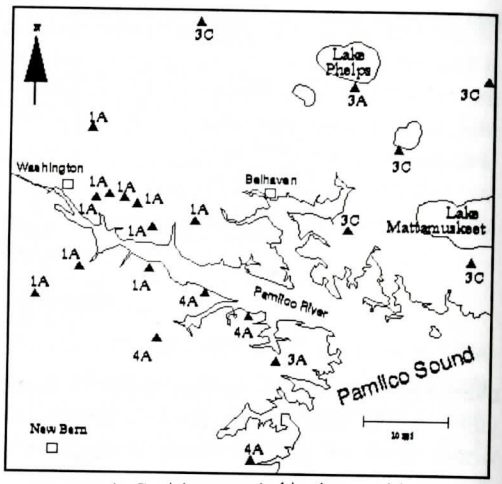

Figure 22. Hydrochemical facies diagram for ground waters of the Upper Castle Hayne.

CONCLUSIONS

Major geochemical processes that appear to affect water chemistry in this region are

(1) dissolution and precipitation of minerals trending toward chemical equilibrium with the water,

(2) mixing of ground water with saline formation water, recharge, or leakage from other aquifers,

(3) ion exchange between the water and the aquifer minerals, and

(4) reactions with soil minerals and fertilizers during recharge.

In the western portion of the study area, the concentrations of ions are due primarily to rainfall, reactions with soil minerals and fertilizers, and dissolution of aquifer minerals. In the eastern portion of the study area, mixing of ground water with saline formation water, derived from various Cenozoic and Upper Cretaceous seawaters, increases the concentrations of many of the ions. Ion exchange appears to be occurring at several localities.

Calcite is saturated in ground waters throughout the study area. The dolomite saturation index increases from west to east in the UCH and waters from all but the nine western-

most UCH wells are saturated. The gypsum saturation index increases from west to east due to an increase in sulfate, but the waters never became supersaturated.

High concentrations of several ions were noted at wells within the cone of depression generated by Texasgulf. Chloride, bromide, and fluoride appear to be higher than would be expected in the area. The increase may be due to the upconing of water from the underlying units. Sodium and potassium seem slightly high, and this may be due to the upconing of brackish water or ion exchange processes.

The L-13 site appears to be an area of recharge because the TDS, chloride, sulfate, magnesium, and calcium concentrations are low, and the alkalinity is high, when compared to surrounding wells.

Chloride, sulfate, fluoride, iron, and manganese concentrations exceed the State drinking water limits in water from some portions of the study area.

The UCH wells in the western portion of the study area exhibit a calcium-rich and bicarbonate-rich hydrochemical facies. Waters within the Texasgulf cone of depression are primarily mixed cations-bicarbonate facies. The wells in the eastern region of the UCH and all the wells in the LCH are alkali-rich and chloride-rich.

Studies of aquifer mineralogy and Sr-isotope geochemistry, and additional work on water chemistry are currently in progress. Hopefully, these studies will answer some of the questions suggested by this preliminary analysis of the chemistry of ground water from the Castle Hayne.

ACKNOWLEDGEMENTS

We are truly grateful to the Water Resources Research Institute of The University of North Carolina for providing financial support for this study (Contract # ECU-42093-1). We would also like to thank William Hardison and Jeff Schaffer of NCDEHNR, Tex Gilmore and Alvin Jarvis of Texasgulf, and Jerry Cutler of the City of Washington, NC. We extend a special thanks to Jim Watson and John Woods for constructing and providing equipment; to many graduate students at ECU who assisted us in the field; to Tim Spruill, Pierre Glynn, Eurybiades Busenberg, Richard Spruill, and Jeff Reynolds who offered insight on sampling techniques and the movement of ground water; to John Bray, Deborah Daniel, Martha Jones, Wendy Jones, and Craig Hamilton for their laboratory assistance; and to Joan Willey and Rudi Kiefer for providing chemical data on precipitation in North Carolina. The careful reviews of Paul Baker, Larry Benninger, John Bray, Richard Mauger, Richard Spruill, and a WRRI reviewer greatly improved this manuscript.

REFERENCES CITED

American Public Health Association, 1992, Standard methods for the examination of water and wastewater, 18th ed.: Washington, D.C.

Baker, P.A., and Kastner, M., 1981, Constraints on the formation of sedimentary dolomite: Science, v. 213, p.214-216.

Chapelle, F.H., 1983, Ground-water geochemistry and calcite cementation of the Aquia aquifer in southern Maryland: Water Resources Research, v. 19, p. 545-558.

DeWiest, R.J.M., 1969, Hydrologic relationship between the Pamlico River and the Castle Hayne aquifer in Eastern North Carolina: Preprint 830: American Society of Civil Engineers, Annual Meeting on Water Resources Engineering, February 1969.

Drever, J.I., 1988, The geochemistry of natural waters, 2nd ed.: Prentice Hall, Englewood Cliffs, N.J., 437 p.

Faure, G., 1991, Principles and applications of inorganic geochemistry: Macmillan Publishing Co., New York, 626 p.

Gambell, A.W. and Fisher, D.W., 1966, Chemical composition of rainfall, western North Carolina and southeastern Virginia: U.S. Geological Survey Water Supply Paper no. 1535-K, 41 p.

Gamus, W.J., 1972, Analysis of factors controlling groundwater flow for prediction of rates of ground-water movement and changes in quality, Atlantic Coastal Plain: Unpublished Ph.D. Thesis, University of Arizona, 113 p.

Giese, G.L., Eimers, J.L., and Coble, R.W., 1991, Simulation of ground-water flow in the coastal plain aquifer system of North Carolina: U.S. Geological Survey Open-File Report 90-372, 178 p.

Giese, G.L., Mason, R.R., and Strickland, A.G., 1987, North Carolina ground-water quality: U.S. Geological Survey Open-File Report 87-0743, 8 p.

Hardy, M.A., Leahy,P.P., and Alley, W.M., 1989, Well instal-

lation and ground-water sampling protocols for the pilot national water-quality assessment program: U.S. Geological Survey Open-File Report 89-396, 36 p.

Harned, D.A., Lloyd, O.B.,Jr., and Treece, M.W., Jr., 1989, Assessment of hydrologic and hydrogeologic data at Camp Lejeune Marine Corps base, North Carolina: U.S. Geological Survey Water-Resources Investigations Report 89-4096, 64 p.

Joint Study, 1971 [North Carolina Board of Water and Air Resources, Texasgulf Sulfur, NC Phosphate Corp.], Hydrogeology and effects of pumping from the Castle Hayne aquifer system, 146 p.

Junge, C.E. and Werby, R.T., 1958, The concentration of chloride, sodium, potassium, calcium and sulfate in rainwater over the United States, Journal of Meteorology, v. 15, p. 417-425.

Knobel, L.L., 1985, Ground-water-quality data for the Atlantic Coastal Plain: New Jersey, Delaware, Maryland, Virginia and North Carolina: U.S. Geological Survey Open-file Report 85-154, 84p.

Lloyd, O.B.,Jr., and Daniel, C.C., 1988, Hydrogeologic setting, water levels, and quality of water from supply wells at the U.S. Marine Corps Air Station, Cherry Point, North Carolina: U.S. Geological Survey Water-Resources Investigations Report 88-4034, 76 p.

Lyke, W.L., and Treece, M.W., Jr., 1988, Hydrogeology and effects of ground-water withdrawals in the Castle Hayne aquifer in coastal North Carolina, *in* Lyke, W.L., and Hoban, T.G., eds., Proceedings of the symposium on coastal water resources, Wilmington, NC, p. 469-478.

Moran, L.K., 1989, Petrography of unconformable surfaces and associated stratigraphic units of the Eocene Castle Hayne Formation, southeastern North Carolina Coastal Plain: Unpublished Masters Thesis, East Carolina University, 337 p.

NCDEHNR, 1981-1992, Unpublished water chemistry data for the Castle Hayne aquifer.

Nesbitt, H.W., and Cramer, J.J., 1993, Genesis and evolution of HCO_3-rich and SO_4-rich ground waters of Quaternary sediments, Pinawa, Canada: Geochimica et Cosmochimica Acta, v. 57, p. 4933-4946.

North Carolina Department of Environment, Health & Natural Resources, Division of Environmental Management (NCDEHNR), 1989, Classification and water quality standards applicable to the ground waters of North Carolina, Subchapter 2L: Environmental Management Commission, Raleigh, NC.

North Carolina Department of Natural and Economic Resources (NCDNER), 1974, Status report on ground-water conditions in Capacity Use Area No. 1, central coastal plain: North Carolina Ground-water Bulletin no. 21, 146p.

North Carolina Department of Natural and Economic Resources (NCDNER), 1976, Interim report on ground-water conditions in Capacity Use Area No.1, central coastal plain, North Carolina,1974-1975, 55 p.

Orion Research, Inc., 1989, Model 94-16 silver/sulfide electrode manual, Part No. 502700-033 Form IM9416/9860 Rev.B.

Otte, L.J., 1981, Petrology of the exposed Eocene Castle Hayne limestone of North Carolina: Unpublished Ph.D. Thesis, University of North Carolina, 183 p.

Otte, L.J., 1986, Regional perspective on the Castle Hayne limestone, *in* Textoris, D.A., ed., SEPM Field Guidebooks: Southeastern United States Third Annual Midyear Meeting: 1986, p. 270-276.

Parkhurst, D.L., Thorstenson, D.C., and Plummer, L.N., 1980, PHREEQE - A computer program for geochemical calculations: U. S. Geological Survey Water-Resources Investigations Report 80-96, 195 p.

Piper, A.M., 1944, A graphic procedure in the geochemical interpretation of water analyses: Trans. American Geophysical Union, v. 25, p. 914-923.

Reynolds, J.W., 1992, Aquifer depressurization for mining at Texasgulf, Inc.: evaluation and modeling of hydrogeologic impacts and potential mitigative strategies: Unpublished Masters Thesis, East Carolina University, 140 p.

Riggs, S.R., 1979, Phosphorite sedimentation in Florida--A model phosphogenic system: Economic Geology, v.74, p.285-314.

Riggs, S.R., 1984, Paleoceanographic model of Neogene phosphorite deposition, US Atlantic continental margin: Science, v. 223, p. 123-131.

Rightmire, C.T., Pearson, F.J., Jr., Back, W., Rye, R.O., and Hanshaw, B.B., 1974, Distribution of sulphur isotopes of sulphates in ground waters from the principal artesian aquifer of Florida and the Edwards aquifer of Texas, U.S.A., *in* Isotope techniques in ground-water hydrology, v. 2., 1974: Vienna, Austria, International Atomic Energy Agency, p. 191-207.

Sherwani, J.K., 1980, Public policy for the management of ground water in the Coastal Plain of North Carolina: University of North Carolina Water Resources Research Institute, Report no. 129, 63 p.

Solorzano, L., 1969, Determination of ammonia in natural waters by the phenol hypochlorite method: Limnol. Oceanogr., v. 14, p. 799-801.

Sprinkle, C.L., 1989, Geochemistry of the Floridan aquifer system in Florida and in parts of Georgia, South Carolina, and Alabama: U.S. Geological Survey Professional Paper 1403-I, 105 p.

Stainton, M.P., Capel, M.J., and Armstrong, F.A.J., 1974, The chemical analysis of fresh water. Environment Canada Miscellaneous Publ. no. 25, Research and Development Directorate, Freshwater Institute, Winnipeg, Canada, 119 p.

Strickland, J.D.H., and Parsons, T.R., 1972, A practical handbook of seawater analyses: Fisheries Research Board of Canada, 311 p.

Stumm, W. and Morgan, J.J., 1981, Aquatic Chemistry: John Wiley and Sons, Inc., New York, 780 p.

Sutton, L.C., and Woods, T.L., 1994, Ground-water geochemistry of the Castle Hayne Aquifer in the region of Capacity Use Area No. 1, Northeastern North Caro-

lina: University of North Carolina Water Resources Research Institute, Report No. 70131, 130p.

Trainer, F.W., and Heath, R.C., 1976, Bicarbonate content of ground water in carbonate rock in eastern North America: Journal of Hydrology, v. 31, p. 37-55.

Trapp, H., Jr., and Meisler, H., 1992, The regional aquifer system underlying the Northern Atlantic Coastal Plain in parts of North Carolina, Virginia, Maryland, Delaware, New Jersey, and New York - Summary: U.S. Geological Survey Professional Paper 1404-A, 30 p.

Warner, D., 1993, Hydrogeologic study of the Castle Hayne aquifer system: northern Beaufort county, N.C.: verification of well field design: Unpublished Masters Thesis, East Carolina University, 163 p.

Wilder, H.B., Robison, T.M., and Lindskov, K.L., 1978, Water resources of northeast North Carolina: U.S. Geological Survey Water-Resources Investigations Report 77-81, 113 p.

Willey, J.D., and Kiefer, R.H., 1990, A contrast in winter rainwater composition: Maritime versus continental rain in eastern North Carolina: Monthly Weather Review, v. 118, p. 488-494.

Willey, J.D. and Kiefer, R.H., 1993, Atmospheric deposition in southeastern North Carolina: Composition and quantity: The Journal of the Elisha Mitchell Scientific Society, v. 109, p. 1-19.

Willey, J.D., Bennett, R.I., Williams, J.M., Denne, R.K., Kornegay, C.R., Perlotto, M.S. and Moore, B.M., 1988, Effect of storm type on rainwater composition in southeastern North Carolina: Environmental Science and Technology, v. 22, p. 41-46.

Winner, M.D., Jr., and Coble, R.W., 1989, Hydrogeologic framework of the North Carolina Coastal Plain aquifer system: U.S. Geological Survey Open-file Report 87-690, 155 p.

ERRATA (VOLUME 35, NO. 1)

GEOPHYSICAL EVIDENCE FOR POST LATE CRETACEOUS REACTIVATION OF BASEMENT STRUCTURES IN THE CENTRAL SAVANNAH RIVER AREA

A. STIEVE AND D. STEPHENSON

Westinghouse Savannah River Company
Savannah River Technology Center
PO Box 616
Aiken, SC 29802

ACKNOWLEDGMENTS

The content and conclusions of this paper are summarized from a 1992 report to U. S. Dept. of Energy under contract DE0AC09-89SR18035. The data were obtained through subcontracts with E. I. DuPont de Nemours Inc. and Westinghouse Savannah River Co. Data collection and processing of the seismic reflection surveys, the TDEM data and the detailed gravity survey were done by Seismograph Services, Inc., Conoco Inc., Coleman Blackhawk, Inc., and Eric Anderson (for MS at University of South Carolina, Columbia) respectively. Most recent reprocessing of the Conoco seismic data was performed under subcontract AA00910-0 under AC09-88SSR18035 with the Virginia Polytechnic Institute and State University Regional Geophysics Lab, to J. Costain and C. Coruh. All Conoco seismic reflection data that appear in this paper were reprocessed by William J. Domoracki for his doctoral degree in geophysics (pending) at the Virginia Polytechnic Institute and State University. Comments on the initial drafts by R. D. Hatcher, Jr., T. Cordone, R. Cumbest and P. Rizzo are gratefully acknowledged. Technical editing and drafting support came from A. Flowers. We would like to thank the anonymous reviewers and D. Heron for their constructive and helpful comments.

Erratum

W. J. Domoracki's name was misspelled in the article on page 5 and 19.